Role of the Extreme Anterior Domain Organizer in Craniofacial Development

A dissertation presented

by

Laura Anne Jacox

to

The Program of Biological Sciences in Dental Medicine

in partial fulfillment of the requirements

for the degree of

Doctor of Philosophy

in the subject of

Biological Sciences in Dental Medicine

Harvard University

Cambridge, Massachusetts

April 2015

Dissertation Advisor

Professor Hazel L. Sive

Author

Laura Anne Jacox

Role of the Extreme Anterior Domain Organizer in Craniofacial Development

Abstract

Craniofacial development is an intricate process, involving cranial neural crest (NC) and anterior facial tissue. NC migration is regulated by multiple mechanisms and activity of one or more organizer regions. Work presented here explores the role of the EAD, an organizer of craniofacial development in *Xenopus*, and its reciprocal signaling with cranial NC. The EAD later contributes to the mouth, nostrils, and anterior pituitary. EAD function involves the Kinin-Kallikrein pathway that was shown for the first time to be necessary for mouth formation. Facial transplants demonstrate that EAD-localized Kinin-Kallikrein function is required for migration of first arch cranial NC into the face. After migration, cranial NC signals back to the EAD to regulate mouth opening via the Wnt/PCP pathway. This pathway is associated with a process consistent with convergent extension of the EAD, whereby a wide and short epithelial mass narrows and lengthens, and cells and nuclei undergo stereotypical changes. The resultant EAD is a bilayered epithelium that later splits to form the mouth opening. Identification of the EAD as a NC organizer, reciprocal interaction of EAD and NC, and convergent extension associated with mouth formation has not previously been described during craniofacial development. Face formation is widely conserved, so findings in frog are likely relevant to amniotes and will provide insight into causes of craniofacial deformities.

Table of Contents

Figures and Tables

Chapter 1

Chapter 2

Chapter 3

Chapter 4

Chapter 5

No figures and no tables

List of Abbreviations

AA	amino acid
ACE	Angiotensin Converting Enzyme
L-Arg, Arg	arginine
AP	anterior pituitary
ANR	anterior neural ridge
atg2b	autophagy related protein 2b
BP membrane	buccopharyngeal membrane
BA	branchial arch
Bdk,bk	Bradykinin
Bkbr, BKB Receptor	Bradykinin B Receptor
BKB1 Receptor	Bradykinin B1 Receptor
BKB2 Receptor	Bradykinin B2 Receptor
BM	Basement membrane
BMP	bone morphogenic protein
cDNA	complementary DNA
CE	convergent extension
CG	cement gland
cGMP	cyclic guanosine monophosphate
Cpn	Carboxypeptidase N
desArg-BK	Des-arginine Bradykinin
dpf	days post fertilization
Dvl	Dishevelled
EAD	extreme anterior domain

EZ	endodermal zone
FEZ	frontonasal ectodermal zone
FNP	frontonasal process, also known as frontonasal prominence
FGF8	Fibroblast growth factor 8
Fzl7	Frizzled7
Frzb-1	Frizzled-Related Protein-1
GFP	green fluorescent protein
GOF	gain of function
GPCR	G-protein coupled receptor
HH	Hamburger Hamilton
hpf	hours post fertilization
IP	inositol phosphate
Kng	Kininogen
LOF	loss of function
LNP	lateral nasal process, also known as lateral nasal prominence
MBS	Modified Barth's Saline
Mo	mouth
MO	morpholino
MN	mandibular process, also known as mandibular prominence
MNP	mandibular nasal process, also known as mandibular nasal prominence
MXP	maxillary process, also known as maxillary prominence
NC	neural crest
No	nose
NO	nitric oxide

NOS	Nitric oxide synthase
nNOS	Neural nitric oxide synthase
NP	nasal placode
NT	neural tube
PA	pharyngeal arch
PCP	Planar Cell Polarity
PCR	polymerase chain reaction
PH3	Phospho-Histone 3
PI	propidium iodide
qPCR	quantitative polymerase chain reaction
rpm	rotations per minute
RT-PCR	reverse transcription polymerase chain reaction
SHH	Sonic Hedgehog
ss	somite stage
TM	transmembrane domain
xBdk	*Xenopus* Bradykinin
8AA	8 amino acids
9AA	9 amino acids

Acknowledgements

I would like to thank my husband, Ilan Moyer, for supporting me through this journey and weathering the storm that is graduate school. I thank him for staying on campus many nights waiting for me to conclude experiments, for bringing me dinner when I did not have time to run to the store, and for camping in the conference room to keep me company when I needed to work late. I thank him for his sound and thoughtful advice, and for loving and encouraging me through this phase. Your friendship and support have made my life so much warmer, more fulfilling, and enjoyable. Thank you.

I want to acknowledge my mom who sparked and fostered my love of learning and new experiences. When I was a child, we would read countless books and travel to museums, zoos, gardens and orchestra concerts nearly every weekend. I value all that she has invested in me, while working full time and raising me on her own. She has always set a high standard for me, yet managed to convince me that I set the bar for myself, a motivational skill I hope to use on my own future children. She is also willing to listen and dispense her sage, down-to-earth advice, more as a friend than as an authority figure, which I have always appreciated. Mom- Thank you for your hard work, perspective, love, and support.

I want to thank my extended family, including my aunts Diane and Anne and my grandparents Joe and Kay and Sanford and Helen for their love and support. Grandma Kay and Aunt Diane are little dynamos who instilled in me the belief that women could and should 'reach for the stars' professionally. Grandpa Joe, or 'Who-Who' as I knew him, taught me to appreciate the simple joys of life as my nanny. Our trips to the park, visits to the neighbor's dog, and mornings spent watching Mr. Roger's Neighborhood, are some of my favorite childhood memories. I miss him greatly.

Much gratitude goes to my advisor, Hazel Sive, for giving me the opportunity and encouragement to pursue research. I have learned a great deal from her about the science and art of biological inquiry. I value Hazel's ability to inspire enthusiasm about science and her commitment to supporting women in research. I will be forever grateful for the advice, mentorship, instruction, and support provided by Hazel and the impact that the graduate school experience has had on me.

Another credit to Hazel is the collaborative and thoughtful environment she has fostered in her lab. My fellow lab-mates are excellent scientists, kind individuals, and patient teachers. They have taught me a great deal about science and regularly offered insightful advice that influenced my approach to projects. I will miss their company and our conversations. I am grateful I had the opportunity to work with Amanda Dickinson, Jasmine McCammon, Ryann Fame, Alyssa Rothman, Heather Ferguson, Isabel Brachman, Alicia Blaker-Lee, Chelsea Chen, Jennifer Gutzman, Jessica Chang, Christian Cortes Campos, Justin Chen, Radek Sindelka, and Olivier Paugois. I am also thankful for the support staff at Whitehead Institute who have made critical graphical, bioinformatic and caloric contributions including Tom DiCesare, Inma Barrasa, George Bell, Prat Thiru, Heather Ferguson and the staff of Salt Creek Catering.

I deeply thank Dr. Ed Seldin, my dental advisor, mentor and friend. I appreciate his advice, encouragement and support, along with his willingness to argue for just causes and speak his mind. I have a deep respect for his brilliance, kindness and good heart.

I would like to acknowledge my Dissertation Advisory Committee: Professors Malcolm Whitman, Richard Maas, and Arkhat Abzhanov. It has been a pleasure to work with such great minds who also are caring mentors. I thank my Dissertation Examining Committee: Professors Arkhat Abzhanov, Richard Maas, Yingzi Yang, and Vicki Rosen for all of their time and care for my defense and dissertation.

I have deep gratitude for Professor Bjorn Olsen, my Harvard-based advisor and Director of the Biological Sciences in Dental Medicine Program. Professor Olsen is not only an exemplary scientist, but he is a great source of advice, inspiration, and mentorship. Professor Olsen's door is almost always open and he is available to thoughtfully discuss projects, career goals, and other topics of interest. Professor Olsen, in collaboration with Diane Spinell, Deborah Milstein, and Patty Cunningham, have done an amazing job helping me navigate transitions from medical school to graduate school and back to dental school. Studying within Professor Olsen's department and getting to know him has been a real pleasure.

Many thanks go to the Harvard-MIT Health Science and Technology (HST) Program for allowing me to pursue a different road to becoming a dentist. The HST curriculum and community has pushed my boundaries and set a high bar for my aspirations as a researcher and clinician. My colleagues and classmates are excellent doctors and scientists while being an invaluable network of kind and caring friends. In particular, I want to thank Professors Richard Mitchell and David Cohen for their excellent teaching, support and for providing me with the opportunity to help teach the HST biochemistry course. I have loved getting to know Rick and David, and the HST students over the years, and have learned a great deal from them about the type of physician-scientist I hope to become in the future. I am also thankful for Patty Cunningham's commitment to managing the HST program and all of its students; she is an indispensible source of kindness, encouragement, and deadline reminders.

I am also grateful for the Harvard School of Dental Medicine (HSDM) and the opportunity to become a dentist and scientist in one of the most vibrant and flexible research-oriented dental schools in the country. Through HSDM, I was able to invent my own HST DMD-PhD program with the support and assistance of many HSDM faculty and staff, including registrar Diane Spinell, and Professors Bjorn Olsen, Nadeem Karimbux, and Sang Park. I appreciate their willingness to pave a new educational road for me, despite the additional work and hassle. My classmates at HSDM have also been wonderful, smart, supportive, and kind friends and colleagues. The administrative support staff and grants office at HSDM have been great resources, and I thank Ashley Congdon, Dawn DeCosta, Deborah Milstein, Lynn Dunham and Mary Lamey for their help at many junctures.

I am deeply thankful for the scientific mentorship I was provided throughout my high school and undergraduate education, with particular gratitude for Sara Sagmiester, Professor James Sherley and Professor Gene Brown. Sara Sagmeister introduced me to the amazing world of biology. Though science had always been an interest of mine, it was Mrs. Sagmeister's interesting and thorough description of biology that sparked a fire in me. Professor Sherley invited me to join his

lab as a freshman, with no prior experience, and paired me with an excellent post-doc, Minsoo Noh. Minsoo was a thoughtful and patient teacher who introduced me to scientific experimentation. Once I learned techniques, I was given the opportunity to work on my own independent project, a responsibility and freedom rarely enjoyed by undergraduates. Professor Sherley spent countless afternoons with me, discussing my project, my future, and careers in science. Had it not been for Professor Sherley's encouragement and support, I likely would not have pursued this degree or science as a career. He is an excellent mentor and human being.

Much gratitude goes to Professor Gene Brown, my undergraduate advisor who offered me the opportunity to be a teaching assistant for his biochemistry course. He has been a great source of advice and encouragement over the years. My involvement with biochemistry unearthed my love of teaching and helped develop my public speaking skills. I still teach biochemistry from notes taken in part from Professor Brown's courses. Professor Brown has had a lasting effect on my life.

Finally, I would like to thank my feline friends, Carmel, Laila and Cleo Bernardi Jacox, for their undying commitment to warming my lap while writing this dissertation and for occasionally distracting me to partake in purr festivals.

Thank you.

“I cannot think of a single field in biology or medicine in which we can claim genuine understanding, and it seems to me the more we learn about living creatures, especially ourselves, the stranger life becomes.”
~Lewis Thomas (1913-1999)

This page has been intentionally left blank.

Chapter 1

Contributions of Craniofacial Organizers to Perioral Development

Author Contributions: L.J. reviewed the literature, wrote and revised the manuscript drafts. H.S. directed and supervised the study and assisted in writing and revising the manuscript.

Publication: Jacox, L., & Sive, H. Contributions of Craniofacial Organizers to Perioral Development. Manuscript in preparation for an invited contribution to *WIREs Developmental Biology*.

1.1 Abstract

Craniofacial development is an intricate process, involving movement of the multipotential cranial neural crest (NC), and organization into anterior facial primordia. Multiple signals regulate NC migration, including activity of one or more organizer regions. One organizer includes the Extreme Anterior Domain (EAD) consisting of directly juxtaposed ectoderm and endoderm, without intervening mesoderm. In *Xenopus laevis,* the EAD is a craniofacial organizer required for NC development. The EAD also contributes to the mouth. While an EAD is present in all vertebrates, it is not clear whether it serves an organizer function in other species. In chick and mice, the frontonasal ectodermal zone (FEZ) is an organizer that forms later in development and more dorsally to the EAD, and directs skeletogenesis. In zebrafish, data is consistent with the existence of a midline organizing domain. Loss of either EAD or FEZ signaling is associated with gross craniofacial abnormalities.

1.2 Introduction

The vertebrate face is one of the most complex regions of the body, and consists of the eyes, nose, mouth and anterior skeletal, nervous, vascular and connective tissues. One third of all birth defects involve deformities of the face and head, which appear in 1 out of every 700 live births (Gorlin, 1990). The intricate complexity of craniofacial development may explain this high rate of anomalies. In most patients, the underlying molecular cause of a craniofacial defect is unknown. Research is needed to identify regulators of face formation and possible disease etiologies, as our knowledge is incomplete.

Despite the complexity of the adult face, the vertebrate mouth and jaws derive from two embryonic origins: the anterior ectoderm and endoderm and the cranial neural crest (NC) (Dickinson and Sive, 2006; Jacox et al., 2014). Cranial NC is a migratory, multipotential population originating from the neural tube (Minoux and Rijli, 2010). Cranial NC segregates into five branchial or pharyngeal arches, which contribute to distinct facial and neck structures (Gilbert, 2010; Minoux and Rijli, 2010). Once the branchial arches arrive in the face, the NC forms facial prominences (mandibular, maxillary, frontonasal, medial nasal, and lateral nasal), which grow and fuse to form the mandible, maxilla, palate, nose, and upper lip (Thomason and Dixon, 2009). Cranial NC in the prominences ultimately differentiates into facial cartilage, bone, connective tissue, and melanocytes (Minoux and Rijli, 2010).

Juxtaposed anterior ectoderm and endoderm constitute the non-crest Extreme Anterior Domain (EAD) (Jacox et al., 2014). The EAD is a conserved structural region that derives from the anterior neural ridge (ANR) (Chapter 3; Couly and Le Douarin, 1985, 1987; Eagleson et al., 1995). Data in chick and frog are consistent with the EAD encompassing the mouth primordium, nasal placodes and the adenohyophyseal anlagen, the precursor of the anterior pituitary (Chapter

3; Couly and Le Douarin, 1985, 1987; Eagleson et al., 1995). These tissues lie within the pan-placodal ectoderm, derived from the ANR region of chick, *Xenopus*, mouse, and zebrafish (Couly and Le Douarin, 1985, 1987; Eagleson et al., 1995; Kozlowski et al., 1997; Osumi-Yamachita et al., 1994). The pan-placodal region is defined by uniform expression of placodal markers including *eya1* and *six1* (Schlosser, 2006; Brugmann and Moody, 2005). In vertebrates, the medial portion of the ANR gives rise to the adenohypophysis while the lateral regions give rise to the olfactory placodes (Couly and Le Douarin, 1985; Eagleson et al., 1986, 1995; Kawamura et al., 2002; Kozlowski et al., 1997; Osumi-Yamachita et al., 1994; Papalopulu, 1995).

Once the ANR gives rise to the EAD, it functions as a craniofacial organizer in *Xenopus*. Previously, it was known that EAD-localized perturbations to *frzb* expression results in gross craniofacial deformities and that *frzb* and Kinin-Kallikrein factors are greatly enriched in the EAD relative to the surrounding face (Dickinson and Sive, 2009). This prompted the question: does the EAD organize the surrounding face through secretion of Kinin-Kallikrein factors and Frzb? Further exploration has shown that the EAD directs cranial NC development and mouth formation through Kinin-Kallikrein signaling and secretion of Wnt inhibitors (Chapter 2; Dickinson and Sive, 2009; Jacox et al., 2014). Another midline craniofacial organizer, known as the Frontoectodermal Zone (FEZ), has been studied in chick and mouse. The FEZ influences facial development, after NC migration into the head, through secretion of Sonic Hedgehog (SHH) and Fibroblast Growth Factor 8 (FGF8) (Hu et al., 2003).

The concept of a developmental organizer was first presented by Spemann and Mangold in their famous 1924 study (Spemann and Mangold, 1924). They define an “organizing center” as a “previously determined part” that “determines the fate of still indifferent parts” by

"emanating determination effects" (Spemann and Mangold, 1924). Both the FEZ and EAD are determined early in facial development and secrete proteins required to determine the "still indifferent" NC. Without proper function of these organizers, craniofacial development is highly aberrant (Dickinson and Sive., 2009; Jacox et al., 2014; Hu et al., 2003; Hu et al., 2009b). Data in zebrafish suggest that a midline organizer is active in their facial development, suggesting broad vertebrate conservation (Eberhart et al., 2006; Kamel et al., 2013).

Following organizer function, EAD basement membrane is broken down, the mouth region invaginates, germ layers intercalate and the buccopharyngeal membrane perforates for mouth opening (Chapter 3; Dickinson and Sive., 2009). Tissue from the EAD contributes to the lining of the mouth, nostrils, and anterior pituitary (Figure 1.1) (Chapter 3; Couly and Le Douarin, 1985, 1987; Eagleson et al., 1995).

Detailed study of early craniofacial development has been conducted primarily in chick, zebrafish and *Xenopus* because of their external development. *Xenopus* is ideal for facial investigation due to its large size and optimal head conformation allowing easy facial visualization and access, unlike chick and zebrafish, which have imposing forebrains. At the start of our investigation, the anatomical record of anterior development was quite incomplete. However, our study of *Xenopus* EAD development from formation to mouth opening has exposed new phases and intricacies of craniofacial development (described in Chapters 1 and 3) whose regulation and conservation can be explored further in frog and other models. As a result, intricacies of oral development observed in *Xenopus* are novel, lacking counterpart in other models, and critical for enriching our knowledge of face formation.

However, phases of craniofacial development are widely conserved among amniotes and anurans, such that findings in frogs are likely broadly applicable (Dickinson and Sive, 2007;

Young et al., 2014). The faces of embryos exhibit the greatest degree of similarity during NC development and prominence fusion (Young et al., 2014). Additionally, steps observed in *Xenopus* development are consistent with chick, mammalian, and zebrafish mouth formation. Stomodeal invagination and ectoderm and endoderm intercalation are widely conserved processes in mouth opening (Hardin and Armstrong, 1997; Manni et al., 2005; Watanabe et al., 1984; Waterman, 1977; Waterman and Schoenwolf, 1980). Avian embryos demonstrate basement membrane dissolution preceding buccopharyngeal membrane perforation, like in frogs (Dickinson and Sive., 2009; Waterman and Balian, 1980; Waterman and Schoenwolf, 1980).

Additionally, broad conservation of craniofacial development and mouth formation is consistent with conservation of midline craniofacial organizers, though it is unknown whether a FEZ organizer exists in frog and fish or whether an EAD organizer operates in mouse and chick. Understanding the conservation, roles and regulation of these organizers will provide crucial insight to craniofacial development and the pathology of human craniofacial deformities.

Figure 1.1: Schematic of EAD development. Data is consistent with the anterior facial region contributing to olfactory placodes, the hypophyseal placode, and the oral epithelia of the mouth in mammals, chick, zebrafish and *Xenopus*. (Chapman et al., 2005; Couly and Le Douarin, 1985, 1987; Eagleson et al., 1995; Helms et al., 1997; Osumi-Yamashita et al.,1994; Schwind, 1928). Purple: Hypophyseal placode (stages 18-35), anterior pituitary (stage 40) and lining of upper mouth. Orange: Nasal placodes (stages 18-35) and nostril lining (stage 40). Blue: future lining of lower mouth. ANR, anterior neural ridge. AP, anterior pituitary. BA1, branchial arch 1. CG, cement gland. EAD, extreme anterior domain. FNP, frontonasal prominence. Hpf, hours post fertilization. No, nose. NT, neural tube. (Adapted from Chapter 3.)

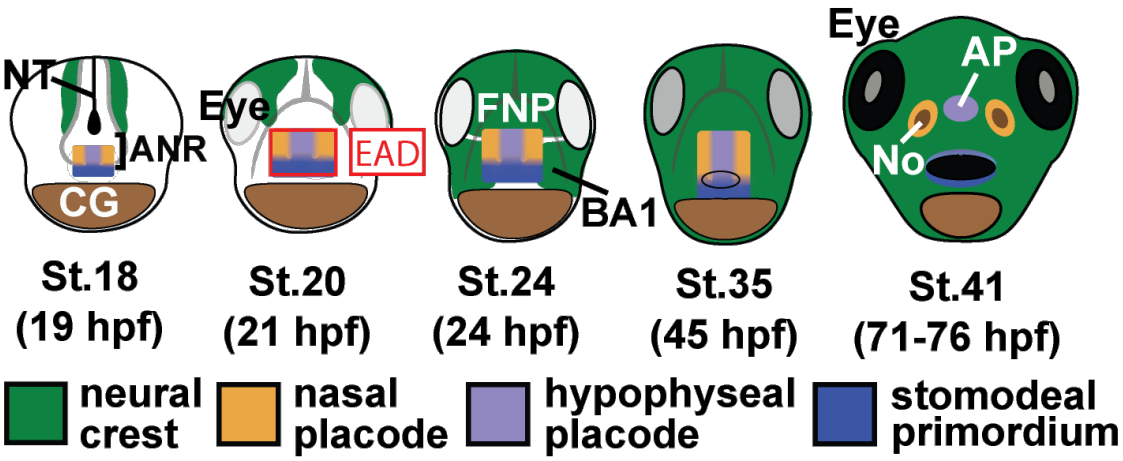
NT
ANR
CG
Eye
EAD
FNP
BA1
Eye
AP
No
St.18
(19 hpf)
St.20
(21 hpf)
St.24
(24 hpf)
St.35
(45 hpf)
St.41
(71-76 hpf)
neural crest
nasal placode
hypophyseal placode
stomodeal primordium

Figure 1.1

1.3 Face Formation and the Cranial Neural Crest

Much of the face derives from NC cells, a migratory, multipotent population. There are many thoughtful reviews detailing NC development (Theveneau and Mayor, 2011, 2012; Mayor and Theveneau, 2013), and the salient points are discussed here. NC is induced during neurulation at the border of the neural plate, where neuroepithelium interfaces with prospective epidermis (Mayor and Theveneau, 2013). Following induction, NC undergoes an epithelial-mesenchymal transition (EMT), allowing NC cells to separate from the neuroepithelium and ectoderm and begin migrating (Duband, 2010; Theveneau and Mayor, 2012). The most anterior, cephalic NC forms the frontonasal prominence (FNP), which contributes to the frontonasal skeleton (Cloutheir et al., 2010). The cephalic NC of the posterior midbrain and hindbrain segregate into paired pharyngeal or branchial arches, which migrate into the presumptive face and neck region (Gilbert, 2010; Minoux and Rijli, 2010). NC migration is governed by a number of mechanisms, including chemotaxis, co-attraction, contact inhibition of locomotion, chase-and-run and guidance through interaction with extracellular matrix, semaphorins, and Eph/Ephrin signals (Theveneau and Mayor, 2012; Mayor and Theveneau, 2013). These mechanisms govern interaction of NC cells with one another and their immediate surroundings. However, they do not provide a long-range signal to guide NC into the face (Hu and Helms, 1999; Jacox et al., 2014).

Following extensive migration, cranial NC cells differentiate into peripheral neurons and glia, cranial ganglia, melanocytes, osteoblasts, fibroblasts, adipocytes, odontoblasts and chondrocytes that produce the peripheral nervous system, pigment, bone, tendon, cartilage, teeth and connective tissue of the face, neck, eyes and ears (Dupin et al., 2006; Le Douarin and Kalcheim, 1999; Le Douarin et al., 2012; Theveneau and Mayor, 2011). NC cells migrate with intrinsic differences that influence their fates along the anteroposterior axis (Noden, 1983;

Trainor et al., 2002). Despite this pre-pattern, NC remains plastic, requiring inductive and guiding signals from surrounding tissue to migrate and develop (Couly et al., 2002; Crump et al., 2004; Hu et al., 2003; Le Douarin et al., 2004; Theveneau and Mayor, 2012).

Though there is literature on NC migratory mechanisms and patterning, we have an imperfect understanding of longer-range signals required to mediate NC migration, development and fate in the face. The EAD and FEZ organizers are critical participants in craniofacial development, releasing peptides that act distally to guide NC movement and development (Jacox et al., 2014; Hu and Helms, 1999). Exposing complex interactions between NC and facial organizers will enrich our knowledge of how NC migrates into the early face and gives rise to adult facial features.

1.4 Face Formation and the Extreme Anterior Domain (EAD)

The developing face includes a contribution from the Extreme Anterior Domain (EAD), an early, non-NC facial structure (Jacox et al. 2014). It consists of juxtaposed ectoderm and endoderm without intervening mesoderm and is highly conserved. An EAD is present in all vertebrates, and indeed in all deuterostomes (Dickinson and Sive, 2007). EAD ectoderm has been shown to arise from the anterior neural ridge (ANR) in *Xenopus* and chick, and undergoes complex morphogenetic changes en route to opening into the adult mouth and nostrils, and contributing to the anterior pituitary (Figure 1.1) (Chapter 3; Couly and Le Douarin, 1985, 1987).

1.4 a. Early EAD Development

Deep EAD ectoderm is enriched in β-catenin and expresses Wnt inhibitor, *frizzled-related protein-1* (*frzb-1*), and Kinin-Kallikrein peptidase, *carboxypeptidase n* (*cpn*) (Chapter 3; Dickinson and Sive, 2009; Jacox et al., 2014). EAD ectoderm is highly enriched in β-catenin, while adjacent ectoderm is not (Figure 1.2, stages 20-40, coronal, parasagittal and sagittal). *frzb-1* and *cpn* expression is restricted to earlier stages when the EAD is forming and cranial NC is migrating into the face (Figure 1.3, *frzb-1* expression: stages 17-28; *cpn* expression: stages 20-28) (Dickinson and Sive, 2009; Jacox et al., 2014). *frzb-1* is also expressed in the endoderm immediately below EAD ectoderm.

Figure 1.2: Sagittal and coronal anatomy of *Xenopus* face development between late neurula and swimming tadpole (stages 20-40), demonstrating convergent extension of midline ectoderm and basement membrane turnover. CG, cement gland. (Adapted from Chapter 3.).

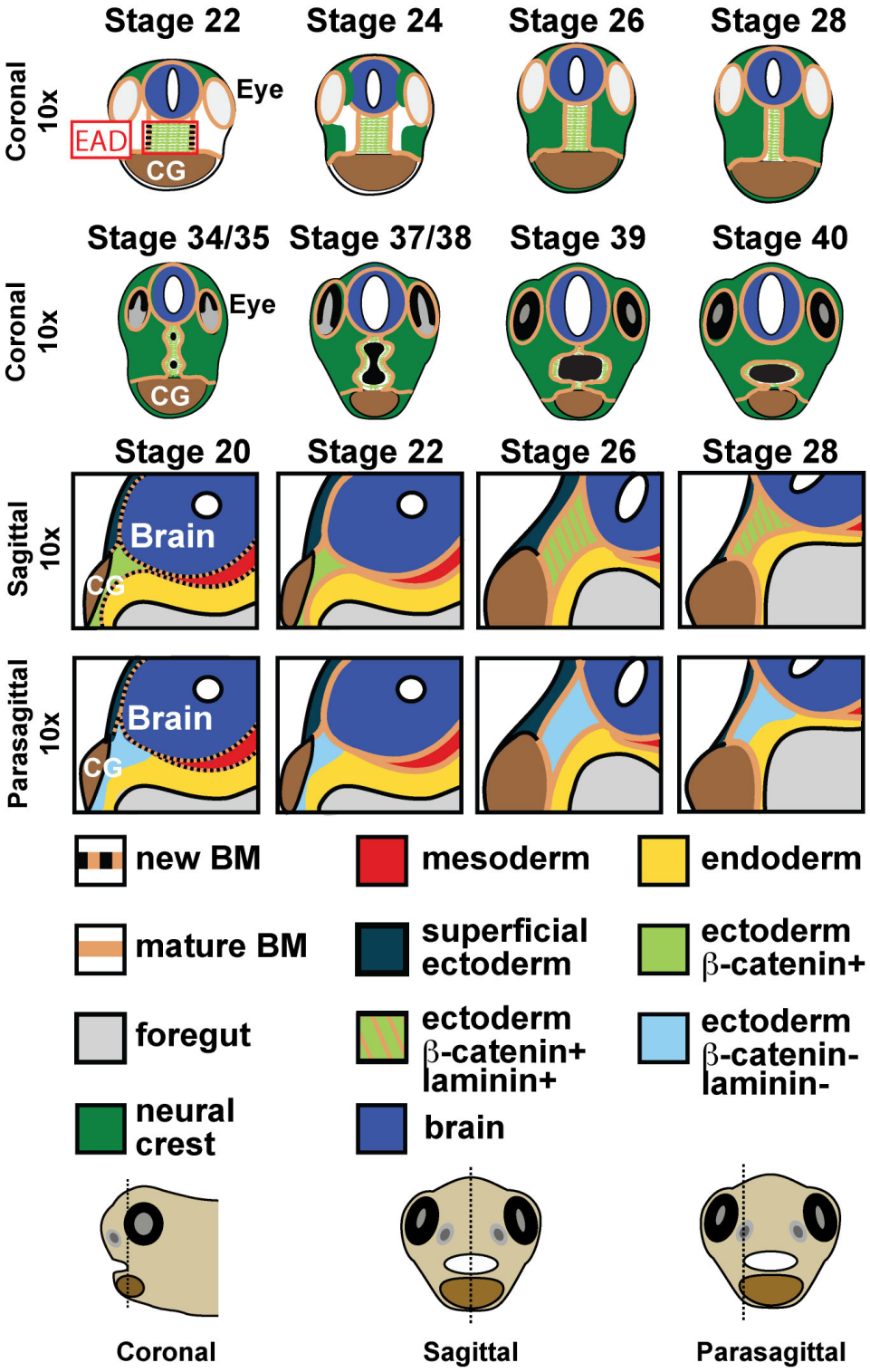
Stage 22
Stage 24
Stage 26
Stage 28
Coronal 10x
Eye
EAD
CG
Stage 34/35
Stage 37/38
Stage 39
Stage 40
Coronal 10x
Eye
CG
Stage 20
Stage 22
Stage 26
Stage 28
Sagittal 10x
Brain
CG
Parasagittal 10x
Brain
CG
new BM
mesoderm
endoderm
mature BM
superficial ectoderm
ectoderm β-catenin+
foregut
ectoderm β-catenin+ laminin+
ectoderm β-catenin- laminin-
neural crest
brain
Coronal
Sagittal
Parasagittal

Figure 1.2

Figure 1.3: Timeline of major events in *Xenopus laevis* craniofacial development. EAD formation is associated with expression of *pitx1c* and *pitx2* at early neurula (stage 13). AP, anterior pituitary. ANR, anterior neural ridge. BA1, branchial arch 1. BM, basement membrane. EAD, extreme anterior domain. NC, neural crest. (Chapter 3; Dickinson and Sive, 2006; Dickinson and Sive, 2007; Dickinson and Sive, 2009; Jacox et al., 2014; Nieuwkoop and Faber, 1994).

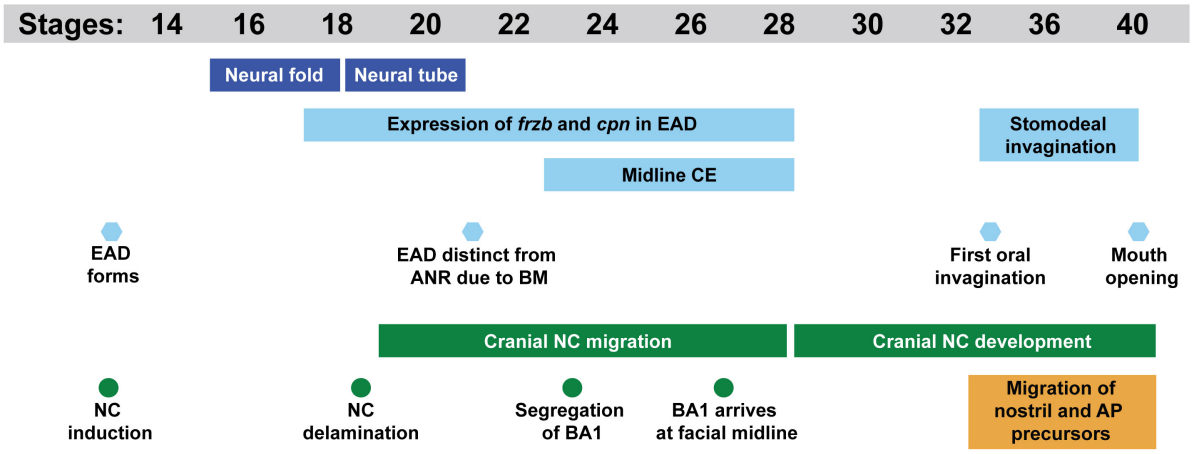
Stages: 14 16 18 20 22 24 26 28 30 32 36 40
Neural fold
Neural tube
Expression of frzb and cpn in EAD
Stomodeal invagination
Midline CE
EAD forms
EAD distinct from ANR due to BM
First oral invagination
Mouth opening
Cranial NC migration
Cranial NC development
NC induction
NC delamination
Segregation of BA1
BA1 arrives at facial midline
Migration of nostril and AP precursors

Figure 1.3

Initially, the EAD is triangular and continuous with the anterior neural tissue when viewed sagittally (Figure 1.2, stages 18-19 neurula, sagittal) (Chapter 3). A basement membrane (BM) is then established, segregating the EAD from neuroepithelium at late neurula (Figure 1.2, stages 20-22, sagittal and parasagittal). At early tail bud, two additional BMs form, separating ectoderm from endoderm and the inner and outer ectodermal layers (Figure 1.2, stage 22, sagittal). Parasagittally, only one BM appears between inner and outer ectodermal layers (Figure 1.2, stage 22, parasagittal). Our prior studies describe a single BM between ectoderm and endoderm in the sagittal plane, but use of improved microscopy and immunohistochemistry has led to identification of a second, more faint BM between outer and inner ectodermal layers (Chapter 3; Dickinson and Sive, 2009).

Coronally, EAD ectoderm begins as a short square of cells, enriched in membranous β-catenin and bounded laterally, anterio-posteriorly, deeply and superficially by BM (Figure 1.2, stage 22, sagittal, parasagittal and coronal); the EAD ectoderm is fully encased in Laminin when cranial NC migrates into the face (Figure 1.2, stages 23-24, coronal) (Chapter 3). At this time, midline ectoderm is expressing high levels of *frzb-1*, *crescent*, and *cpn* (Figure 1.3). Frzb-1 and Crescent are canonical Wnt inhibitors that regulate BM remodeling required for mouth opening. CPN cleaves the N-terminal Arginine from small peptides, including Braydkinin, a 9-amino acid protein required for cranial NC migration and cartilaginous skeleton formation (Dickinson and Sive, 2009; Jacox et al., 2014).

At tail bud stages, sagittal EAD ectoderm lengthens and widens, forming a large rectangle stretching from brain to cement gland (Figure 1.2, stages 22-26, sagittal) (Chapter 3). As previously reported, the well-defined BM of the sagittal EAD is eliminated, but prior to breakdown, it is accompanied by Laminin uniformly coating midline EAD cells, concomitant

with NC abutting EAD ectoderm (Figure 1.2, stages 26-27, coronal and sagittal) (Chapter 3; Dickinson and Sive, 2009). This Laminin coating is a novel observation and may act as a structural barrier for migrating NC as it approaches the facial midline and EAD bilaterally. Once NC has reached the facial midline at stage 28, Laminin and BM dissipate to form a patchy haze (Figures 1.2 and 1.4, stage 28, sagittal). Parasagittally, a thin perimeter of Laminin wraps around the deep ectoderm, separating it from the brain superiorly, cement gland inferiorly, outer ectoderm anteriorly, and endoderm posteriorly; it is likely that NC migrates into this ectodermal space bounded by BM (Figure 1.2, stage 26, parasagittal) (Chapter 3). By stage 28, the parasagittal Laminin separating ectoderm from endoderm disappears (Figure 1.2, stage 28, parasagittal). The BMs of the EAD are more complex than previously reported, and their roles and regulation are in need of further study.

As cranial NC migrates towards and arrives at the midline during tail bud stages, the EAD ectoderm undergoes significant lengthening in height and thinning in width, transitioning from a square of flat, elongated cells (6-8 cells across) to a tall column of rectangular cells arranged in two parallel rows (Fig. 1.2, stages 24-28, coronal) (Chapter 3). This morphogenetic process is consistent with convergent extension (CE), and its features and regulation is discussed in Chapter 3.

Figure 1.4: Mouth formation from the EAD in *Xenopus laevis*. At neurula stages (stage 17-22), *frzb-1*, *crescent*, and *cpn* are expressed in a subset of EAD cells. By tail bud stages (stage 27-28), basement membrane (bm) and Laminin is broken down and appears patchy. BM dissolution is followed by cell migration, cell death, invagination of the stomodeum, thinning of the stomodeal region to form the buccopharyngeal (BP) membrane, intercalation of germ layers in the BP membrane, and finally perforation. *frzb-1*, *crescent*, and *cpn* expressing cells are colored purple; *cpn* is only expressed in the EAD ectoderm while *frzb-1* and *crescent* are expressed in the ectoderm and superficial endoderm. Ectoderm, blue. Endoderm, yellow. BM is indicated by an orange line. Laminin is indicated by an orange haze. hpf, hours post fertilization. (Chapter 3; Dickinson and Sive, 2006; Dickinson and Sive, 2007; Dickinson and Sive, 2009; Jacox et al., 2014; Nieuwkoop and Faber, 1994).

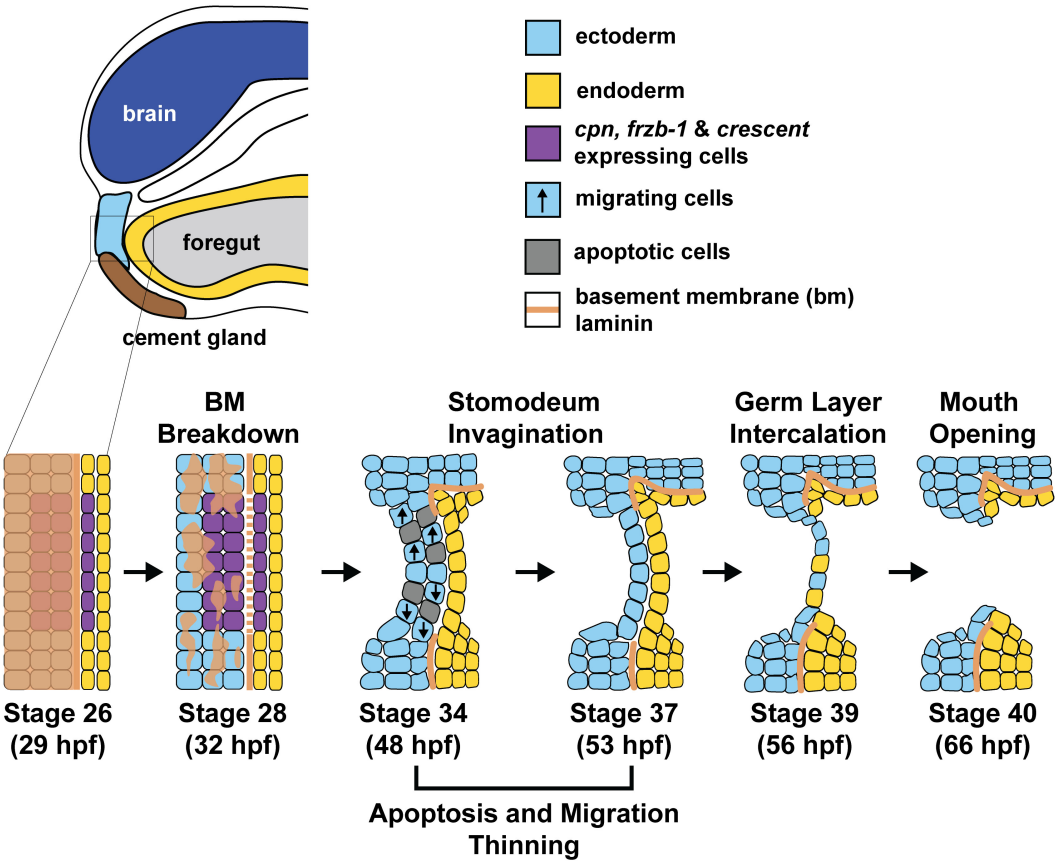
brain
foregut
cement gland
ectoderm
endoderm
cpn, frzb-1 & crescent expressing cells
migrating cells
apoptotic cells
basement membrane (bm) laminin
BM Breakdown
Stomodeum Invagination
Germ Layer Intercalation
Mouth Opening
Stage 26 (29 hpf)
Stage 28 (32 hpf)
Stage 34 (48 hpf)
Stage 37 (53 hpf)
Stage 39 (56 hpf)
Stage 40 (66 hpf)
Apoptosis and Migration Thinning

Figure 1.4

1.4 b. Late EAD Development

Following midline CE, EAD ectoderm segregates into precursors of nasal epithelia, the anterior pituitary and oral epithelia, which migrate, invaginate, and develop into their final structures (Figures 1.1 and 1.3, stages 33/34-40) (Chapter 3). EAD cells migrate out of the oral region (stages 32-40) and undergo a burst of apoptosis (stage 34/35) forming an enlarging stomodeal invagination (Figures 1.1, 1.3 and 1.4, stage 33/34) (Dickinson and Sive, 2006; Nieuwkoop and Faber, 1994). Coronally, the two rows of EAD ectodermal cells separate down the midline (Figure 1.2, stage 34/35) and form an oval oral orifice, surrounded by Laminin BM (Figure 1.2, stages 37-40, coronal) (Chapter 3). Sagittally, the ectoderm and endoderm layers intercalate to form a one cell thick, buccopharyngeal (BP) membrane that perforates to form the mouth opening (Figure 1.4, stage 40) (Dickinson and Sive, 2006). During these terminal stages of mouth opening, Hedgehog signaling regulates BM turnover, BP membrane perforation, and mouth size (Tabler et al., 2014).

While the stomodeum invaginates, tissue moves internally and posteriorly to contribute to the anterior pituitary, and nasal precursors migrate superiorly and laterally where they invaginate to form nostrils, consistent with placodal development in other models (Figures 1.1, 1.2 and 1.3, stages 33/34-40) (Chapter 3; Dickinson and Sive, 2007; Nieuwkoop and Faber, 1994; Park and Saint-Jeannet, 2010). The cranial NC is concomitantly differentiating into progenitors and forming facial structures. By the time of mouth opening (stage 40), the craniofacial cartilages and masticatory apparatus have formed and the tadpole will begin feeding thereafter (Chapter 3; Dickinson and Sive, 2006; Nieuwkoop and Faber, 1994.)

1.5 Phases of Mouth Development

The Sive group initially defined the primary mouth as the first opening to connect the gut cavity with the outside (Dickinson and Sive, 2006; Dickinson and Sive, 2007). The secondary or adult mouth was defined as the final oral structure consisting of teeth, tongue, palate and jaws that form from cranial NC and grow around the primary mouth (Dickinson and Sive, 2006).

More recently, we have understood that the division into primary and secondary development cannot be drawn. Cranial NC migrates into the face and arrives at the midline (stage 28) stages before the stomodeum begins invaginating to form the buccopharyngeal (BP) membrane (stage 33/34) (Jacox et al., 2014; Nieuwkoop and Faber, 1994). By the time the BP membrane perforates (stage 40), cranial NC has formed all facial rudiments. In mammals, a persistent BP membrane localizes to the back of the oral cavity, inserting inferiorly into the posterior tongue and superiorly in the soft palate (Ramachandran et al., 2010; Verma and Geller, 2009). This location does not indicate a chronology where the BP membrane perforates and then cranial NC gives rise to secondary mouth structures. Instead, the BP membrane perforates once cranial NC has migrated into the face and undergone much of its development, allowing the tadpole to feed (Nieuwkoop and Faber, 1994). As a result, we are retiring the use of a primary and secondary mouth nomenclature since it is not possible to temporally or spatially separate these stages of mouth development.

1.6 The *Xenopus* EAD Is a Craniofacial Organizer

Extirpation and grafting experiments revealed the organizing potential of the EAD during craniofacial development. Removal of EAD endoderm or EAD and neural ectoderm yields embryos with narrow, deformed faces and un-perforated, oddly shaped stomodea (Dickinson and Sive, 2006). However, embryos with extirpated EAD ectoderm develop normally (Dickinson and Sive, 2006). Based on our study of Kinin-Kallikrein signaling, EAD ectoderm is locally required for global craniofacial development, suggesting that either neural tissue can induce regeneration of EAD ectoderm or that EAD ectoderm has provided its NC and BM regulatory cues by the time of extirpation at tail bud, stage 24 (Dickinson and Sive, 2009; Jacox et al., 2014). At stage 24, cranial NC has segregated into BA1 and migrated into the face, and *frzb-1* and *crescent* are down-regulated in the EAD (Nieuwkoop and Faber, 1994; Dickinson and Sive, 2009). *frzb-1* and *crescent* likely inhibit Wnt-8. Wnt-8 overexpression in the EAD ectoderm during stages 25-28 mildly reduces mouth size while GOF between stages 17-24 causes gross craniofacial abnormalities with narrow faces, hypotelorism, and no mouth (Figure 1.1 and 1.3) (Dickinson and Sive, 2009). The data suggest that the EAD serves its inductive, organizing role between stages 20 and 24/25, similar to the avian facial organizer, the FEZ, which exercises its effect during a limited time window between stages HH20 and HH24 (Hu et al., 2003). It would be interesting to repeat the ectodermal extirpation and EAD grafting experiments with earlier surgeries to investigate these hypotheses. The gross abnormalities associated with extirpation show that the EAD is required for craniofacial development.

Grafting experiments clarified the importance of the EAD as an organizer. Grafting an ectopic EAD with surrounding tissues adjacent to the host EAD induces formation of a second mouth (Dickinson and Sive, 2006). When an EAD is grafted into host flank tissue, a second

mouth does not form. Explant assays corroborate these findings; an EAD alone does not produce a mouth but an EAD plus lateral NC and anterior neural tissue results in mouth formation. Therefore, the EAD is able to induce formation of a second oral opening when the necessary neighboring tissues are present. BA1 NC, pharyngeal endoderm, and anterior neural plate are likely required for mouth formation. This inductive capability qualifies the EAD as an organizing center, based on the criteria set forth in Spemann and Mangold's treatise (Spemann and Mangold, 1924).

Further study of the EAD has revealed two signaling pathways required for its organizing capacity: suppression of canonical Wnt signaling via Frzb-1 and Crescent and the Kinin-Kallikrein pathway. Local EAD loss of function (LOF) in *frzb-1* and *crescent* is associated with narrow, deformed faces, retained BMs, and no mouth or stomodeum (Dickinson and Sive, 2006). *frzb-1*, *crescent*, and *wnt8* GOF cause a similar abnormal facial phenotype except *frzb-1* GOF embryos have a markedly enlarged stomodeum (Dickinson and Sive, 2006). Though this earlier study did not look at NC development, craniofacial deformities resulting from local LOF suggest Wnt inhibitors are required for development of the surrounding face including cranial NC. Kinin-Kallikrein signaling is also required for cranial NC migration and formation of the cartilaginous skeleton and mouth, as will be discussed in chapter 2.

The EAD is an organizer of *Xenopus* craniofacial development. Localized EAD LOF in *frzb-1*, *crescent* and *cpn* are associated with global craniofacial deformities. The EAD organizes surrounding tissues via secreted proteins, *frzb-1*, *crescent* and *cpn,* which regulate NC migration and development, BM remodeling, and mouth size and opening.

1.7 The FEZ, an Amniote Organizer

Studies in mouse and chick suggest conservation of a midline organizer required for craniofacial development, known as the Frontonasal Ectodermal Zone (FEZ) (Figure 1.5). The boundary between *Fgf8* and *Shh* expression in the anterior ectoderm sets up the FEZ, an organizer that signals to NC to control jaw growth (Hu and Marcucio, 2009b) (Figure 1.5, Table 1.1). The FEZ signaling center spans the avian FNP, while mice have FEZ regions on their medial nasal processes (Figure 1.5). *Fgf8* is expressed in dorsal frontonasal prominence (FNP) ectoderm while *Shh* is expressed in stomodeal roof ectoderm adjacent to but not overlapping with *Fgf8* (Hamburger Hamilton (HH) stage 20) (Hamburger and Hamilton, 1951; Marcucio et al., 2005; Shigetani et al., 2000; Tucker et al., 1999). *Fgf8* expression in the FEZ domain is established prior to arrival of NC in the early face, like the *Xenopus* EAD (Hu et al., 2003; Marcucio et al., 2001). However, the FEZ organizer, with juxtaposed *Fgf8* and *Shh* expression, is not established until much later when NC has completed its migration into the face (Stage HH20 in chick; Stage E9.5 in mouse) (Hu and Marcucio, 2009b).

The FEZ patterns NC-derived mesenchyme of the frontonasal and mandibular processes, along with dorso-ventral and rostro-caudal patterning of the upper beak (Hu et al., 2003; Abzhanov et al., 2007). FEZ ectodermal grafts are uniquely capable of re-patterning FNP and BA1 NC and duplicating FNP and skeletal elements, at a late stage in craniofacial development (HH stage 20) (Hu et al., 2003). Like FEZ grafts, ectopic *Shh* and *Fgf8* expression induces outgrowth and chondrogenesis in the avian facial skeleton (Abzhanov and Tabin, 2004). Ectopic application of FGF8 protein alters target gene expression and re-patterns the mandibular arch and trigeminal nerve tracts (Shigetani et al., 2000).

Figure 1.5: Craniofacial organizers in *Xenopus*, chick, and mouse. *Xenopus* is shown at tail bud, stage 24, as cranial neural crest (NC) is migrating into the face, towards the midline. Chick is shown at HH stage 20 and mouse is shown at stage E10.5, after NC has migrated into the face and formed prominences. Pale green represents cranial neural crest (NC) that contributes to the frontonasal prominence (FNP). Dark green represents cranial NC that contributes to the branchial arches (BA) and medial nasal prominence (MNP). Tan is non-NC tissue. Red represents the EAD craniofacial organizer in *Xenopus*. Orange represents the FEZ craniofacial organizer in chick and mouse. BA1, branchial arch 1. BA2, branchial arch 2. BA3, branchial arch 3. CG, cement gland. EAD, extreme anterior domain. FEZ, frontonasal ectodermal zone. FNP, frontonasal process, also known as frontonasal prominence. LNP, lateral nasal process, also known as lateral nasal prominence. Mo, mouth. MN, mandibular process, also known as mandibular prominence. MNP, medial nasal process, also known as medial nasal prominence. MXP, maxillary process, also known as maxillary prominence. NP, nasal placode. (Chapter 3; Hamburger and Hamilton, 1951; Hu and Marcucio, 2009b).

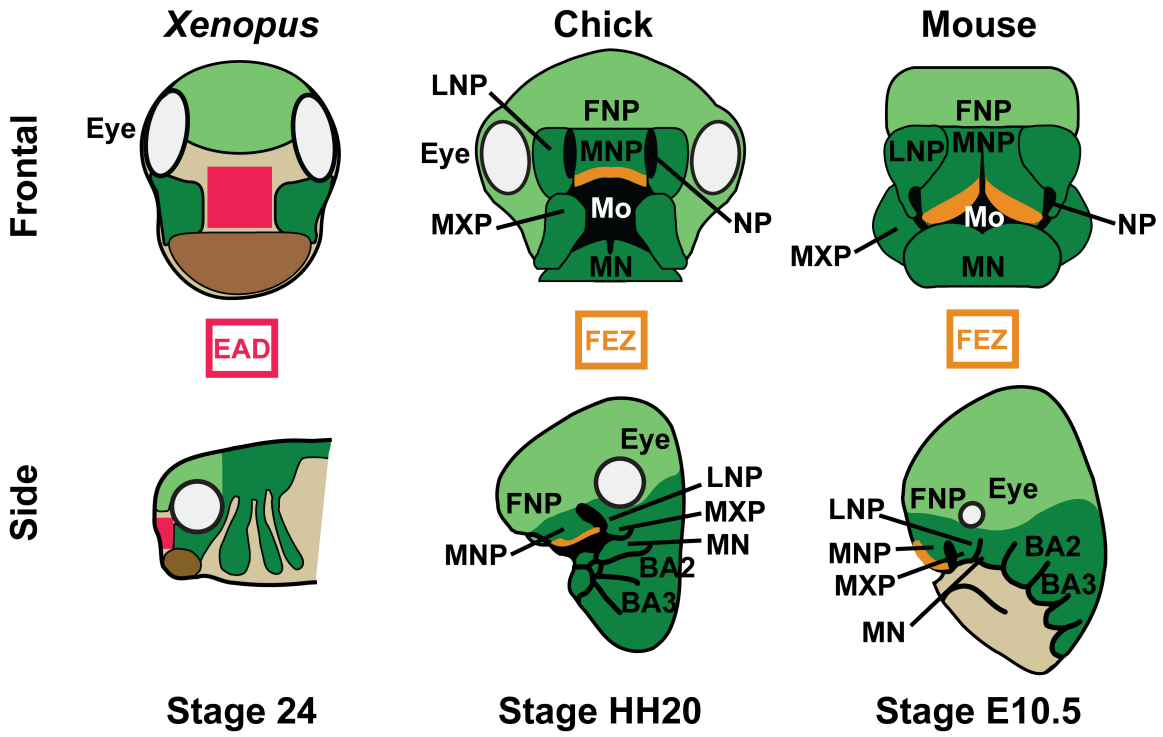
Xenopus
Chick
Mouse
Frontal
Side
Eye
LNP
FNP
MNP
Mo
MXP
NP
MN
EAD
FEZ
FEZ
BA2
BA3
Stage 24
Stage HH20
Stage E10.5

Figure 1.5

Table 1.1: FEZ craniofacial organizer secreted proteins and their roles, expression domains, and LOF phenotypes. Secreted proteins of the EAD include the Wnt inhibitor Frzb-1 and Kinin-Kallikrein factors, Carboxypeptidase-N (CPN), and Kininogen, discussed in Chapter 2. BA, branchial arch. EAD, extreme anterior domain. FEZ, frontonasal ectodermal zone. FGF8, Fibroblast Growth Factor-8. FNP, frontonasal prominence, also known as the frontonasal process. HH, Hamburger Hamilton chick stages. LOF, loss of function. MXP, maxillary process, also known as the maxillary prominence. NC, neural crest. SHH, Sonic Hedgehog.

Table 1.1: FEZ craniofacial organizer secreted proteins.

Secreted Protein	FGF8	Sonic hedgehog
Roles in Craniofacial Development	Chick: Survival, proliferation, migration directionality and patterning of BA1, FNP and trigeminal nerves (Abzhanov et al., 2007; Creuzet et al., 2004; Shigetani et al., 2000) Mice: BA1 cell survival and development into cranial bones (Abu-issa et al., 2002; Trumpp et al., 1999)	Chick, Human, Mouse, Zebrafish: Midline development of brain and face Proper growth and fusion of facial prominences Establishing medio-lateral facial dimension Formation of facial bones/cartilages (Abzhanov et al., 2007; Belloni et al., 1996; Chen et al., 2001; Chiang et al., 1996; Eberhart et al., 2006; Hu et al., 2003; Hu et al., 2015; Hu and Helms, 1999; Hu and Marcucio, 2009b; Jeong et al., 2004; Odent et al., 1999; Wada et al., 2005)
Human LOF phenotypes	hypogonadotropic hypogonadism, olfactory abnormalities (Kallmann syndrome), renal agenesis, cleft lip and/or palate, tooth agenesis, and bimanual synkinesis (Trarbach et al., 2010)	holoprosencephaly, microcephaly, cyclopia, ocular hypotelorism, arhinia (congenital absence of a nose), proboscis nose (a primitive, abnormal nasal structure), missing nasal bones or nasal defects, upper lip and palate clefting, premaxillary hypoplasia, a single central incisor, sensorineural hearing loss, pituitary hypoplasia and absence of olfactory neurons or corpus callosum (Belloni et al., 1996; Chiang et al., 1996; Roessler et al., 1996)
Model organisms	Chick Mouse	Chick Mouse Zebrafish (Human)
Anterior expression during craniofacial development	Chick: HH9-20 (all stages examined): epithelia of nasal pits and maxillary processes (Helms et al., 1997) HH11 (13 somite stage (ss)): ventral ectoderm over future presumptive BA1 and maxillomandibular region, pharyngeal ectoderm (Creuzet et al., 2004; Shigetani et al., 2000) HH12-18: ectoderm over mandibular processes (Shigetani et al., 2000) HH13-HH15: oral ectoderm (Creuzet et al., 2004) HH14-HH15 (24ss): superficial ectoderm of BA1-4, prosencephalon neuroepithelium and adjacent superficial ectoderm, neuroepithelium of isthmus (Creuzet et al., 2004) HH18: ectoderm over maxillary processes (Shigetani et al., 2000) HH20: expression in the FEZ (ectoderm of FNP overlying NC, stretching across M-L width, opposing SHH domain), dorsal FNP and ventral MNP (Hu et al., 2003; Hu and Marcucio, 2009b) HH22: nasal pit epithelium (Marcucio et al., 2005) Mouse: E8.5-10.5: superficial ectoderm of head, BA1, oral ectoderm (Abu-issa et al., 2002; Trumpp et al., 1999; Tucker et al., 1999)	Chick: HH7-8: midline of neural plate (Marcucio et al., 2005) HH9: ventral prosencephalon, pharyngeal endoderm, prechordal plate (Marcucio et al., 2005) HH12: buccopharyngeal membrane including ectoderm and endoderm (Marcucio et al., 2005) HH17: diencephalon and telencephalon (Marcucio et al., 2005), expression first seen in endoderm of pharyngeal pouches 1-3 and at anterior attachment of ruptured buccopharygeal membrane attachment site between Rathke's and Sessel's pouches (Helms et al., 1997) HH18: stomodeal roof ectoderm which contributes to future olfactory and nasal epithelium (Helms et al., 1997) HH18-20: posterior border of hyoid arch, pharyngeal endoderm, FNP and MXP ectoderm (Helms et al., 1997) HH20 expression in the FEZ (ectoderm of FNP overlying NC, stretching across M-L width, opposing FGF8 domain) (Hu et al., 2003; Hu and Marcucio, 2009b; Marcucio et al., 2005) HH23: roof of stomodeum and inferior border of BA2 (Helms et al., 1997) HH24-29: midline of FNP epithelia (Helms et al., 1997)

Table 1.1 (Continued): FEZ craniofacial organizer secreted proteins.

Secreted Protein	FGF8	Sonic hedgehog
Anterior expression during craniofacial development (Continued)	E9.5: expression detected in forebrain and surface ectoderm of medial and lateral domains (Abu-issa et al., 2002; Trumpp et al., 1999; Tucker et al., 1999) E10-10.5: expression in the FEZ (ectoderm of median nasal processes overlying NC, stretching across M-L width opposing SHH domains) (Hu and Marcucio, 2009b)	HH29: midline of stomodeum, distal tip of tongue, FNP and MXP (Helms et al., 1997) HH31: presumptive dental lamina of mandible (Helms et al., 1997) Human: superficial ectoderm of median nasal processes (Hu and Marcucio, 2009b; Odent et al., 1999) Mouse: E9.5-10.5: expression in ventral forebrain epithelium, oral ectoderm and pharyngeal endoderm (Jeong et al., 2004; Hu and Marcucio, 2009b) E10-10.5: expression in the bilateral FEZ domains (superficial ectoderm of median nasal processes overlying NC, opposing FGF8 domain) (Hu and Marcucio, 2009b) E12.5: expressed in the ventral nasal pit and tongue epithelium (Jeong et al., 2004) Zebrafish: 14hpf-42hpf: oral ectoderm, ventral neural tube (Eberhart et al., 2006; Wada et al., 2005)
Oral Ectodermal Expression	Chick: HH10: midline superficial ectoderm HH13-HH15: oral ectoderm (Creuzet et al., 2004) Mouse: E8.5-E10.5: oral ectoderm (Abu-issa et al., 2002; Trumpp et al., 1999; Tucker et al., 1999)	Chick: HH12-18: buccopharyngeal membrane (Helms et al., 1997; Marcucio et al., 2005) HH18-29: stomodeal roof (Helms et al., 1997; Marcucio et al., 2005) Mouse: E9.5-10.5: oral ectoderm (Jeong et al., 2004; Marcucio et al., 2009) Zebrafish: 14hpf-42hpf: oral ectoderm (Eberhart et al., 2006; Wada et al., 2005)

1.7 a. Contributions of FGF8 to the FEZ Organizer

Prior to development of the FEZ, the avian anterior neural ridge (ANR) is a signaling center for the brain and NC. The ANR releases FGF8 needed for subsequent NC development, survival, proliferation and chemotaxis (Creuzet et al., 2004; Sato et al., 2011; Trumpp et al., 1999). Before NC migration into the face (at chick HH10 or mouse E10), FGF8 is expressed in midline, ventral ectoderm, near the future stomodeum in chick and mouse (Shigetani et al., 2000; Tucker et al., 1999). The FEZ is established with juxtaposed *Fgf8* and *Shh* expression in the ectoderm above the mouth, before outgrowth of the FNP at HH stage 20 (Figure 1.5, Table 1.1) (Hu et al., 2003). *Fgf8* and *Shh* expression domains reciprocally inhibit each other (Abzhanov et al., 2007). *Fgf8* overexpression in head ectoderm results in expanded head size, deformation and truncation of the FNP, and disappearance of the egg tooth, a landmark of distal FNP polarity (Abzhanov et al., 2007). *Fgf8* LOF via RNAi is associated with a decrease in FNP width, a reduced beak length, and elimination of the egg tooth. Proper FGF8 production is a prerequisite for normal craniofacial development, and likely influences NC proliferation and dorsal specification.

In mouse, *Fgf8* is expressed in oral ectoderm and superficial ectoderm of BA1 between stages E8.5-10.5 (Table 1.1) (Trumpp et al., 1999; Tucker et al., 1999). Loss of *Fgf8* function by Cre-Lox recombinase is associated with significant apoptosis in BA1; embryos are born with gross craniofacial deformities, lacking all proximal BA1-derived bone, nerve and cartilage (Abu-issa et al., 2002; Trumpp et al., 1999). Interestingly, *Fgf8* LOF embryos also have an un-perforated buccopharyngeal membrane and die shortly after birth from asphyxiation due to their craniofacial and hyoid abnormalities. Humans with mutations in FGF8 also have a range of phenotypes, which include hypogonadotropic hypogonadism, olfactory abnormalities (Kallmann

Syndrome), bimanual synkinesis, renal agenesis, cleft lip and/or palate and selective tooth agenesis, suggesting that the role of FGF8 in craniofacial and nerve development is conserved (Table 1.1) (Trarbach et al., 2010).

1.7 b. Contributions of SHH Signaling to the FEZ Organizer

FGF8 works in concert with Hedgehog signaling to pattern the early face, as both are components of the FEZ. *Shh* is expressed as part of the avian FEZ in the ectoderm stomodeal roof at HH stage 20, and remains expressed in the frontonasal and maxillary processes (FNP and MXP) through HH stage 25 (Figure 1.5, Table 1.1) (Abzhanov et al., 2007; Hu and Helms, 1999; Marcucio et al., 2005). The FNP and MXP give rise to the upper beak, primary palate, secondary palate and side of the face in chick (Hu and Helms, 1999). In mouse, *Shh* is also expressed in the stomodeal ectoderm and FEZ, but the murine FEZ and associated *Shh* domains are localized to the left and right median nasal processes (Figure 1.5, Table 1.1) (Hu and Marcucio, 2009b). Human embryos display a similar bilateral expression pattern of *SHH* (Hu and Marcucio, 2009b; Odent et al., 1999). The juxtaposed expression of *Shh* and *Fgf8* in the FEZ is relatively brief, lasting from HH stage 20-22 in chick and E9.5-10.5 in mouse (Hu and Helms, 1999; Hu et al., 2015). Once the *Fgf8* and *Shh* boundary is established in the FEZ, *Fgf8* is downregulated and restricted to nasal pit epithelia (Marcucio et al., 2005).

SHH is critical for craniofacial and skeletal development in mammals; mutations in human and mouse disturb mediolateral patterning of the neural plate, producing embryos with holoprosencephaly, cyclopia, and arhinia or a primitive nasal structure known as a proboscis (Table 1.1) (Belloni et al., 1996; Chiang et al., 1996; Roessler et al., 1996). Milder human phenotypes are associated with brain and facial abnormalities, including ocular hypotelorism,

microcephaly, upper lip clefting, nasal defects, premaxillary hypoplasia, a single central incisor, sensorineural hearing loss, pituitary hypoplasia, and absence of olfactory neurons or the corpus callosum (Belloni et al., 1996; Odent et al., 1999; Roessler et al., 1996). Mice mutant in *Shh* or *Smoothened* (*Smo)*, the SHH receptor, lack nearly all craniofacial bones, though the BAs appear to form and initiate migration normally (Chiang et al., 1996; Jeong et al., 2004). *Smo* mutants demonstrate increased BA1 apoptosis and diminished proliferation producing facial truncation by E11.5 (Jeong et al., 2004). *Shh* mutants also inappropriately retain the BP membrane past E9 (Tabler et al., 2014). SHH is critical for facial development in mammals.

Mammalian *Shh* mutants have early, profound defects in axial mesoderm, precluding detailed study of Hedgehog signaling in later development (Jeong et al., 2004). As a result, researchers have focused on chick and zebrafish. Transient loss of *Shh* causes collapse of the facial midline and reduced NC proliferation in chick. Lack of midline NC results in deficient FNP and MXP outgrowth, primary palatal clefting, and hypotelorism (Abzhanov et al., 2007; Hu and Helms, 1999; Hu et al., 2003; Hu et al., 2015). Egg teeth also fail to form (Abzhanov et al., 2007). Ectopic SHH stimulates cell proliferation leading to growth of ectopic upper beak-like structures, extra egg teeth, hypertelorism and medial-lateral widening of the FNP, upper beak, face and brain (Hu and Helms, 1999; Hu et al., 2003; Abzhanov et al., 2007). This medial-lateral enlargement prevents palatal shelves from fusing, resulting in a secondary palatal cleft analogous to mammalian cleft palate, and the FNP fails to fuse with maxillary and lateral prominences causing nasal clefting (HH stage 31) (Abzhanov et al., 2007; Hu et al., 2015). SHH signaling balances apoptosis and proliferation in the cranial NC needed for prominence growth and fusion (Kurosaka et al., 2014). *Shh* expression in the FEZ patterns the mediolateral axis of the face, and

perturbations affect underlying NC, producing a range of craniofacial malformations analogous to mammalian congenital defects.

FEZ *Shh* expression in chick is regulated by SHH and BMP signaling within facial ectoderm. To induce *Shh* expression, there must be a SHH signal from the forebrain and a BMP signal from within the FNP and NC (Foppiano et al., 2007; Hu and Marcucio, 2009a; Marcucio et al., 2005). SHH and BMP then promote expansion of *Shh* expression from the FNP ectoderm at HH stage 20 to the epithelium of the nasal pits, maxillary process and FNP globular processes by HH stage 22 (Foppiano et al., 2007; Hu and Marcucio, 2009b; Hu et al., 2015). Subsequently, the FEZ regulates BMP expression in adjacent NC mesenchyme, including *Bmp-2*, *Bmp-4* and *Bmp-7* (Hu and Marcucio, 2009b). BMP signaling has been implicated in species-specific patterning of the upper jaw (BMP-2, BMP-4) and establishment of growth zones in upper jaw mesenchyme (BMP-4) (Abzhanov et al., 2004; Wu et al., 2006). The FEZ acts upstream of signaling pathways regulating jaw development, including the BMP pathway.

1.7 c. Comparison of the FEZ and EAD Organizers with the Zebrafish Stomodeam

In chick, a SHH signal from the forebrain induces *Shh* expression in the FEZ, which acts as an organizer of craniofacial development (Hu and Marcucio, 2009a; Marcucio et al., 2005). Zebrafish appear to have a similar signaling mechanism, whereby stomodeal ectoderm receives a Hh signal from the ventral neural keel at the end of gastrulation (10hpf). This causes a change in stomodeal ectoderm promoting BA1 cranial NC condensation on the stomodeal roof (18-20hpf) (Eberhart et al., 2006). *Smo* LOF embryos have a marked reduction in anterior cranial cartilages, despite normal cranial NC migration and survival, due to failed NC condensation (Chen et al., 2001; Eberhart et al., 2006). *Sonic you* (*syu*) mutant fish, which have a disrupted *shh* gene,

recapitulate features of other *Shh* LOF organisms with profound medio-lateral patterning defects (Eberhart et al., 2006). Embryos lack anterior cartilage and demonstrate trabecular midline fusions, palatal clefting and cyclopia. SHH GOF imparts mediolateral broadening and increased chondrogenesis, akin to ectopic SHH in chick. SHH release from the ventral neural tube directs trabecular midline morphogenesis of cranial NC, while SHH from oral ectoderm promotes subsequent chondrogenesis (Wada et al., 2005).

Akin to the *Xenopus* EAD, zebrafish express *frzb* in the developing mouth (55hpf), but at a later stage than in frogs; *frzb* is expressed in chondrocytes of the anterior palate, derived from the proximal first and second BAs (Kamel et al., 2013). LOF in *frzb* is associated with smaller craniofacial structures and an absence of the lower jaw, ceratobranchial cartilages and anterior palatal segment, as it is required for convergence and extension of palatal elements and convergence of mandibular prominences (Kamel et al., 2013). As will be discussed in chapter 2, Kinin-Kallikrein LOF in zebrafish causes failure of NC condensation, cranial cartilage formation, and mouth opening, reminiscent of *Xenopus* LOF (Jacox et al., 2014). Peri-oral expression of the Wnt inhibitor Frzb and Kinin-Kallikrein factors is required for craniofacial development in both *Xenopus* and zebrafish (Dickinson and Sive, 2009; Jacox et al., 2014; Kamel et al., 2013).

Though a zebrafish FEZ or EAD has not been described, we hypothesize that the stomodeal region promoting mouth opening, BA1 condensation, chondrogenesis and prominence convergence is an equivalent midline organizing center in fish. Zebrafish demonstrate *fgf8* expression in the lateral stomodeum and *shh* expression in the medial stomodeum, directly adjacent and without overlap, akin to the avian and murine FEZ (Eberhart et al., 2006). This region of oral ectoderm is required for formation of the anterior craniofacial skeleton, like the

murine and avian FEZ (Eberhart et al., 2006). Peri-oral expression of *frzb* and Kinin-Kalikrein factors are required for mouth and neural crest development in zebrafish, similar to *Xenopus.* (Jacox et al., 2014; Kamel et al., 2013). The zebrafish stomodeal region serves analogous functions to the FEZ and EAD, indicating it should also be considered a midline organizing center. Findings in zebrafish corroborate data in mice, *Xenopus*, and chick that midline organizing domains are a conserved feature of vertebrate craniofacial development, acting through Hedgehog, FGF, Wnt inhibitors, and Kinin-Kallikrein signaling to pattern the early face.

1.8 Relationship of the EAD and FEZ

The EAD and FEZ share features consistent with organizers. However, they are distinct midline organizers active at different times in craniofacial development and studied in separate species. The EAD is a midline craniofacial organizer identified in *Xenopus*, with activity between late neurula (stages 20) and mid tail bud (stage 24/25), when cranial NC migrates away from the neural plate, forms into distinct branchial arches and moves into the face (Jacox et al., 2014). The FEZ is a facial organizer studied in mice and chick, acting at later stages (Chick: HH20-HH22, Mouse: E9.5-10.5) after cranial NC migration, during facial prominence development (Hu et al., 2003; Hu and Marcucio, 2009b; Hu et al., 2015). The FEZ encompasses ectodermal cells, overlying NC of the frontonasal prominence in chick and medial nasal prominences in mouse, expressing juxtaposed *Shh* and *Fgf8* (Hu et al., 2003; Hu and Marcucio, 2009b). Though a portion of the EAD is characterized by expression of *frzb* and *cpn*, the EAD is defined structurally, as the region of ectoderm juxtaposed with endoderm that gives rise to the presumptive mouth (Jacox et al., 2014). The EAD and FEZ are distinct midline craniofacial organizers, identified in separate species, acting at different points in facial development, and defined in separate ways.

All vertebrate faces have an EAD, with juxtaposed ectoderm and endoderm, but it is unknown whether the EAD serves organizer functions in species outside of *Xenopus* (Dickinson and Sive, 2006; Dickinson and Sive, 2007; Jacox et al., 2014). Similarly, all vertebrates have ectoderm overlying their cranial NC prominences, but it is unclear whether the FEZ region secretes SHH and FGF8 to pattern facial development in species beside mouse, chick and possibly zebrafish. One hypothesis is that vertebrates begin facial development with a conserved EAD organizer active during cranial NC migration, and later generate a FEZ organizer signaling

for prominence development and chondrogenesis. Future inquiry into organizer conservation and development is necessary to address these hypotheses.

1.9 Endodermal Contributions to Facial Organizers

Our discussion has focused on ectodermal tissue in the FEZ and EAD, but endoderm is influential in neurocranial morphogenesis. Branchial arch 1 NC is an "equivalence group" in that a small portion of cells can regenerate the entire arch and facial skeleton, suggesting NC cells are not committed to particular facial bones (Couly et al., 2002). Anterior foregut and pharyngeal endoderm act as a NC specification map, directing overlying NC to their facial fates (Benouaiche et al., 2008; Couly et al., 2002; Ruhin et al., 2003). Data in zebrafish mutants corroborate the findings in chick suggesting broad conservation of an endodermal topographic map for NC (David et al., 2002; Piotrowski and Nusslein-Volhard, 2000).

The anterior-most foregut, known as stripe 1 or endoderm zone 1 (EZ-1), is the endoderm of the facial primoridum, lying deep to the ectoderm of the EAD. EZ-1 directs overlying NC to form mesethmoid cartilage, the source of upper beak cartilage in chick and nasal septum and vomer bones in humans (Benouaiche et al., 2008). Ablation of EZ-1 is associated with agenesis or reduction of the nasal capsule, nasal septum, and upper beak (Benouaiche et al., 2008; Couly et al., 2002). EZ-1 degenerates after forming Sessel's pouch, but expresses *Shh* prior to its atrophy (Couly et al., 2002). Early *Shh* expression is limited to EZ-1 (5ss), and is necessary and sufficient for development of the nasal capsule into mesethmoid cartilage. Grafting of EZ-1 and SHH beads induce ectopic *Gli1* expression, a SHH target, and mesethmoid cartilages (Benouaiche et al., 2008). Extirpation of EZ-1 tissue in *Xenopus* and the salamander *Amblystoma punctatum* prevents nostril and mouth formation; a detailed analysis of missing cartilages was not completed in these studies, but the phenotypes suggest EZ-1 may serve a conserved role in these species (Adams, 1931; Dickinson and Sive, 2006). Stomodeal endoderm, EZ-1, is a

signaling center required for nasal development, and is part of the NC specification map provided by the pharyngeal endoderm.

EZs 2-6 are caudal to the early face, but are required for patterning *Hox*-negative (BA1) and *Hox*-positive (BA2-6) arches (Benouaiche et al., 2008; Couly et al., 2002; Ruhin et al., 2003). EZs 2-4 are necessary for morphogenesis of bones derived from the maxillary and mandibular processes of BA1 (Couly et al., 2002) and EZs 5-6 are required for hyoid bone development from BA2-4 (Ruhin et al., 2003). *Shh* expression in anterior pharyngeal and BP membrane endoderm is required to induce and maintain *fgf8* expression in adjacent oral ectoderm and presumptive first arch ectoderm (HH stages 8-14) (Haworth et al., 2004; Haworth et al., 2007). *Shh* and *Fgf8* expression in the perioral region and FEZ is crucial for NC patterning and craniofacial development, as discussed previously.

1.10 The EAD and FEZ are Organizers of Perioral Development

Spemann and Mangold define an "organization center" as a "previously determined part" of the embryo that "determines the fate of still indifferent parts" by "emanating determination effects of a certain quantity in certain directions" (Spemann and Mangold, 1924).

In sum, the EAD and FEZ have multiple characteristics of an organizer. They are determined early, prior to NC development. These domains secrete proteins, including SHH, FGF8, Frzb-1, and CPN, required for determination and development of "still indifferent" NC mesenchyme. Organizer-localized LOF and GOF in SHH, FGF8, Frzb-1 and CPN perturb development of surrounding tissues, demonstrating that the EAD and FEZ "emanate determination effects." Duplicating EAD plus neighboring tissue in *Xenopus* and FEZ tissue in chick results in duplication of mouth formation and skeletal elements, respectively, akin to the capacity of the blastopore lip to induce duplicate body axes.

The EAD and FEZ are craniofacial organizers identified in *Xenopus laevis*, chick and mouse. The phases of craniofacial development are conserved among amniotes and anurans, suggesting that vertebrates possess midline craniofacial organizing centers (Dickinson and Sive, 2007; Young et al., 2014). Further study is needed to investigate whether a midline organizer domain exists in primates and if perturbation of organizer signaling underlies human craniofacial malformations.

1.11 Dissertation Overview

Prior work by Dickinson and Sive, 2009 suggests that the EAD has organizer capacity, as localized *frzb* LOF was associated with marked craniofacial abnormalities. However, our knowledge of EAD organizer function and development was very limited. As a result, I began my graduate studies posing the following questions. Is the EAD a craniofacial organizer? Does the EAD influence cranial NC migration and mouth development via Kinin-Kallikrein signaling? Does cranial NC reciprocally signal with the EAD to control midline morphogenesis? In the following chapters, I address these queries. I present data that the EAD is a discrete organizer region that influences NC development through Kinin-Kallikrein factors and later forms the mouth. I then present an investigation of reciprocal signaling between the EAD and NC, responsible for stimulating a morphogenetic process consistent with convergent extension.

In Chapter 2, I discuss our study of Kinin-Kallikrein signaling in the EAD, where we identify members of the pathway as novel craniofacial regulators and demonstrate the organizing capacity of the EAD to influence cranial NC migration and development. A parallel study in zebrafish indicates that the stomodeal region utilizes Kinin-Kallikrein signaling and is required for condensation of cranial NC to form anterior cartilages.

In Chapter 3, I present a morphogenetic study of mouth formation in *Xenopus laevis* that reveals a new phase reminiscent of convergent extension. The study indicates that Wnt11 ligand released by the NC is necessary and sufficient to bind Frzl7 receptors on EAD cells to initiate convergent extension.

In Chapter 4, I describe the experimental technique of facial transplants in *Xenopus* embryos. These transplants can provide localized LOF or GOF in EAD tissue.

In Chapter 5, I conclude by presenting future directions in craniofacial developmental research. I pose questions and hypotheses derived from my studies and literature review, and propose some experimental approaches to address them. I finish by emphasizing the importance and promise of craniofacial research for biologists and clinicians alike.

Chapter 2

The Extreme Anterior Domain Is an Essential Craniofacial Organizer Acting through Kinin-Kallikrein Signaling

Author Contributions: L.J. designed and conducted all bead, extirpation, transplant, migration LOF and rescue assays (Figures 2.7, 2.9S–2.9T', 2.11, and 2.12), NO and urea quantification assays (Figures 2.9Y–2.9c, and 2.11I–2.11J), and in situ hybridization experiments (Figures 2.5Q–2.5g, 2.7J–2.7L, and 2.11G–2.11H'). L.J. wrote and revised the manuscript drafts. R.S. designed and tested morpholinos, executed LOF rescues with cognate RNA and SNAP, and conducted immunohistochemistry and NO staining (Figures 2.5A–2.5D', 2.5I–2.5P, 2.9A–2.9L', 2.9Q–2.9R', and 2.9U–2.9X), except for Ph3 and TUNEL experiments, conducted by L.J. (Figures 2.5h–2.5l). R.S. contributed in situ hybridization data (Figures 2.9M–2.9P' and 2.5E–2.5H''') and obtained or cloned all plasmids. R.S. and L.J. assembled and modified figures and contributed in situ hybridization data shown in Figure 2.2. J.C. designed and conducted all experiments in zebrafish (Figures 2.13 and 2.14) and contributed to manuscript preparation. A.R. contributed in situ hybridization data (Figures 2.5Y–2.5Z and 2.5a–2.5g). A.D. identified Cpn and Kininogen in the EAD and performed initial experiments. H.S. directed and supervised the study and assisted in writing and revising the manuscript.

Publication: Jacox, L.*, Sindelka, R.*, Chen, J., Rothman, A., Dickinson, A., & Sive, H. (2014). The extreme anterior domain is an essential craniofacial organizer acting through Kinin Kallikrein signaling. *Cell Rep, 8*(2), 596-609. doi: 10.1016/j.celrep.2014.06.026

(* equally-contributing first authors)

This chapter has been kept largely unchanged from its published form, with the exception of minor changes in figure and section order and number. To help orient the reader to the figures in this chapter and associated publication, the numbering of figures is summarized in Table 2.1

Table 2.1: Table associating Chapter 2 figures with figures of Jacox et al., 2014.

Chapter 2 Figures	Jacox et al., 2014 Figures
2.1	Graphical Abstract
2.2	Figure 1
2.3	Supplementary Figure 1
2.4	Supplementary Figure 2
2.5	Figure 2
2.6	Supplementary Figure 3
2.7	Figure 3
2.8	Supplementary Figure 4
2.9	Figure 4
2.10	Supplementary Figure 5
2.11	Figure 5
2.12	Figure 6
2.13	Figure 7
2.14	Supplementary Figure 6

2.1 Abstract

The extreme anterior domain (EAD) is a conserved embryonic region that includes the presumptive mouth. We show that the Kinin-Kallikrein pathway is active in the EAD and necessary for craniofacial development in *Xenopus* and zebrafish (Figure 2.1). The mouth failed to form and neural crest (NC) development and migration was abnormal after loss of function (LOF) in the pathway genes *kng*, encoding Bradykinin (xBdk), *carboxypeptidase-N* (*cpn*), which cleaves Bradykinin, and *neuronal nitric oxide synthase* (*nNOS*). Consistent with a role for nitric oxide (NO) in face formation, endogenous NO levels declined after LOF in pathway genes, but these were restored and a normal face formed after medial implantation of xBdk-beads into LOF embryos. Facial transplants demonstrated that Cpn function from within the EAD is necessary for the migration of first arch cranial NC into the face and for promoting mouth opening. The study identifies the EAD as an essential craniofacial organizer acting through Kinin-Kallikrein signaling.

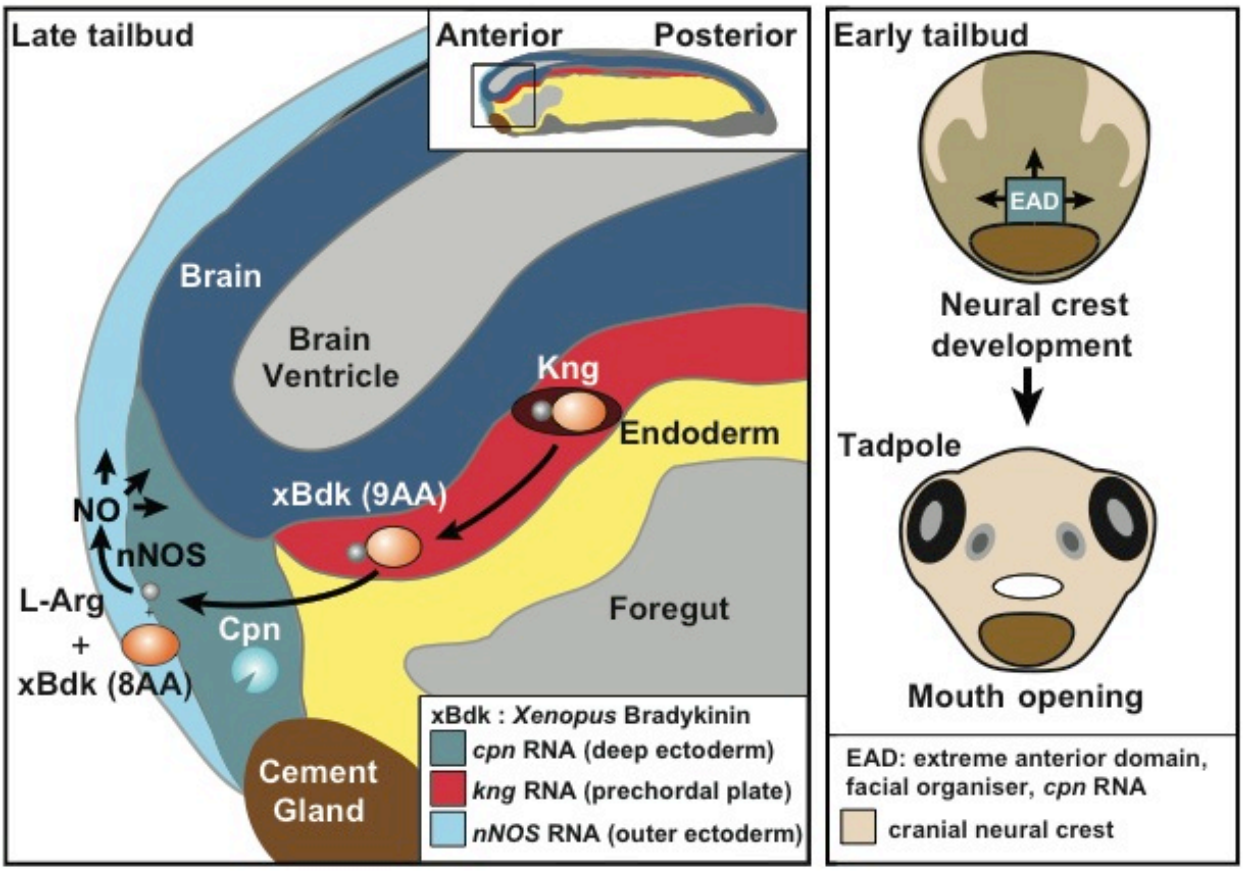

Figure 2.1: Graphical Abstract.

2.2 Introduction

The face derives from both neural crest and non-neural crest derivatives. The presumptive mouth arises from a conserved extreme anterior domain (EAD) where ectoderm and endoderm are juxtaposed (Dickinson and Sive, 2006). The cranial neural crest (NC) migrates into the future facial region to abut the EAD (Dickinson and Sive, 2007; Spokony et al., 2002) during tail bud stages in *Xenopus*. At mouth opening, the cranial NC has begun differentiating into cranial nerves, melanocytes, connective tissue, and chondrocytes that contribute to the jaws and other facial bones (Santagati and Rijli, 2003). The EAD expresses signaling regulators (Dickinson and Sive, 2009), which suggested that the region might act as a facial organizer. We addressed this possibility using transplant assays where EAD lacking the secreted Wnt regulators Frzb-1 and Crescent replaced the EAD of a control embryo. Not only did the mouth fail to form, but surrounding facial regions appeared abnormal, suggesting more global activity of the EAD. However, this putative organizer activity was not extensively explored for other factors impacting mouth formation and cranial NC migration.

Molecular rules for NC movement have been extensively described and include contact inhibition of locomotion, coattraction, chase-and-run strategies (Theveneau et al., 2013), and guidance through interaction with extracellular matrix, semaphorins, and Eph/Ephrin signals (Mayor and Theveneau, 2013). Despite these elegant conclusions, the mechanisms that direct the cranial NC into the facial primordium, and the identity of localized guidance signals that facilitate this migration are not known.

In a microarray screen to identify regulatory genes expressed in the EAD that may regulate mouth and other aspects of face formation, we isolated *carboxypeptidase N* (*cpn*), *kininogen* (*kng*), and *neural nitric oxide synthase* (*nNOS*). These genes are members of the

Kinin-Kallikrein pathway (Kakoki and Smithies, 2009), a regulator of blood pressure (Sharma, 2009) that also participates in inflammation (Bryant and Shariat-Madar, 2009) and renal function. This pathway had not been described as necessary for craniofacial development in any animal. In the adult mammalian Kinin-Kallikrein pathway (Figure 2.2A), Kallikrein, a protease, cleaves KNG to yield Bradykinin, a 9 amino acid (9AA) peptide. Bradykinin is a vasodilator that binds the Bradykinin B2 (BKB2) G-protein-coupled receptor. BKB2 receptor activates NOS, which converts L-Arginine (Arg) to nitric oxide (NO) and citrulline. Bradykinin can also be cleaved by CPN, yielding 8AA desArg-Bradykinin and Arg that can be converted to NO (Moncada and Higgs, 1995). The BKB2 receptor is constitutively expressed in adult mammals and binds Bradykinin, but not desArg-Bradykinin, to activate NOS (Kakoki and Smithies, 2009). A BKB1 receptor is conditionally expressed during inflammation and binds desArg-Bradykinin but not Bradykinin. Angiotensin Converting Enzyme (ACE) degrades both Bradykinin and desArg-Bradykinin.

Figure 2.2: Mammalian Kinin-Kallikrein pathway and putative pathway genes are expressed in the developing face. (**A**) Adult mammalian Kinin-Kallikrein pathway (Kakoki and Smithies 2009). (**B–G'**) In situ hybridization for *kng* (**B, B', E, and E'**), *cpn* (**C, C', F, and F'**), and *nNOS* RNA (**D, D', G, and G'**) RNA is purple. Cement gland marker (*xcg*) is red. Arrow: presumptive mouth. cg, cement gland. (**B–G**) frontal views; (**B'–G'**) sagittal sections. Scale bars: 200 μm.

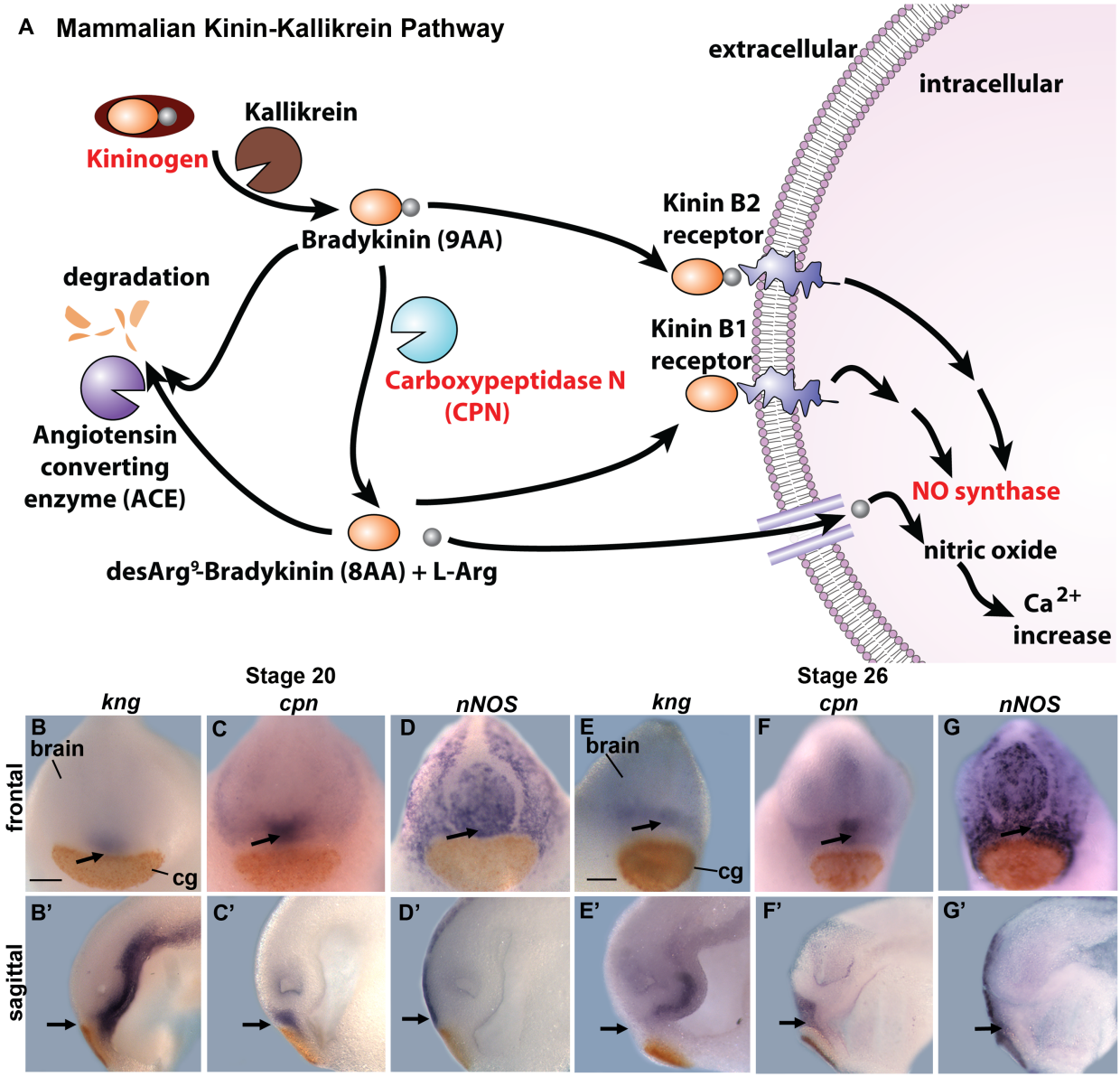
A Mammalian Kinin-Kallikrein Pathway
extracellular
intracellular
Kallikrein
Kininogen
Bradykinin (9AA)
Kinin B2
receptor
degradation
Kinin B1
receptor
Carboxypeptidase N
(CPN)
Angiotensin
converting
enzyme (ACE)
NO synthase
nitric oxide
Ca 2+
increase
desArg9-Bradykinin (8AA) + L-Arg
Stage 20
Stage 26
kng
cpn
nNOS
kng
cpn
nNOS
frontal
sagittal
B
brain
cg
C
D
E
brain
cg
F
G
B'
C'
D'
E'
F'
G'

Figure 2.2

In addition to its role in the Kinin-Kallikrein pathway, NO participates in multiple processes including wound healing, tissue regeneration (Filippin et al., 2011), angiogenesis (Cooke, 2003), neurotransmission (Contestabile and Ciani, 2004), and possibly malignancy (Olson and Garban, 2008). NO has been implicated in developmental contexts including neuronal development (Bradley et al., 2010), bone growth regulation, (Yan et al., 2010), cardiac endothelial-to-mesenchymal transition (Chang et al., 2011), and control of organ size and developmental timing (Kuzin et al., 1996). Elevated NO production has been found in developing epithelial tissues, ganglia, and the notochord (Lepiller et al., 2007). In *Xenopus*, NO is a potent parthenogenetic activator of *Xenopus* eggs (Jeseta et al., 2012) and is correlated with movement in tadpoles (McLean and Sillar, 2000).

The strong expression of *kng*, *cpn*, and *nNOS* in the EAD led us to hypothesize that the Kinin-Kallikrein pathway is active during embryogenesis and required for facial development. We present data that support this hypothesis, and additionally show that Kinin-Kallikrein signaling localized to the EAD is necessary for movement of the first arch cranial NC into the face, and for mouth formation. The study identifies the EAD as an essential craniofacial organizing center acting through Kinin-Kallikrein signaling.

2.3 Methods

2.3 a. Embryo Preparation

Xenopus laevis and zebrafish, *Danio rerio*, embryos were cultured using standard methods (Sive et al., 2000; Westerfield et al., 2001). *Xenopus* embryos were staged according to Nieuwkoop and Faber, 1994; *Danio* embryos were staged according to Kimmel et al., 1995. Lines used were Sox10::GFP (Curtin et al., 2011). All animal use is reviewed and approved by MIT IACUC, under protocol number 0414-026-17.

2.3 b. RNA and qPCR

RNA extraction, cDNA preparation, and qPCR measurements were conducted according to Dickinson and Sive, 2009. Primer sequences are available on request. Three sets of five heads at stage 22 for *sox10* and at stage 26 for *sox9* were collected for each of four conditions, including control MO, *cpn* MO, *kng* MO, and *nNOS* MO to provide biological replicates. Equal amounts of RNA were used for reverse transcription (RT) and qPCR to measure *sox9* or *sox10* RNA. qPCR data from three readings for each of four conditions were averaged, and their distribution was plotted to determine SD. Average morphant qPCR value divided by control morphant qPCR value gave expression level relative to control.

2.3 c. In Situ Hybridization

cDNA sequences used to transcribe in situ hybridization probes including *cpn* (BC059995), *kng* (BC083002), *nNOS* (Peunova et al., 2007), *sox9* (AY035397), *sox10* (Aoki et al., 2003), *xanf1* (Ermakova et al., 2007), *frzb1* (BC108885), and *XCG* (Sive et al., 1989). In situ hybridization was performed as described by Sive et al., 2000, without proteinase K treatment.

Double-staining protocol adapted from Wiellette and Sive, 2003.

2.3 d. Morpholinos and RNA Rescues

Xenopus antisense morpholino-modified oligonucleotides (morpholinos [MOs]) included one start site MO targeting *cpn*, two splice site MOs against *kng* and *nNOS* and a standard control MO. Sequences are as follows: *cpn* MO 5'-ACCACAATCCCAGTGCCATTCTCCC-3', *kng* MO 5'-TTTTACCC ATTGTCTCTTACCTGTC-3', *nNOS* MO 5'-TGGCTAAAAGAACACAGGACATCAA-3. *nNOS* MO resulted in an intron inclusion with an early stop codon at AA313, whereas *kng* MO resulted in an aberrant transcript that could not be amplified by RT-PCR, suggesting it was too large to be amplified or the primer binding sites spanning the MO sequence were missing. qPCR in Figure S2E confirms a reduction in normal *kng* mRNA transcript following MO treatment. *Danio* morpholinos include a start site and a splice site MO targeting *kng1*. Sequences are *kng1* MO (5'-CAAGCTCTTGTCCAGCGCCATTGTC-3') and *kng1* MO (5'-AGCCTGAGGAAACACAAACGCACGT-3'). The splice site *kng1* morpholino binds the terminal 22bp of intron 2 and the first 3bp of exon 3.

kng cDNA, *nNOS* cDNA, and *cpn* cDNA without 5' UTRs were cloned into the $CS2^{+}$ vector. RNA was generated in vitro using the mMESSAGE mMACHINE kit (Ambion). RNA (~1ng) and morpholino (14–18ng) were coinjected at the one-cell stage to test morpholino specificity via RNA rescue.

2.3 e. Peptide and NO Donor Rescues

Peptides (Thermo Scientific) were designed according to predicted sequences including 9

amino acid (AA) *Xenopus* Bradykinin (xBdk) (SYKGLSPFR) and 8AA Des-Arg xBdk (SYKGLSPF) and diluted to 0.1 or 0.2mg/ml. Affi-gel blue agarose beads (50–100 mesh, Bio-Rad) loaded with peptides were prepared according to Carmona-Fontaine, 2011. For rescues, beads resuspended in 0.1mg/ml peptide solution were implanted in the presumptive mouth region at stage 22 and scored at stage 40. For NC assays, beads resuspended in 0.2mg/ml peptide solution were implanted in the side of the head or presumptive mouth at stages 20–22. Embryos were fixed at tail bud (stage 26) for in situ hybridization analysis. For peptide-rescue assays, partial LOF morphants were employed to maximize viability.

NO donor, S-Nitroso-N-acetyl-DL-penicillamine (SNAP) (Sigma) was diluted to 100mM in a 50% DMSO solution. For early rescues, 1nl of SNAP was co-injected with 17ng of morpholino into one-cell stage embryos. For late rescues (stage 20), 2–3nl of SNAP was injected into the presumptive mouth region. The nNOS inhibitor, TRIM (Sigma, T7313), was diluted to 1M concentration in DMSO and applied to late neurula (stage 20) embryos. Embryos were collected at tail bud (stage 26) for *sox9* in situ hybridization and at swimming tadpole (stage 40) for craniofacial morphology.

2.3 f. Nitric Oxide Staining and Quantification

Embryos were incubated in NO indicator 4-amino-5-methylamino-2',7' -di-fluorofluorescein diacetate (1:150), (DAF-FM diacetate; Invitrogen; Lepiller et al., 2007) for 2–3 hours at 26°C. Embryos were fixed in 4% paraformaldehyde overnight, embedded in 4% agarose, vibrotome sectioned (100μm), counter-stained with DAPI, and imaged on a Zeiss LSM 700 Laser Scanning Confocal. For NO quantification, 120 embryos per condition were decapitated, washed, dounced, and spun (10 min, 1,300rpm). The clear fraction was divided in

triplicate and loaded on a microplate (Corning 3993- half-area, flat bottom, black), and fluorescence was measured using a Teican microplate reader. Untreated head solution was used to measure background fluorescence.

2.3 g. Urea Assay

A bovine Arginase solution (2mg/ml lyophylized bovine Arginase [Sigma # A3233] in 50mM $MnCl_2$) was incubated for 1 hour at 37°C. Stage 28–29 embryos were anesthetized and decapitated, with 180 heads per condition. Heads were dounced in 90μl of water, spun for 10 min at 1,100rpm at 4°C, and 100μl of clear, cytoplasmic fraction was mixed with 75μl of Arginase solution for a 2 hour incubation at 37°C. Urea content was detected using the Abcam Urea Assay Kit (Abcam #AB83362). Absorbance was read on a Teican ‘‘Infinite Pro’’ microplate reader and calculated as a percentage of wild-type or control morphant level.

2.3 h. Immunohistochemistry

Immunohistochemistry was performed as described (Dickinson and Sive, 2006). Primary antibodies included polyclonal anti-laminin antibody (Sigma L-9393) diluted 1:150 and polyclonal anti-β-catenin (Invitrogen) diluted 1:100. Secondary antibody was Alexa 488 goat anti-rabbit (Molecular Probes) diluted 1:500 with 0.1% propidium iodide as a counterstain. Sections were imaged on Zeiss LSM 700 and 710 Laser Scanning Confocal microscopes. Images were analyzed using Imaris (Bitplane) and Photoshop (Adobe).

2.3 i. Whole-Mount TUNEL, PH3, and Alcian Blue Labeling

TUNEL and PH3 labeling were performed according to Dickinson and Sive, 2006 and

2009. Alcian blue staining was performed according to Kennedy and Dickinson, 2012.

2.3 j. Transplants and Head Extirpation

EAD transplants were performed according to Jacox et al., 2014; NC transplants were performed according to Mancilla and Mayor, 1996. For head extirpation, morphant and wild-type embryos were grown to stage 31–32, when the stomodeum forms. Embryos were anesthetized in Tricaine, and heads were removed below the cement gland excluding the developing heart. Heads were moved to 0.5x Modified Barth's Saline (MBS) for healing and growth. Whole embryos and heads were scored for facial and mouth development at stage 40.

2.4 Results

2.4 a. *kininogen*, *carboxypeptidase N*, and *neural nitric oxide synthase* Are Expressed in the EAD during Initial Stages of Craniofacial Development

kng, *cpn*, and *nNOS* expression was identified in the *Xenopus* EAD region (Dickinson and Sive, 2009; Figure 2.3A), suggesting activity of an embryonic Kinin-Kallikrein pathway (Figure 2.2A). Protein alignment showed high conservation of Cpn and nNOS (Figures 2.3B–2.3D). Gene expression was examined by in situ hybridization and quantitative RT-PCR (qPCR) (Figures 2.2B–2.2G' and 2.3E–2.3G). At tail bud (stages 20 and 26) when the EAD is present and cranial NC is migrating, *kng* is expressed in the prechordal plate with anterior expression adjacent to the EAD (Figures 2.2B, 2.2B', 2.2E, and 2.2E'). At stage 20, *cpn* was expressed in deep EAD layers (Figures 2.2C and 2.2C') and by stage 26 at low intensity in the first branchial arch (Figures 2.2F and 2.2F'). *nNOS* RNA is present in outer ectoderm of the face, excluding hatching and cement glands (Figures 2.2D, 2.2D', 2.2G, and 2.2G'). Later, *nNOS* is expressed in the head and notochord (Peunova et al., 2007). These data show that putative Kinin-Kallikrein pathway genes are simultaneously expressed in adjacent regions of the presumptive face.

Figure 2.3: Temporal expression profiles, expression in the presumptive mouth, and homology of protein sequences. (**A**) Three tissues were dissected from stage 26 heads: cg - cement gland, mouth, and brain - neural and expression of *kng*, *cpn*, and *nNOS* were determined by microarrays - m (Dickinson and Sive, 2009) and qPCR - q. *kng*, *cpn*, and *nNOS* displayed 4-fold enrichment, 5-fold enrichment, and 4-fold enrichment, respectively, in the presumptive mouth region relative to surrounding tissue. (**B-D**) Percentage values correspond to sequence identity of protein sequences among human, mouse, zebrafish, *Xenopus laevis*, and *Xenopus tropicalis*. Protein sequences were obtained from NCBI Gene. Homologs were aligned using several different algorithms (t-coffee, mafft, probcons, and muscle), with the final alignment determined by consensus as implemented by t-coffee. Phylogeny was estimated with a maximum likelihood method (proml), using default parameters, in the phylip package. (**E-G**) 5 embryos per biological replicate (error bars: 3 biological replicates) were collected for developmental stages from oocyte (stage 1) to swimming tadpole (stage 42). Total RNA was extracted and expression profiles of *kng*, *cpn* and *nNOS* were measured by qPCR. All genes showed low maternal level of expression and rapid increase of expression after mid-blastula and between stages 20 and 26.

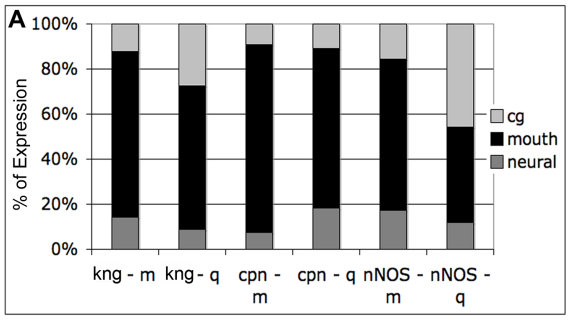

B

kng	human	mouse	zebrafish	*X. laevis*
mouse	58%			
zebrafish	16%	13%		
X. laevis	30%	27%	13%	
X. tropicalis	27%	26%	15%	75%

C

cpn	human	mouse	zebrafish	*X. laevis*
mouse	83%			
zebrafish	66%	64%		
X. laevis	68%	67%	67%	
X. tropicalis	68%	67%	67%	91%

D

nNOS	human	mouse	zebrafish	*X. laevis*
mouse	94%			
zebrafish	73%	74%		
X. laevis	78%	77%	74%	
X. tropicalis	78%	78%	74%	95%

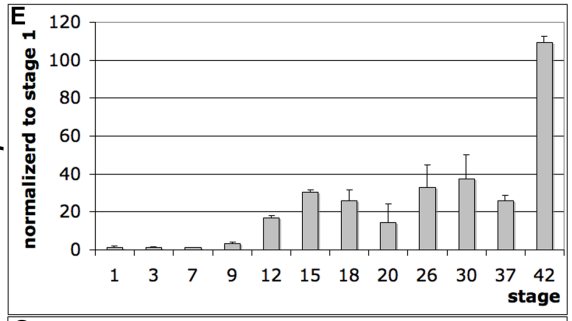

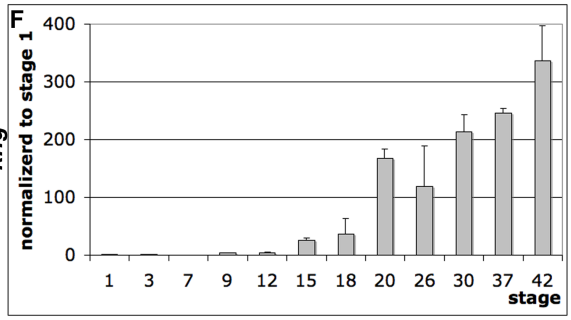

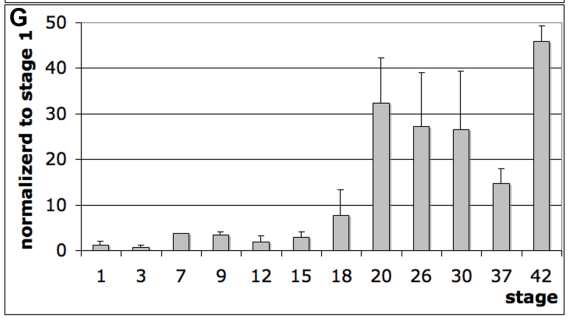

Figure 2.3

2.4 b. Putative Kinin-Kallikrein Pathway Genes Are Required for Mouth Formation and Neural Crest Development

A requirement for *kng*, *cpn*, and *nNOS* during craniofacial development would be consistent with activity of the Kinin-Kallikrein pathway. This was tested by loss of function (LOF) using injection of morpholino antisense oligonucleotides (morpholinos, MOs) at the one-cell stage. Specificity of MO targeting was demonstrated by using two MOs, or more importantly, by ‘‘rescue’’ assays where a normal phenotype was observed when MO was coinjected with cognate mRNA lacking the MO target site (Figures 2.4A–2.4D’ and 2.4B’’). For *kng* and *nNOS* MOs targeting splice sites, qPCR showed a strong decrease in endogenous RNA levels (Figures 2.4E and 2.4F). At late hatching stage (stage 40), LOF animals (‘‘morphants’’) displayed abnormal body morphology and no open mouth, with a small stomodeal invagination (Figures 2.5A–2.5D’, bracket). Nostrils were absent, eyes were small, pigment was reduced, and the face was narrow (Figures 2.5A’ –2.5D’). Morphant phenotypes were apparent at early tail bud (stage 22, Figures 2.6A–2.6L’) and were accompanied by elevated cell death but normal proliferation (Figures 2.6M–2.6V). Despite abnormal mouth phenotypes, the EAD was correctly specified as shown by expression of *frzb1* and *xanf1* (Figures 2.5E–2.5H’’’).

Figure 2.4: Morpholino specificity and efficiency. (**A-D, B'-D', B''**) The specificity of the morphant phenotypes was confirmed by rescue with 800pg of *kng* mRNA (**B'**), 800pg of *nNOS* mRNA (**D'**), and 1ng of *cpn* mRNA (**C'**), which does not hybridize to the start site *cpn* morpholino. (**B''**) *kng* LOF phenotype was also overcome with human *KNG* mRNA. Embryos were co-injected using a mixture of morpholino and mRNA at the one cell stage. The craniofacial phenotype of *kng*, *cpn* and *nNOS* LOF was completely rescued by coinjection with mRNAs, i.e. *kng* (**B'**) 70% normal, n= 162; *cpn* (**C'**) 74% normal, n=112; *nNOS* (**D'**) 44% normal, n=94 and human *kng* (**B''**) 32% normal, n=40. Scale bar: 200μm. Phenotypes of *kng* (**B**), *cpn* (**C**), and *nNOS* (**D**) loss of function using antisense morpholinos are described in detail in Figure 2.5. When injected into control embryos alone, the *kng*, *cpn*, and *nNOS* RNA did not alter mouth morphology, despite the Kinin-Kallikrein GOF (data not shown). (**E** and **F**) Using qPCR, levels of *kng* and *nNOS* mRNA in LOF embryos were determined to be 6-10% and 25-34% of control levels, respectively. Two independent experiments are shown. Three independent groups of embryos (n=5 for each group) were analyzed by qPCR (biological replicates).

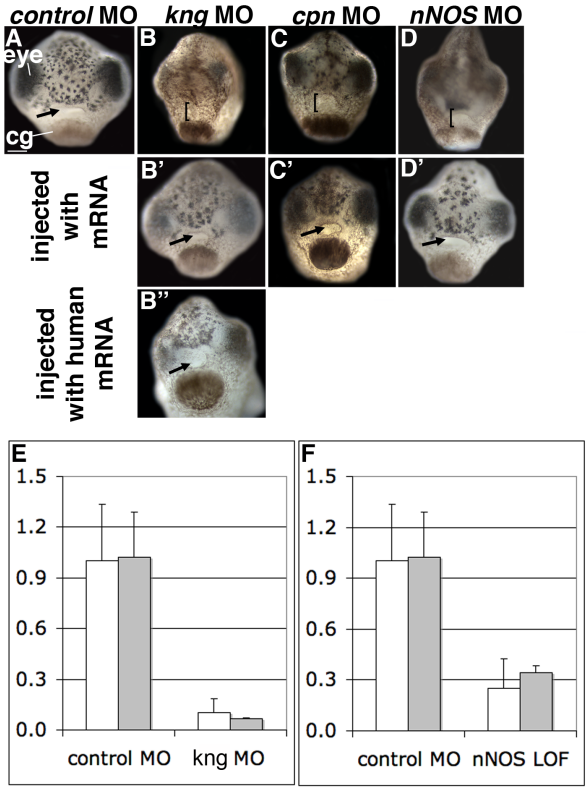
control MO
kng MO
cpn MO
nNOS MO
A
eye
cg
B
C
D
injected with mRNA
B'
C'
D'
injected with human mRNA
B''
E
1.5
1.2
0.9
0.6
0.3
0.0
control MO
kng MO
F
1.5
1.2
0.9
0.6
0.3
0.0
control MO
nNOS LOF

Figure 2.4

Figure 2.5: *kng*, *cpn*, and *nNOS* are required for mouth opening and face formation. (**A–D'**) *kng*, *cpn*, and *nNOS* loss of function (LOF) using antisense morpholinos. Embryos assayed at stage 40, in four independent experiments. Arrow: mouth region. Bracket: unopened mouth. cg, cement gland. Scale bar in (**A–D**): 2,000μm. Scale bar in (**A'–D'**): 200μm. (**A and A'**) Control morphants (100% normal, n = 97). (**B–D'**) *kng*, *cpn*, and *nNOS* morphants (*kng* [**B'**] 0% normal, n = 102; *cpn* [**C'**] 2% normal, n = 105; *nNOS* [**D'**] 0% normal, n = 129). (**E–H'''**) Kinin-Kallikrein pathway morphants at stage 22 express presumptive mouth markers, *frzb1* and *xanf*1. Scale bars: 200μm. (**I–P and I'–L'**) Histology of *kng*, *cpn*, and *nNOS* LOF. Coronal sections (**I–L**, control morphant 100% normal, n = 5; each Kinin-Kallikrein morphant, 0% normal, n = 9) assayed at stage 26 in two independent experiments with β-catenin immunolabeling. Parasagittal sections with anterior to the left (**I'–L'**, control morpholino 100% normal, n = 5; each Kinin-Kallikrein pathway morpholino, 0% normal, n = 12).

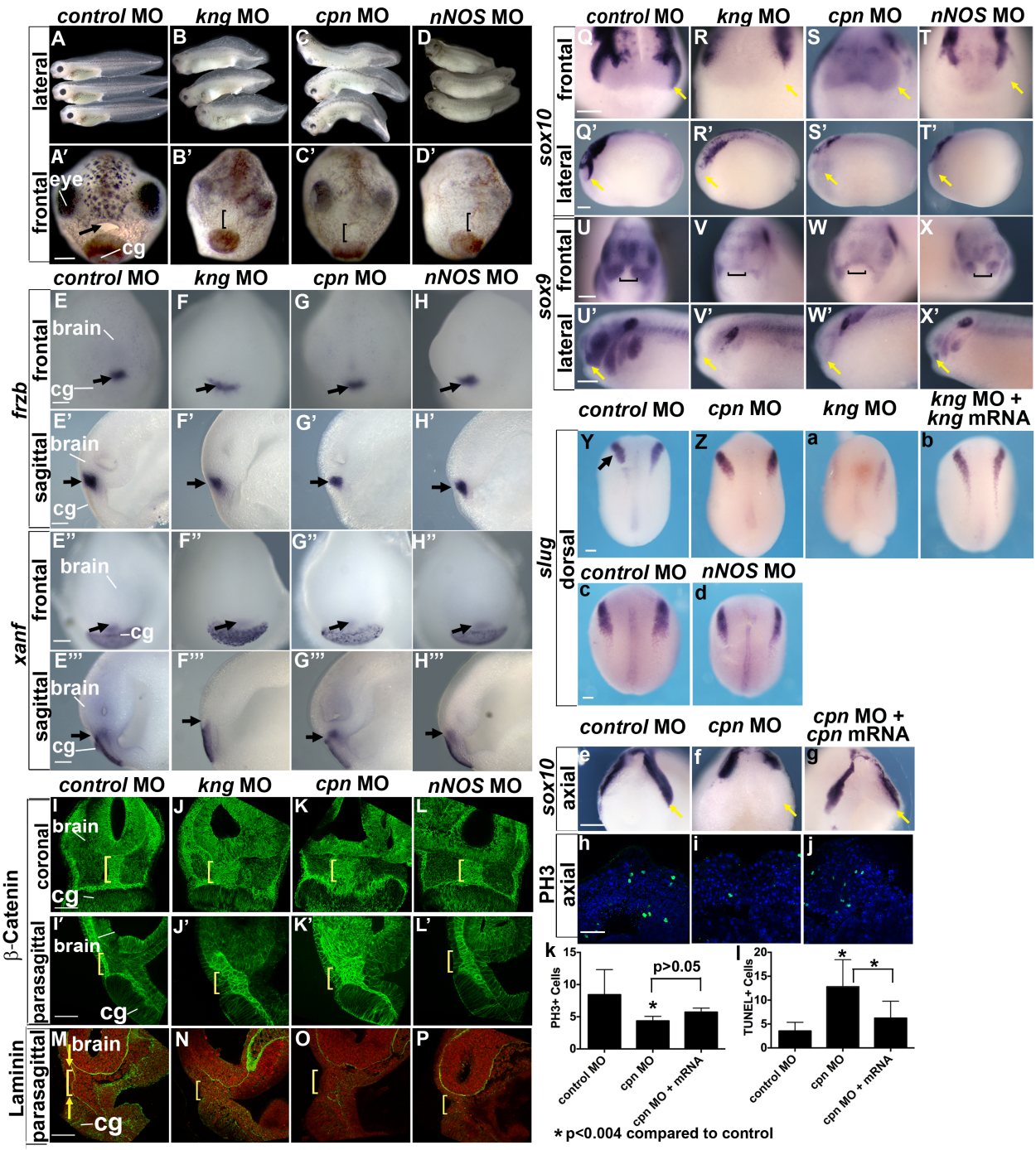
control MO
kng MO
cpn MO
nNOS MO
lateral
frontal
eye
cg
frzb
brain
sagittal
xanf
sox10
sox9
slug
dorsal
kng MO + kng mRNA
cpn MO + cpn mRNA
axial
PH3
β-Catenin
coronal
parasagittal
Laminin
PH3+ Cells
p>0.05
TUNEL+ Cells
control MO
cpn MO
cpn MO + mRNA
* p<0.004 compared to control

Figure 2.5

Figure 2.6: Phenotypic comparison at early stages and TUNEL, PH3 staining. (**A-L**) Frontal views of control and LOF embryos at earlier stages 22, 26 and 30. Scale bar: 200μm. (**A'-L'**) Lateral views of control and LOF embryos at earlier stages 22, 26 and 30. Scale bar: 500μm. Whole body phenotypes vary from morphant to morphant. *kng* morphants displayed a normal head size (**B, F, J**). Pockets of edema frequently formed in the presumptive heart region starting at stage 26. *cpn* morphants displayed a larger head relative to the posterior, most obvious at stage 22 (**C, G, K**). These morphants showed a tendency to disintegrate at high MO levels after stage 30 (hatching), suggesting abnormal epithelial integrity. *nNOS* morphants showed a diminished overall head size and expanded posterior (**D, H, L**). All morphants had reduced pigment and diminished movement at low MO levels, and no ability to move at high levels. Cell death was increased in LOF embryos. (**M-P**) Histological coronal sections showing TUNEL labeling in the presumptive mouth (brackets) at stage 26. Scale bar: 100μm. (**Q-T**) Histological coronal sections with PH3 labeling in the presumptive mouth (brackets) at stage 26. Scale bar: 100μm. (**U**) Graph showing TUNEL data. *kng* (average n=13.3 positive cells), *cpn* (average n=23.0 positive cells), and *nNOS* (average n=17.0 positive cells) morphants have an increase in cell death, respectively, compared with control morphants (average n = 1 positive cell), n = 8 embryos counted per condition, p values < 0.05. (**V**) Graph showing PH3 positive cells (green) compared to negative cells (red). *kng* (5% of total cells), *cpn* (16% of total cells), and *nNOS* (8% of total cells) morphants have a similar level of cell proliferation, respectively, compared with control morphants (10% of total cells), n = 8 embryos per condition, p values > 0.2.

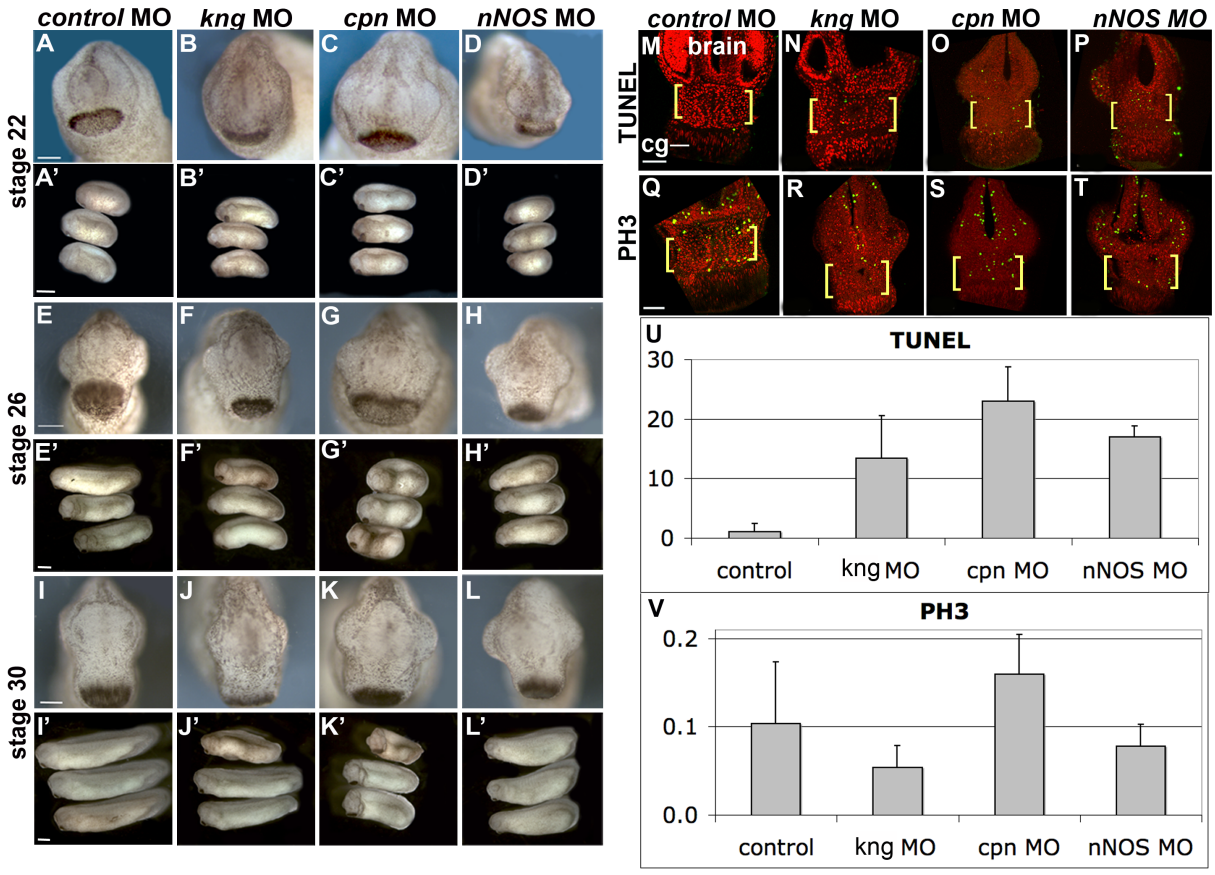
control MO
kng MO
cpn MO
nNOS MO
stage 22
stage 26
stage 30
A
B
C
D
A'
B'
C'
D'
E
F
G
H
E'
F'
G'
H'
I
J
K
L
I'
J'
K'
L'
control MO
kng MO
cpn MO
nNOS MO
TUNEL
PH3
M
brain
cg
N
O
P
Q
R
S
T
U
TUNEL
30
20
10
0
control
kng MO
cpn MO
nNOS MO
V
PH3
0.2
0.1
0.0
control
kng MO
cpn MO
nNOS MO

Figure 2.6

To understand LOF defects, we analyzed tail bud embryos (stage 26) for β-catenin indicating adherens junctions, and laminin indicating basement membrane using immunostaining. In coronal (frontal) sections, controls displayed a narrow midline strip of β-catenin-positive cells running from brain to cement gland, two to four cells wide (Figure 2.5I). However, in morphants this strip was six to eight cells wide, indicating abnormal epithelial organization (Figures 2.5J–2.5L), also apparent in parasagittal sections (Figure 2.5I', bracket) where morphants showed a deep region of β-catenin-positive tissue (Figures 2.5J'–2.5L'). In morphants, Laminin localization was largely absent from the basement membrane extending from brain to cement gland and separating epidermis and deep ectoderm (Figures 2.5M– 2.5P, arrows). These data demonstrate epithelial and basement membrane abnormalities at tail bud after *kng*, *cpn*, and *nNOS* LOF.

Reduction of pigment and narrow faces in morphants suggested cranial NC may be abnormal, and, consistently, RNA expression of cranial NC markers *sox9* and *sox10* (Aoki et al., 2003; Mori-Akiyama et al., 2003) was reduced at early tail bud (stage 22) and at late tail bud (stage 26) (Figures 2.5Q–2.5X') as assayed by in situ hybridization. This was confirmed by qPCR, with >50% reduction in RNA levels (data not shown). Frontal views of control embryos at stage 26 showed a midline strip negative for NC markers (Figure 2.5U, bracket) that was not apparent or wider in morphants (Figure 2.5V–2.5X). These data suggest cranial NC induction, survival, proliferation, or migration is abnormal.

To assay NC induction in morphants, expression of *slug* (LaBonne and Bronner-Fraser, 1998) was examined at early neurula (stage 15) (Figures 2.5Y–2.5d). Although *nNOS* and *cpn* morphants displayed normal *slug* expression (Figures 2.5Y, 2.5Z, 2.5c, and 2.5d), *kng* morphants showed a decrease that was prevented by coinjection of *kng* mRNA (Figures 2.5a and 2.5b).

Because *cpn* morphants show normal NC induction but a later deficit in NC marker expression, morphants were analyzed for alterations in proliferation and cell death. Axial sections of *sox10* in situ embryos confirmed NC identity (Figures 2.5e–2.5h). PH3 labeling demonstrated 50% reduction in mitotic cells (Figures 2.5i–2.5j and 2.5l) and TUNEL demonstrated a 100% increase in dying cells in *cpn* morphants relative to controls (Figure 2.5m) that was partially prevented by coinjecting cognate mRNA (Figures 2.5k–2.5m). The data show a requirement for *kng*, *cpn*, and *nNOS* during craniofacial development, including mouth opening. After LOF, multiple changes are observed, in epithelial organization and NC induction, proliferation, or survival, consistent with an active embryonic Kinin-Kallikrein pathway.

2.4 c. *kng* and *cpn* LOF Phenotypes Are Prevented by *Xenopus* Bradykinin Peptides

In the adult, the Kng precursor is processed to release a 9AA peptide, Bradykinin (Bdk) and desArg-xBdk, an 8AA peptide, after cleavage by Cpn. *Xenopus* Bdk (xBdk) peptide was predicted by aligning Kng protein sequence across species and identifying putative Kallikrein cleavage sites (Figure 2.7A) (Borgono et al., 2004). Considering the adult mammalian pathway, we predicted that both the 9AA and 8AA peptides should prevent the *kng* LOF phenotype, whereas only the 8AA peptide should prevent the *cpn* LOF phenotype (Figure 2.2A). Beads soaked in peptides were implanted medially in the future facial region of *kng* or *cpn* LOF embryos at tail bud (stage 22), which were scored at tadpole (stage 40) for mouth and facial phenotypes (Figure 2.7B). Relative to a scrambled xBdk peptide (Figures 2.7C and 2.7F), 9AA and 8AA peptides prevented the *kng* morphant phenotype (Figures 2.7D, 2.7E, and 2.7I), as predicted. In *cpn* morphants, mouth opening was restored by 8AA but not by 9AA peptide, consistent with the adult model (Figures 2.7G–2.7I). However, both peptides restored normal

pigment, overall facial symmetry, and head size to *cpn* morphants (Figure 2.7I).

To investigate whether xBdk peptide could restore NC development after *kng* LOF, 9AA scrambled or xBdk soaked-beads were implanted medially (Figures 2.7J–2.7L) or anterolaterally below the eye (Figures 2.8A–2.8C') at stage 22, and *sox9* expression was later assayed. Normal *sox9* expression was observed with 9AA xBdk beads (Figures 2.7J–2.7L). Consistent data were obtained with lateral implants (Figures 2.8B–2.8C'); however, these failed to rescue mouth formation at stage 40 (Figures 2.8D–2.8F). These data support the hypothesis that xBdk peptides derived from Kng direct mouth and NC formation.

Figure 2.7: Bradykinin-like peptides prevent *cpn* and *kng* loss of function phenotypes. (**A**) Amino acid sequence alignment of region around Bdk-l peptide. Gray highlights: Bdk-l peptide sequence; red: conserved amino acids; black arrows: Kallikrein and Cpn cleavage sites. Bdk-l (9AA) and Des-Arg Bdk-l peptides (8AA) used. (**B**) Experimental design. (**C–H**) Abnormal mouth phenotype after *kng* LOF prevented by 9AA and 8AA peptides, whereas in *cpn* morphants was prevented only by the 8AA peptide. (**C**) *kng* morphants implanted with 9AA scrambled (9AAscr) peptide bead (28% normal, n = 60). Embryos scored as abnormal if mouth failed to open, was tiny or asymmetric, nostrils failed to form, pigment was absent, or face was abnormally narrow. (**D–E**) *kng* morphant implanted with 9AA (**D**, 60% normal, n = 105) or 8AA bead (**E**, 57% normal, n = 75). (**F**) *cpn* morphants implanted with 9AAscr bead (mouth: 43% normal, n = 67; face: 27% normal, n = 67). (**G–H**) *cpn* morphants implanted with 9AA bead (mouth: 41% normal, n = 54; face: 44% normal, n = 54) or 8AA bead (mouth: 65% normal, n = 79; face: 51% normal, n = 79). Scale bar: 200μm. (**I**) Graph depicting percent of morphants implanted with beads, displaying normal mouth and face formation. p values: one-tailed Fisher's exact test. (**J–L**) Expression of neural crest marker *sox9* in *kng* morphants implanted with 9AA bead. Arrow: normal extent of first arch cranial NC. Wild-type expression of *sox9* (**J**, 100% normal, n = 13). *kng* morphant with a 9AAscr bead (**K**, 8% normal, n = 12) and 9AA bead (**L**, 39% normal, n = 13). Scale bar: 200μm.

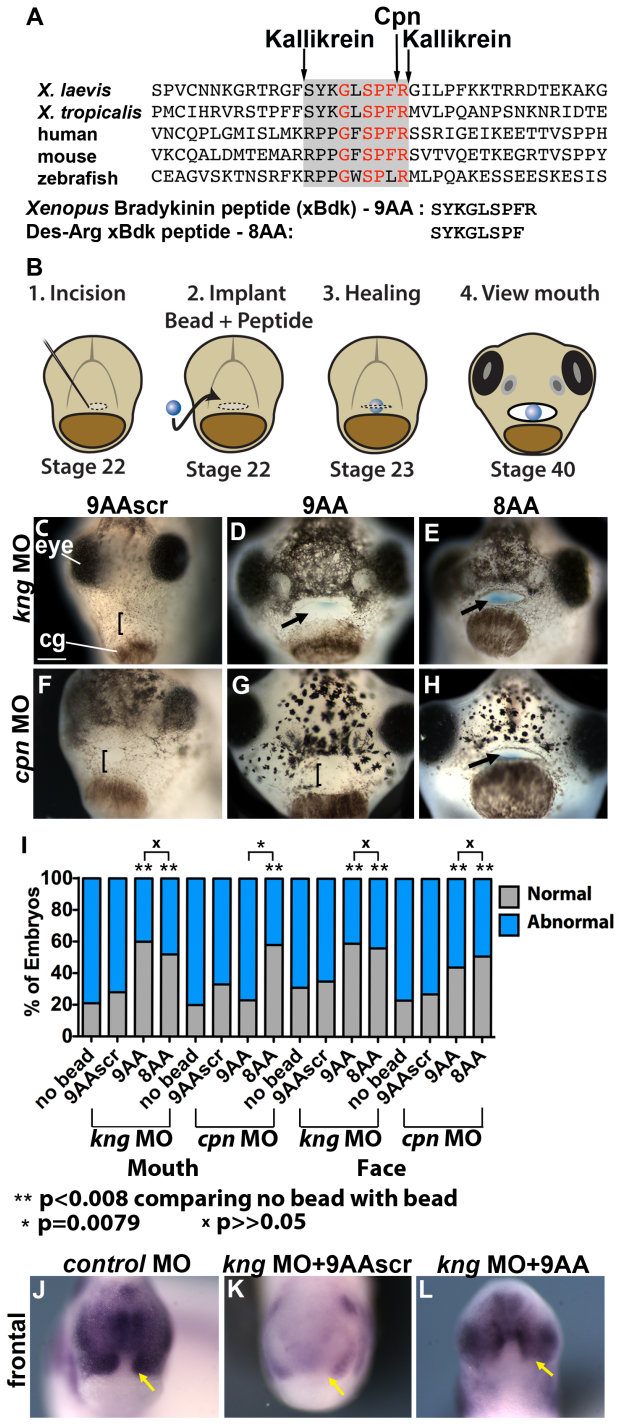
A
Cpn
Kallikrein
Kallikrein
X. laevis SPVCNNKGRTRGFSYKGLSPFRGILPFKKTRRDTEKAKG
X. tropicalis PMCIHRVRSTPFFSYKGLSPFRMVLPQANPSNKNRIDTE
human VNCQPLGMISLMKRPPGFSPFRSSRIGEIKEETTVSPPH
mouse VKCQALDMTEMARRPPGFSPFRSVTVQETKEGRTVSPPY
zebrafish CEAGVSKTNSRFKRPPGWSPLRMLPQAKESSEESKESIS
Xenopus Bradykinin peptide (xBdk) - 9AA : SYKGLSPFR
Des-Arg xBdk peptide - 8AA: SYKGLSPF
B
1. Incision
2. Implant Bead + Peptide
3. Healing
4. View mouth
Stage 22
Stage 22
Stage 23
Stage 40
9AAscr
9AA
8AA
kng MO
cpn MO
C
eye
cg
D
E
F
G
H
I
% of Embryos
Normal
Abnormal
no bead
9AAscr
9AA
8AA
kng MO
cpn MO
Mouth
Face
** p<0.008 comparing no bead with bead
* p=0.0079
x p>>0.05
control MO
kng MO+9AAscr
kng MO+9AA
frontal
J
K
L

Figure 2.7

Figure 2.8: Laterally located Bradykinin-like peptides promote cranial neural crest migration but do not restore mouth opening in *kininogen* (*kng*) morphants. (**A**) Schematic. (**B, B'**) *kng* morphant with no beads (35% with right side expression, n=17). (**C, C'**) *kng* morphant plus implanted beads (74% with right side expression, n=19). *kng* morphants had 9AA peptide implanted on the right side of the head, and 9AAscr peptide implanted on the left side of the head. Bracket: normal location of branchial arch 2. Scale bar: 120μm. (**D**) *kng* morphant with 9AAscr peptide (28% with a normal mouth, n=14). (**E**) *kng* morphant with 9AA peptide (21% with a normal mouth, n=14). (**F**) *kng* morphant with 8AA peptide (28% with a normal mouth, n=14). Bracket: unopened mouth. Scale bar: 100μm.

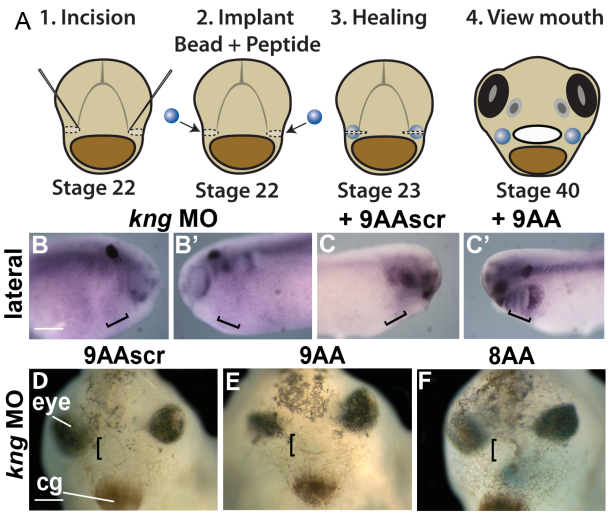
A
1. Incision
2. Implant
Bead + Peptide
3. Healing
4. View mouth
Stage 22
Stage 22
Stage 23
Stage 40
kng MO
+ 9AAscr
+ 9AA
lateral
B
B'
C
C'
9AAscr
9AA
8AA
kng MO
D
eye
cg
E
F

Figure 2.8

2.4 d. Nitric Oxide Prevents *kng*, *cpn*, and *nNOS* LOF Phenotypes, and Endogenous NO Production Is Regulated by xBdk

In mammals, the Kinin-Kallikrein pathway leads to production of the signaling molecule NO. We therefore hypothesized that LOF phenotypes would be prevented by application of the NO donor S-Nitroso-N-Acetyl-D,L-Penicillamine (SNAP). SNAP was coinjected with MO at the one-cell stage or injected into the face at late neurula (stage 20). When applied at the one-cell stage, SNAP prevented craniofacial and whole-body phenotypes (Figures 2.9A–2.9D'; Figures 2.10A–2.10G, 2.10B'–2.10D', and 2.10J) and corrected β-catenin and laminin localization and *sox9* expression (Figures 2.9E–2.9P'). When injected into the presumptive facial region, SNAP improved facial development (Figures 2.10A–2.10D') indicating NO can act at later stages. This rescue was not due to a general effect on all MOs, because the *par1* phenotype (Ossipova et al., 2005) was not prevented by SNAP (Figures 2.10H–2.10J). Consistent data were obtained using the NO antagonist TRIM applied at stage 20, resulting in abnormal mouth, face, and *sox9* expression (Figures 2.9Q–2.9R'). Although the Kinin-Kallikrein pathway has a role in angiogenesis (Westermann et al., 2008), craniofacial phenotypes did not result from altered blood flow, shown by a head extirpation assay. Thus, an open mouth developed in isolated heads lacking a heart and cultured from prehatching stages 31 and 32, before a heartbeat, until stage 41 (swimming tadpole) (Figures 2.9S–2.9T').

Figure 2.9: *kng*, *cpn*, and *nNOS* loss of function phenotypes are prevented by the NO donor, SNAP, and Kinin-Kallikrein morphants show reduced NO production that is increased by xBdk. (**A–D'**) Facial morphology of *kng*, *cpn*, and *nNOS* loss of function (**A–D**) and with SNAP (**A'–D'**). Embryos assayed at stage 40 in three independent experiments and scored as abnormal if mouth failed to open, was tiny or asymmetric, nostrils failed to form, pigment was absent, or face was abnormally narrow. Arrow: mouth region. Bracket: unopened mouth. cg, cement gland. (**A**) Control MO injected (98% normal, n = 427) (**B–D**) *kng*, *cpn*, or *nNOS* MO injected. (**A'**) SNAP plus control MO. (**B'–D'**) *kng*, *cpn*, or *nNOS* MO plus SNAP coinjection (*kng* [**B'**] 85% normal, n = 105; *cpn* [**C'**] 86% normal, n = 98; *nNOS* [**D'**] 90% normal, n = 87). Scale bars: 100μm. (**E–L'**) Histology of *kng*, *cpn*, and *nNOS* LOF embryos after SNAP treatment. Parasagittal sections with anterior to left assayed at stage 26 with β-catenin (**E–H'**) and laminin immunolabeling (**I–L'**). β-catenin: green. Laminin: green, with nuclear propidium iodide: red. cg, cement gland. (**E–H'**) β-catenin in control embryos (**E and E'**), LOF embryos (**F–H**), and LOF embryos coinjected with SNAP (**F'–H'**) (*kng* [**F'**] 100% normal, n = 5; *cpn* [**G'**] 100% normal, n = 5; *nNOS* [**H'**] 100% normal, n = 5). (**I–L'**) Laminin staining in control embryos (**I and I'**), LOF embryos (**J–L**), and LOF embryos coinjected with SNAP (**J'–L'**) (*kng* [**J'**] 75% normal, n = 4; *cpn* [**K'**] 80% normal, n = 5; *nNOS* [**L'**] 100% normal, n = 4). Scale bars: 170μm. (**M–P'**) Expression of *sox9* RNA (in situ hybridization) after SNAP injection into *kng* (**N, N'**), *cpn* (**O, O'**), and *nNOS* (**P, P'**) LOF embryos. Lateral view. Scale bar: 100μm. (**Q–R'**) NOS inhibitor TRIM prevents mouth formation and reduces *sox9* expression. (**Q and Q'**) Wild-type embryos (100% normal, n = 6). (**R and R'**) TRIM-treated embryos (17% normal, n = 6). (**Q and R**) Frontal view at stage 40. (**Q' and R'**) Lateral view of *sox9* in situ hybridization at stage 26. Scale bars in (**Q**) and (**R**): 100μm. Scale bars in (**Q'**) and (**R'**): 400μm. (**S–T'**) Extirpated heads show open mouth and

normal pigmentation at swimming tadpole (stage 41). (**S and S'**) Control heads (96% normal, n = 27). (**T and T'**) Isolated heads (92% normal, n = 26). (**S and T**) frontal view. (**S' and T'**) side view. Scale bar: 100μm. (**U–X**) Fluorescence after incubation with NO sensor DAF-FM in control embryos (**U**), *kng* (**V**), *cpn* (**W**), and *nNOS* (**X**) LOF embryos. cg, cement gland. Sagittal view. Scale bar: 170μm. (**Y–c**) Control morphant with no bead (**Y**). *kng* morphant with no bead (**Z**), with 9AA xBdk scrambled bead (**a**) or 9AA xBdk bead (**b**). Images collected with same exposure, gain, and fluorescent illumination. *kng* morphants implanted with 9AA xBdk bead displayed 50% of control florescence compared with 23% of control fluorescence in morphants treated with 9AAscr xBdk peptide. Frontal view. Scale bar: 100μm. (**c**) Graph showing morphant fluorescence as percentage of control fluorescence; *cpn* morphants: 49%, *kng* morphants: 24%, and *nNOS* morphants: 64%. Each dot represents average of three biological replicates from independent experiments. p values: one-tailed t-test.

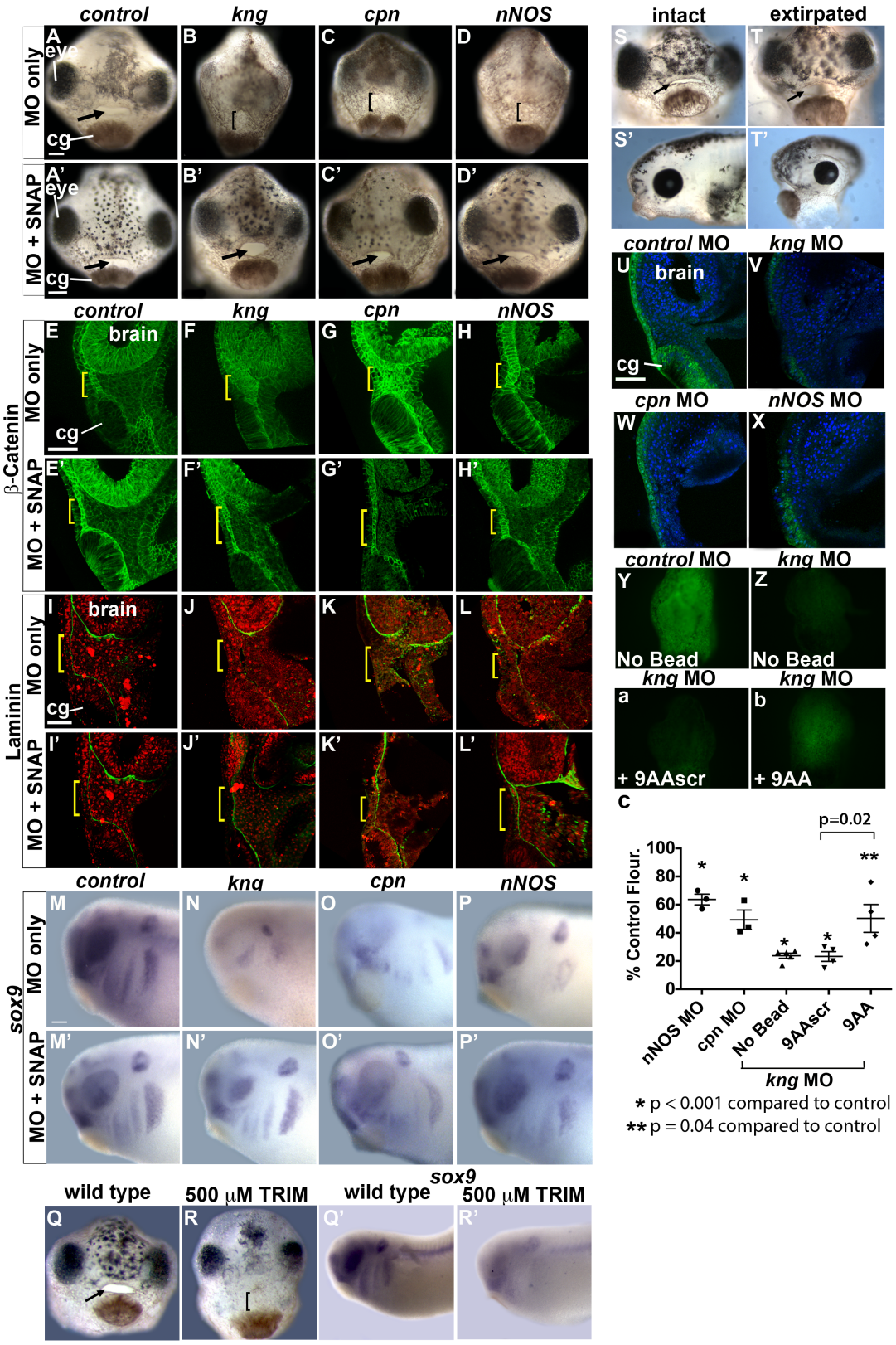
control
kng
cpn
nNOS
MO only
MO + SNAP
eye
cg
brain
β-Catenin
Laminin
sox9
intact
extirpated
control MO
kng MO
cpn MO
nNOS MO
No Bead
+ 9AAscr
+ 9AA
p=0.02
% Control Flour.
kng MO
* p < 0.001 compared to control
** p = 0.04 compared to control
wild type
500 μM TRIM

Figure 2.9

Figure 2.10: NO donor (SNAP) prevented *cpn*, *kng* and *nNOS* LOF phenotypes when injected late, and SNAP rescue is a specific effect. (**A-D**) Embryos were injected with morpholino at the one cell stage. NO donor (SNAP) was injected into the presumptive mouth region at stage 20. Phenotypes of *kng* (**B**), *cpn* (**C**), and *nNOS* (**D**) loss of function using antisense morpholinos are described in detail in Fig. 2.5. (**B'-D'**) Embryos injected with NO donor late, at stage 20. The craniofacial phenotype of *kng*, *cpn* and *nNOS* LOF was prevented by injection of NO donor into the EAD. (*kng* (**B'**) 54% normal, n= 48; *cpn* (**C'**) 79% normal, n=34; *nNOS* (**D'**) 53% normal, n=15) Scale bar: 100μm. (**E-J**) NO specificity for the Kinin-Kallikrein pathway was tested by co-injecting SNAP and morpholino at the one cell stage. Embryos were scored at stage 26. (**E**) Control morphants. (**F-G**) The phenotype of *cpn* LOF was prevented by injection of NO donor SNAP with 82% normal embryos. (**H-I**) No rescue was obtained when SNAP was injected with *par1* morpholino with 0% normal embryos. *Par1* morpholino sequence and phenotype were published by Ossipova et al., 2005. (**J**) Quantification of results.

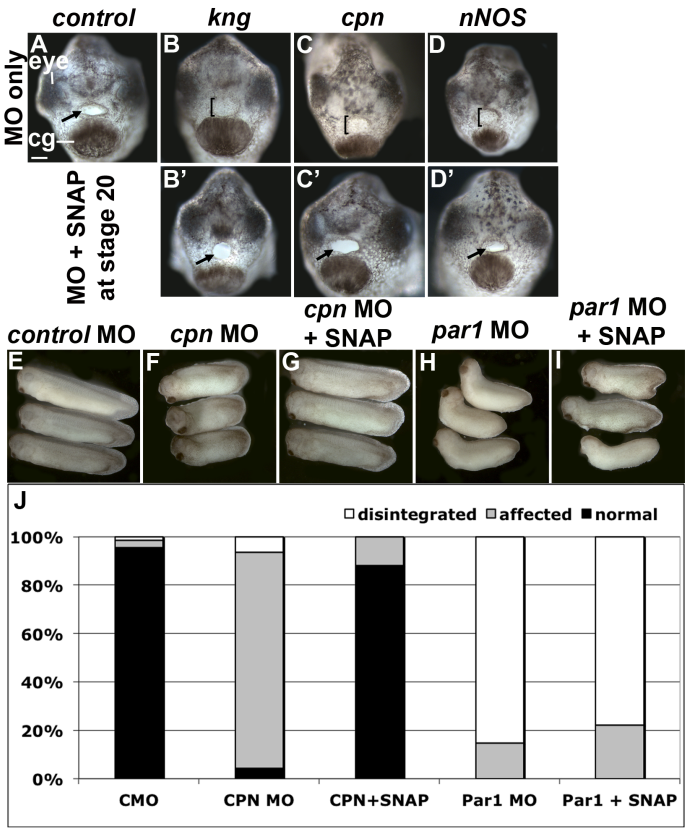
control
kng
cpn
nNOS
A
eye
cg
B
C
D
MO only
B'
C'
D'
MO + SNAP at stage 20
control MO
cpn MO
cpn MO + SNAP
par1 MO
par1 MO + SNAP
E
F
G
H
I
J
disintegrated
affected
normal
100%
80%
60%
40%
20%
0%
CMO
CPN MO
CPN+SNAP
Par1 MO
Par1 + SNAP

Figure 2.10

If NO mediates craniofacial development, it should be detectable in developing facial regions and decrease after *kng*, *cpn*, and *nNOS* LOF. NO was measured by incubating late neurula (stage 20) embryos with DAF-FM diacetate, which emits green fluorescence after reacting with NO. Tail bud (stage 26) control embryos showed fluorescence in the outer epidermis (Figure 2.9U), where *nNOS* is strongly expressed. Diminished fluorescence was seen and quantified in *kng*, *cpn*, and *nNOS* LOF embryos (Figures 2.9V–2.9X and 2.9c). *nNOS* LOF was associated with the smallest reduction in NO production, perhaps due to other NOS isoforms. We predicted that xBdk peptides would increase NO production (Figure 2.2A), and this was confirmed by implanting xBdk-beads into the presumptive mouth region of *kng* morphants (Figures 2.9Y–2.9c). These data demonstrate production of NO in the EAD is dependent on Kinin-Kallikrein gene function, occurs during facial development, and is responsive to xBdk.

2.4 e. *cpn* Is Expressed in the EAD and Is Required Locally for Mouth Opening and Modulates Arginine Levels

Based on LOF phenotypes, we hypothesized that *kng*, *cpn*, and *nNOS* function in the EAD is locally required in the presumptive mouth and globally required for cranial NC development. This was tested by transplanting the EAD from *kng*, *cpn*, and *nNOS* LOF embryos at early tail bud (stage 22) into sibling controls (Figure 2.11A) (Jacox et al., 2014). Control transplants led to normal mouth opening, nostril formation, and pigmentation (Figures 2.11B and 2.11B', and quantified in Figure 2.11F). Strikingly, when *cpn* LOF EAD was transplanted into control embryos, open mouths or nostrils failed to form, and heads were narrow and lacked pigment, similar to global *cpn* LOF (Figures 2.11C and 2.11C'). In contrast, transplant of *nNOS*

and *kng* LOF EAD into control embryos led to milder phenotypes (Figures 2.11D–2.11E'), consistent with the highly preferential expression of *cpn* in the EAD, and more widespread expression of *kng* and *nNOS*. We further showed that *cpn* expression in the EAD is required for cranial NC formation because *sox9* expression at late tail bud is abnormal and reduced after EAD *cpn* LOF transplants (stage 28, Figures 2.11G–2.11H').

The activity of Cpn predicts it modulates levels of Arg (Figure 2.2A). To examine this, we used a quantitative assay where Arg is converted into urea whose levels can be measured (Figure 2.11I). As hypothesized, after *cpn* LOF, lower levels of urea relative to control embryos were present. Specificity was demonstrated as urea levels increased after injection of *cpn* mRNA into LOF embryos (Figure 2.11J). Together, these data indicate a requirement for Cpn activity localized in the EAD during mouth, cranial NC, and face development.

Figure 2.11: Local *cpn* expression is required for mouth opening. Local requirement of *kng*, *cpn*, and *nNOS* expression tested with EAD transplants. (**A**) Experimental design: donor morphant tissue was transplanted to uninjected sibling recipients. (**B–E'**) EAD transplant outcome from control, *cpn*, *kng*, or *nNOS* morphant donor tissue (control [**B**] 100% normal, n = 11; *cpn* [**C**] 28% normal, n = 14; *kng* [**D**] 83% normal, n = 24; *nNOS* [**E**] 61% normal mouth phenotype, 72% normal facial phenotype, n = 18). (**B'–E'**) Overlay of (**B**)–(**E**) with GFP fluorescence indicating donor tissue. Dots surround open mouths. Bracket: unopened mouth. Frontal view. Scale bar: 100μm. (**F**) Quantification of structure depending on morphant background of facial tissue. (**G–H'**) *sox9* expression in *cpn* morphant donor tissue transplants, compared with control morphant transplants. *sox9* in situ hybridization in control morphant transplants (**G**, **G'**, 70% with normal expression, n = 10) and *cpn* morphant transplants (**H** and **H'**, 36% with normal expression, n = 11). Two representative embryos shown. Scale bar: 100μm. (**I and J**) (**I**) Summary of urea assay for analysis of Cpn activity. (**J**) Chart summarizing level of urea derived from free Arg in *cpn* morphants or morphants coinjected with *cpn* RNA, as percent of urea derived from free Arg in control morphants. Urea levels in control morphants and wild-type embryos were equivalent. Each dot represents an independent experiment. p value: one-tailed t test.

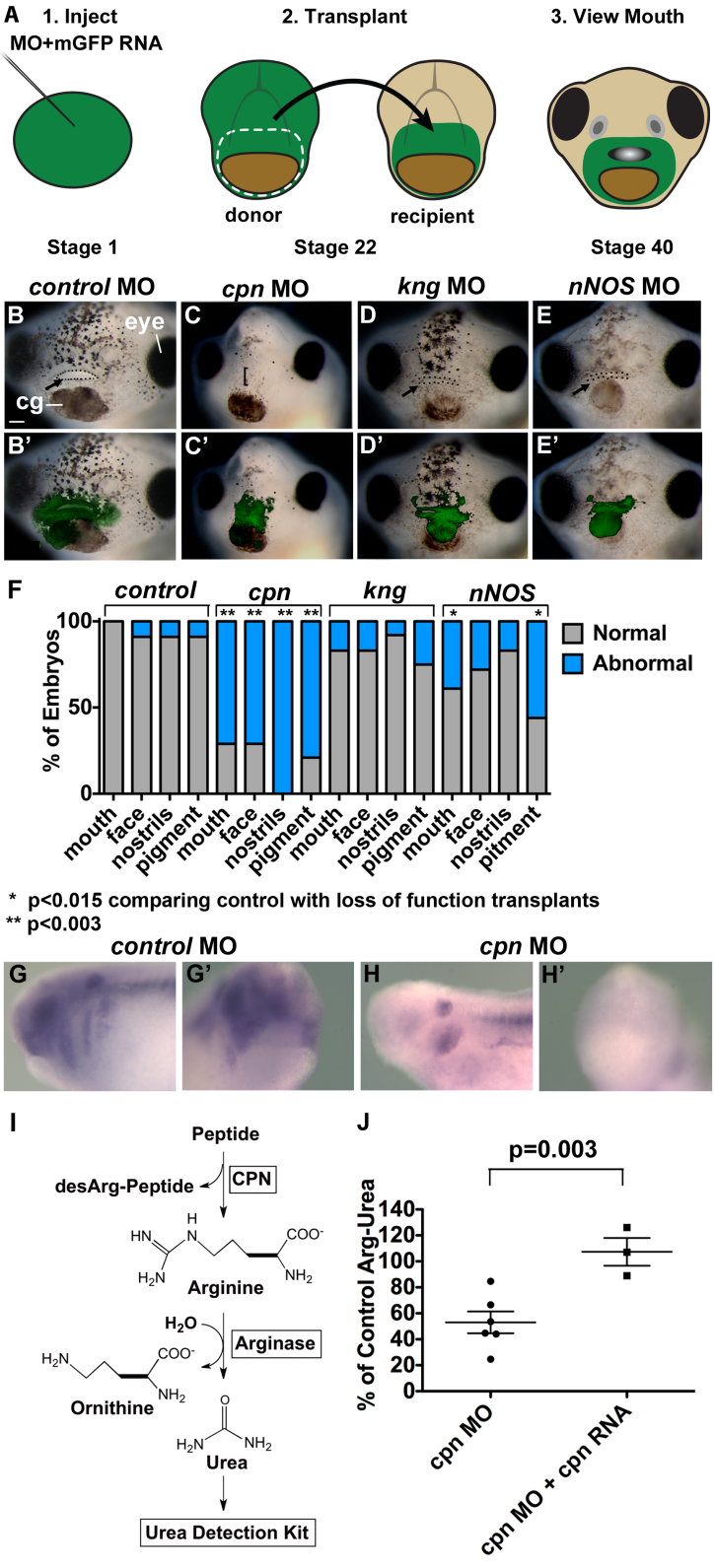
A
1. Inject
MO+mGFP RNA
2. Transplant
3. View Mouth
donor
recipient
Stage 1
Stage 22
Stage 40
control MO
cpn MO
kng MO
nNOS MO
B
eye
cg
C
D
E
B'
C'
D'
E'
F
control
cpn
kng
nNOS
% of Embryos
100
50
0
Normal
Abnormal
mouth
face
nostrils
pigment
pitment
* p<0.015 comparing control with loss of function transplants
** p<0.003
control MO
cpn MO
G
G'
H
H'
I
Peptide
desArg-Peptide
CPN
Arginine
H2O
Arginase
Ornithine
Urea
Urea Detection Kit
J
p=0.003
% of Control Arg-Urea
140
120
100
80
60
40
20
0
cpn MO
cpn MO + cpn RNA

Figure 2.11

2.4 f. Localized *cpn* Activity in the EAD Is Necessary for Migration of First Arch Neural Crest into the Face

The reduction in *sox9* expression with *cpn* LOF suggested that *cpn* expression is required for NC migration. To analyze migration, fluorescent cranial NC was transplanted into control or *cpn* morphant hosts at neurula (stage 18) and scored at late tail bud (stage 28) (Figure 2.12A). Although control transplants displayed three or four distinct branchial arches at late tail bud (stage 28) (Figures 2.12B and 2.12B'), control NC transplanted into *cpn* morphants failed to segregate into branchial arches and did not migrate (Figures 2.12C and 2.12C'), indicating a requirement for Cpn in cranial NC migration.

We extended this to ask whether local *cpn* expression is required for cranial NC migration, using double NC and EAD transplants, where control cranial NC was first transplanted into control embryos, followed by a control or *cpn* morphant EAD transplant (Figure 2.12D). Relative to controls (Figures 2.12E–E'', 2.12I, and 2.12I'), embryos with a c*pn* LOF EAD showed reduced NC migration at late tail bud (stage 28) (Figures 2.12F–2.12F'', 2.12J, and 2.12J'). In particular, first arch NC showed highly reduced migration anteriorly and medially (Figures 2.12J and 2.12J'), demonstrating that *cpn* expression in the EAD is necessary to guide the cranial NC into the face. At tadpole (stage 40), control transplants developed a normal mouth and face with extensive NC-derived tissue (Figures 2.12G–2.12G'') and a normal cartilaginous skeleton (Figures 2.12K and 2.12K'). However, *cpn* EAD LOF transplants failed to form normal mouths or faces (Figures 2.12H and 2.12H') and had substantially less NC-derived tissue (Figure 2.12H'') with deformed Meckel's and ceratohyal cartilages (Figures 2.12L and 2.12L'). These data demonstrate that local Cpn activity in the EAD is required for migration of the first branchial arch into the face, putatively through processing of Kng-derived peptides.

Figure 2.12: Global and local *cpn* expression is required for cranial neural crest migration. Global requirement for *cpn* expression tested with cranial NC transplants. Embryos scored as normal if three or four distinct branchial arches formed and migrated normally. (**A**) Experimental design: donor wild-type cranial NC transplanted into *cpn* morphant sibling recipients. (**B–C'**) (**B and C**) Cranial NC transplant outcomes in control and *cpn* morphant recipients with GFP fluorescence overlay, indicating location of donor transplant at stage 28 (control [**B**] 69% normal, n = 36; *cpn* [**C**] 27% normal, n = 29). (**B' and C'**) GFP fluorescence of cranial NC in control and *cpn* morphant recipient. Numbers indicate branchial arches. Side view. cg, cement gland. Scale bar: 200μm. (**D**) Experimental design: donor *cpn* morphant EAD transplanted into control morphant sibling recipients with fluorescent cranial NC. (**E–H''**) (**E, F, G, and H**) Bright-field view of control and *cpn* morphant transplants at stages 28 and 40. (**E', F', G', and H'**) Cranial NC in control and *cpn* morphant EAD recipients at stages 28 and 40 with GFP fluorescence overlay, indicating location of cranial NC and mCherry fluorescence overlay, indicating location of EAD transplant. (control stage 28 [**E'**] 85% normal, n = 41; *cpn* stage 28 [**F'**] 57% normal, n = 42; control stage 40 [**G'**] 63% normal, n = 38; *cpn* stage 40 [**H'**] 17% normal, n = 35). (**E'', F'', G'', and H''**) GFP fluorescence of cranial NC in control and *cpn* morphant EAD recipients at stage 28 and 40. Arrow: Open mouth. Bracket: unopened mouth. Frontal view. cg, cement gland. Scale bar: 100μm. (**I–J'**) (**I and J**) Cranial NC outcome in control and *cpn* morphant EAD recipients with GFP fluorescence overlay, indicating location of cranial NC at stage 28. (**I' and J'**) GFP fluorescence of cranial NC in control and *cpn* morphant EAD recipients. Numbers indicate branchial arches. Side view. cg, cement gland. Scale bar: 200μm. (**K–L'**) Cartilage in control morphant EAD recipients (**K, K'** 78% normal, n = 14) and *cpn* morphant EAD recipients (**L, L'** 6% normal, n = 16). (**K and L**) Ventral view. (**K' and L'**)

Dorsal view. M, Meckel's cartilage. C, ceratohyal cartilage. Scale bar: 100μm.

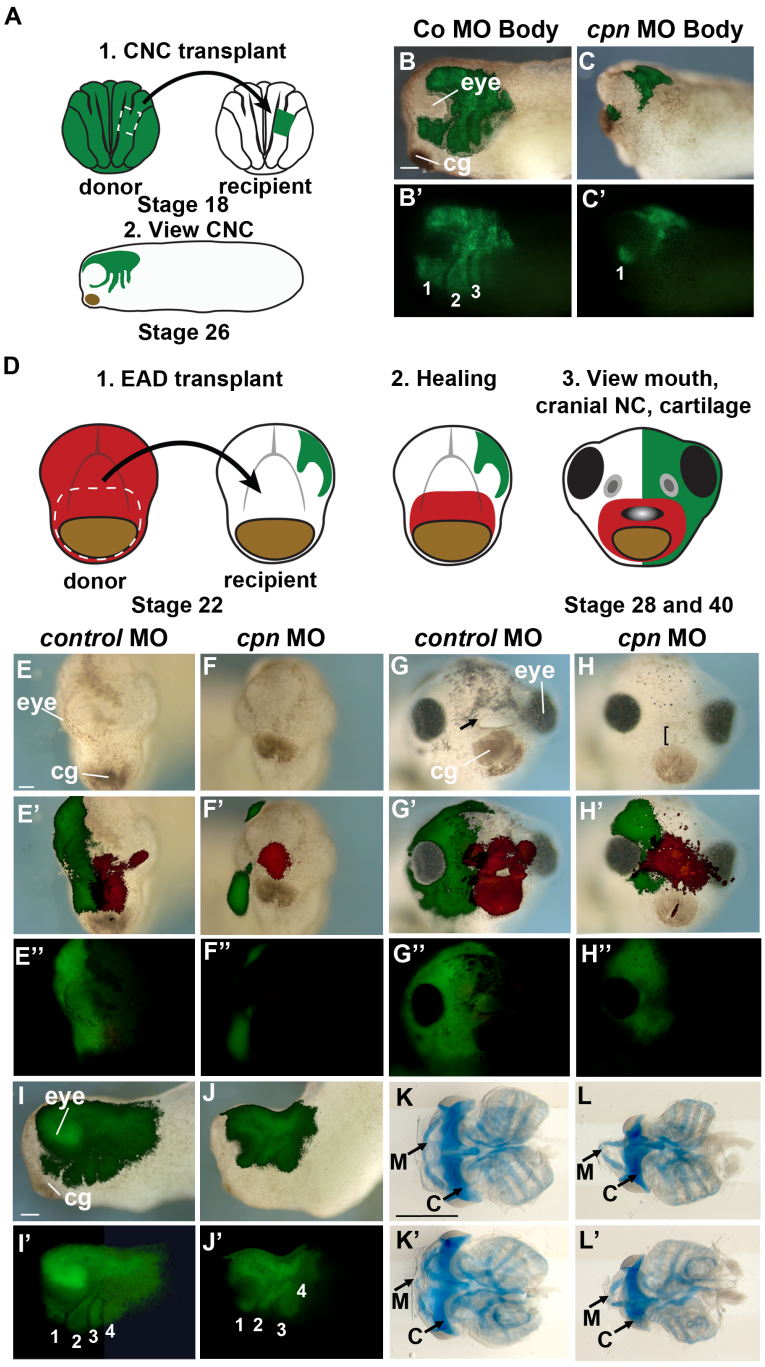
A
1. CNC transplant
donor
recipient
Stage 18
2. View CNC
Stage 26
Co MO Body
cpn MO Body
B
eye
cg
C
B'
1 2 3
C'
1
D
1. EAD transplant
donor
recipient
Stage 22
2. Healing
3. View mouth, cranial NC, cartilage
Stage 28 and 40
control MO
cpn MO
control MO
cpn MO
E
eye
cg
F
G
eye
cg
H
E'
F'
G'
H'
E''
F''
G''
H''
I
eye
cg
J
K
M
C
L
M
C
I'
1 2 3 4
J'
4
1 2 3
K'
M
C
L'
M
C

Figure 2.12

2.4 g. Conservation of *kng* Function during Craniofacial Development in Zebrafish

To investigate whether the function of *kng* in face formation is conserved, we used antisense MOs to target zebrafish (*Danio*) *kng* and assayed facial cartilages in 5 day postfertilization embryos by Alcian blue staining (Figures 2.13A–2.13E' and 2.13F; Figures 2.14A–2.14C' and 2.14D). The MOs used target the *kng1* isoform, the only transcript that includes the 9AA Bdk-l peptide. Zebrafish *kng* is expressed during NC development and mouth opening (Figures 2.14E and 2.14F). *kng* LOF led to abnormally shaped Meckel's and ceratohyal cartilages, or abnormal spacing between Meckel's cartilage and the ethmoid plate. As in *Xenopus*, LOF led to absence of an open mouth (Figures 2.13G–2.13I). The LOF phenotype was prevented by coinjection of zebrafish *kng* that does not bind the MO (Figures 2.13D and 2.13D') or by human *KNG* RNA indicating specificity (data not shown). Morphants injected with *Xenopus laevis kng* RNA showed no rescue (Figures 2.13E and 2.13E') consistent with the greater identity between human and zebrafish Bradykinin than with *Xenopus* (Figure 2.7A).

Sox10::GFP transgenic fish were used to observe NC specification and migration after *kng* LOF. In both controls and morphants, NC was properly specified at the 10-somite stage (data not shown), and migration to form the first and second pharyngeal arches was normal until 48 hpf (Figures 2.13J–2.13Q'). However, by 60 hpf, Meckel's cartilage, derived from the first pharyngeal arch, fails to condense in morphants (Knight and Schilling, 2006). We conclude that zebrafish *kng* is necessary for NC and mouth development, demonstrating a conserved requirement for Kinin-Kallikrein signaling. The phenotypes observed in zebrafish are apparent at a later stage than those observed in *Xenopus*, indicating that temporal control of facial development by Kinin-Kallikrein signaling may differ between species.

Figure 2.13: Function of *kng* in craniofacial development is conserved in zebrafish (**A and A'**) Camera lucida of facial cartilages. E, ethmoid plate. C, ceratohyal cartilage. M, Meckel's cartilage. (**B–E'**) *kng* loss of function using splice morpholinos and rescue with zebrafish (zf) *kng* mRNA. Embryonic cartilage scored at 5 dpf after Alcian blue staining in three independent experiments. Scale bar: 250μm. (**B and B'**) Control morphants co-injected with mRNA were normal (88% normal, n = 50). (**C, C', E, and E'**) *kng* morphants and *kng* morphants coinjected with 200ng *Xenopus kng* mRNA showed abnormal facial cartilage. Meckel's cartilage was truncated, boxy, and pointed at an abnormal angle. The ceratohyal cartilage was positioned at an abnormal angle, perpendicular to the midline. (*kng* [**C and C'**] 3% normal, n = 61; *kng* mo plus frog mRNA [**E and E'**] 0% normal, n = 65). (**D and D'**) *kng* morphants coinjected with 200ng zebrafish (zf) mRNA showed partial rescue. Embryos scored as partially rescued if Meckel's cartilage was longer, more rounded, and pointed dorsally and if ceratohyal cartilage pointed more anteriorly, compared to *kng* morphants (54% partial rescue, n = 89). (**F**) Quantification of phenotypes. p values: one-tailed Fisher's exact test. N, normal or partially rescued phenotype. A, abnormal phenotype. (**G–I**) Ventral views of mApple-injected embryos at 48hpf. White arrow: open mouth. White bracket: closed mouth. Scale bar: 100μm. (**G**) Control morphants (100% normal, n = 5). (**H**) *kng* splice morphants failed to form open mouths (0% normal, n = 6). (**I**) *kng* splice morphants coinjected with 200ng zf mRNA had open mouths (67% normal, n = 6). (**J–Q'**) Confocal images of Sox10::GFP zebrafish coninjected with 75pg mApple and 4ng control morpholino (100% normal, n = 5) or 4ng *kng* splice morpholino (0% normal, n = 5). Paired images of the same embryo show GFP signal alone and GFP with mApple. Numbers indicate pharyngeal arches (PA). Bracket: uncondensed/disorganized cartilage. Lateral view. M, Meckel's cartilage. Scale bar: 100μm. (**J–K'**) At 36 hpf, NC has migrated

into the face of both morphant and control embryos to form first and second PA. (**L–M'**) At 48 hpf, the first PA has begun to extend under eye to form the lower jaw in both morphant and control embryos. (**N and N'**) At 60 hpf, first PA has condensed into Meckel's cartilage in control embryos. (**O and O'**) At 60 hpf, first PA remains disorganized in morphants and does not condense. (**P and P'**) At 72 hpf, Meckel's cartilage is prominent in control embryos. (**Q and Q'**) At 72 hpf, cartilage of the lower jaw remains disorganized and uncondensed in morphants.

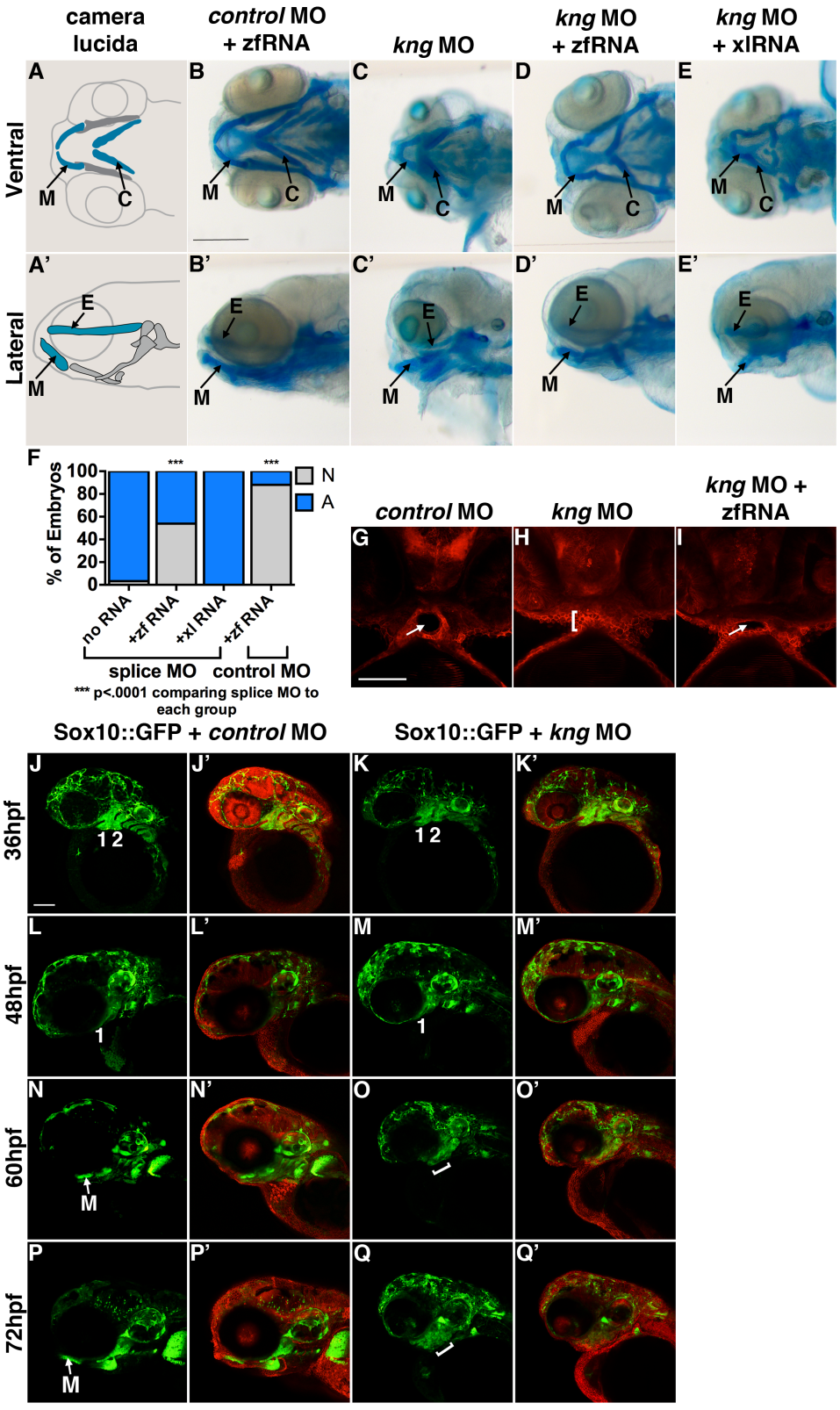
camera lucida
control MO + zfRNA
kng MO
kng MO + zfRNA
kng MO + xlRNA
Ventral
Lateral
A
B
C
D
E
A'
B'
C'
D'
E'
M
C
E
F
% of Embryos
100
80
60
40
20
0
N
A
***
***
no RNA
+zf RNA
+xl RNA
+zf RNA
splice MO
control MO
*** p<.0001 comparing splice MO to each group
control MO
kng MO
kng MO + zfRNA
G
H
I
Sox10::GFP + control MO
Sox10::GFP + kng MO
36hpf
48hpf
60hpf
72hpf
J
J'
K
K'
L
L'
M
M'
N
N'
O
O'
P
P'
Q
Q'
1 2
1

Figure 2.13

Figure 2.14: *kininogen* (*kng*) is expressed throughout zebrafish craniofacial development and loss of function results in craniofacial cartilage abnormalities. (**A-C, A'-C'**) *kng* loss of function using splice site and start site morpholinos. Embryonic cartilage was observed at 5dpf using alcian blue staining in three independent experiments. E, Ethmoid plate. C, Ceratohyal cartilage. M, Meckel's cartilage. Scale bar: 250μm. (**A, A'**) Control morpholino injected embryos appeared normal (95% normal, n=43). (**B-B', C-C'**) Splice and start morphants showed abnormal facial cartilage. Meckel's cartilage is truncated and lies at an abnormal angle. The ceratohyal cartilage points at an abnormal angle, perpendicular to the midline. (*kng* splice morpholino (**B, B'**) 7% normal, n=95; *kng* start morpholino (**C, C'**) 6% normal, n=47). (**D**) Quantification of morphant phenotypes. P-values: one-tailed Fisher Exact test. (**E**) Non-quantitative RT-PCR. *kng* expression is present at bud stage and extends until 72hpf. Expression spans mouth opening at 48hpf and formation of facial cartilage at 72hpf. (**F**) Non-quantitative RT-PCR. RNA was extracted at 24hpf. Controls yield normal length *kng* transcripts, while splice morphants yield fewer normal length transcripts and a truncated transcript. Arrow: truncated transcript band.

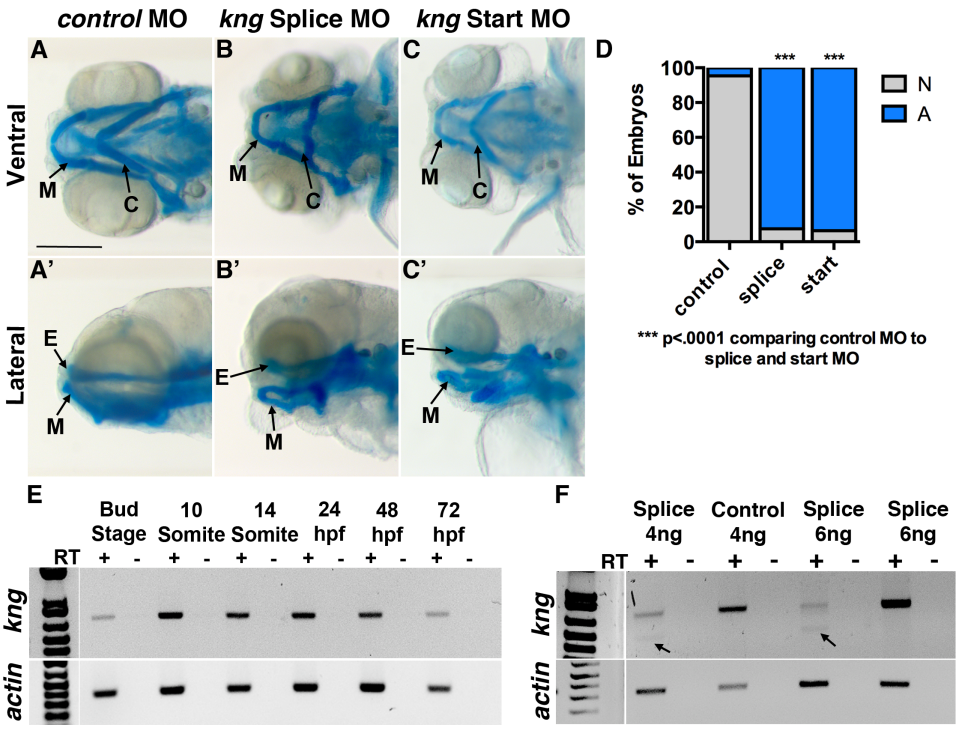
control MO
kng Splice MO
kng Start MO
A
B
C
D
Ventral
M
C
A'
B'
C'
Lateral
E
% of Embryos
100
80
60
40
20
0
***
***
N
A
control
splice
start
*** p<.0001 comparing control MO to splice and start MO
E
Bud Stage
10 Somite
14 Somite
24 hpf
48 hpf
72 hpf
RT + - + - + - + - + - + -
kng
actin
F
Splice 4ng
Control 4ng
Splice 6ng
Splice 6ng
RT + - + - + - + -
kng
actin

Figure 2.14

2.5 Discussion

This study demonstrates activity of the Kinin-Kallikrein pathway during embryogenesis and localized control of craniofacial development through this pathway. Three major conclusions are reached. First, the embryonic pathway in *Xenopus* functions through a signaling sequence similar to that described for the adult mammalian pathway, and conservation is present in zebrafish. Second, nitric oxide (NO) production is an outcome of the pathway and is necessary for mouth and neural crest (NC) development. Third, the extreme anterior domain (EAD) functions as craniofacial organizer and facilitates migration of first arch cranial NC into the face via Kinin-Kallikrein signaling. These findings add insight into localized signaling essential for craniofacial development.

Epistatic relationships demonstrated for the adult pathway appear to be conserved in the embryo, such that loss of function in *kng*, *cpn*, and *nNOS* is overcome by application of the predicted peptide xBdk or by the downstream effector NO. Further, *cpn* activity and xBdk modulate levels of endogenous NO, connecting NO and Kinin-Kallikrein signaling. Consistent with a role in craniofacial signaling, pathway genes are expressed at the front of the embryo; however, their nonoverlapping expression domains suggest that initial processing of Kng to yield xBdk occurs distal to the site of xBdk processing and NO production. We did detect different sensitivity of the embryo for intact xBdk and xBdk after C-terminal Arg removal. Thus, with reduced *cpn* activity, an open mouth is formed in response only to the 8AA peptide, whereas overall face morphology is corrected by both peptides, suggesting that different downstream receptors or alternate forms of peptide processing may be available to the NC.

NO has not previously been appreciated as critical for craniofacial development. In *Xenopus,* it was proposed that NO suppresses cell proliferation and promotes convergent

extension, but a facial phenotype was not explored (Peunova et al., 2007). The requirement for *kng* in zebrafish facial development implies involvement of NO, and this is in accord with effects of treating zebrafish embryos with a NO inhibitor (Kong et al., 2014). In Zebrafish, *NOS* isoforms are expressed in the developing face, specifically in the mandibular primordium and surrounding the oral cavity, consistent with this role (Poon et al., 2003, 2008). Another route to NO production is the endothelin pathway and consistent with our results, mice deficient in *endothelin-1* have craniofacial abnormalities (Kurihara et al., 1994).

The demonstration that the EAD is necessary for migration of the first arch NC into the facial region addresses the long-standing question of what region might guide the migratory cranial NC into the face. Our findings not only underscore the organizer capacity of the EAD, but identify *cpn* locally expressed in the EAD as required for NC ingress, possibly through processing of Kng-derived peptides. Consistent with a guidance function for xBdk, midline or lateral placement (into the EAD) of xBdk-impregnated beads was sufficient to overcome the NC migration defect after Kinin-Kallikrein LOF. Bradykinin is promigratory in other settings, for malignant cells and trophoblasts, whereas NO is involved in inflammation-induced cell migration (Chen et al., 2000; Cuddapah et al., 2013; Erices et al., 2011; Yu et al., 2013). Interestingly, another substrate for CPN is C3a, a small complement peptide required for more local aspects of cranial NC migration (Carmona-Fontaine et al., 2011; Matthews et al., 2004).

In addition to a role for Kinin-Kallikrein signaling in NC migration, *kng* is necessary for NC induction, whereas *cpn* is needed later for NC proliferation and survival, highlighting complex spatiotemporal requirements for Kinin-Kallikrein signaling during NC development. Unlike NC specification, mouth specification does not depend on Kinin-Kallikrein signaling. However, mouth opening is tightly linked to NC that abuts the EAD, suggesting that the Kinin-

Kallikrein pathway may indirectly regulate mouth opening through the NC. Consistently, application of a xBdk peptide or NO donor after mouth specification and neural tube closure restored a normal NC, normal face morphology, and concomitantly an open mouth to LOF embryos.

Genes that encode Kinin-Kallikrein pathway factors are found in all vertebrates, raising the question of whether activity of this pathway during craniofacial development is conserved. The requirement for *kng* function during zebrafish NC development and mouth formation supports broad conservation. Additionally, ACE inhibitors that stabilize Bradykinin, used to treat high blood pressure, are teratogens associated with human craniofacial defects (Barr and Cohen 1991). In mammals, single-gene LOF in Kinin-Kallikrein pathway proteins do not obviously result in craniofacial defects (Cheung et al., 1993; Mashimo and Goyal, 1999; Merkulov et al., 2008; Mueller-Ortiz et al., 2009); however, certain double mutants or compound heterozygotes have not been examined. Humans heterozygous for CPN function suffer from angioedema without developmental manifestation; however, no reported patients have complete CPN deficiency, indicating an essential function for this protein (Matthews et al., 2004). A screen for mouse genes involved in craniofacial development identified a Glutamate Carboxypeptidase and a Protein Inhibitor of Nitric Oxide (PIN), suggesting that NO activity is involved in mammalian facial development (Fowles et al., 2003). It is also possible that redundant genes or another pathway such as endothelin signaling work together with Kinin-Kallikrein signaling.

Our study defines the Kinin-Kallikrein pathway and nitric oxide as key for craniofacial development in *Xenopus* and zebrafish and addresses the long-standing question of how the NC specifically moves into the face. The observations suggest important future directions, including mechanistic studies addressing a putative NC guidance function for xBdk and other EAD-

derived activities, and the relationship between NC migration and mouth formation.

2.6 Acknowledgements

We thank our colleagues for discussion and critical input, especially Jasmine McCammon and Ryann Fame. Thanks to George Bell for help with bioinformatics, Nicki Watson and Wendy Salmon for imaging support, and Tom diCesare for assistance with graphics. We thank Eric Liao for his gift of Sox10::GFP fish, for collegial discussion, and for communicating results prior to publication. Thanks to Natalia Peunova, Andrey Zaraisky, and Jean-Pierre Saint-Jeannet for gifts of plasmids. We are grateful to the NIDCR for support (1R01 DE021109-01 to H.S. and F30DE022989 to L.J.), Harvard University for the Herschel Smith Graduate Fellowship (to L.J.), and the American Association of Anatomists (for a postdoctoral fellowship to R.S.).

Chapter 3

Mouth Morphogenesis Requires Interaction Between Neural Crest and the Extreme Anterior Domain through Wnt/PCP Signaling

Author Contributions: L.J. designed and conducted all experiments, and wrote and revised the manuscript drafts with H.S. Technical assistance was provided by A.R. for in situ hybridizations and immunohistochemistry in Figures 3.4, 3.5, 3.7, 3.8, and 3.9. H.L. created the claymation demonstrating midline convergent extension shown in Figure 3.4X-a. H.S. directed and supervised the study and assisted in writing and revising the manuscript.

Publication: Jacox, L., Rothman, A., Lathrop-Marshall, H., & Sive, H. Mouth morphogenesis requires interaction between neural crest and the extreme anterior domain through Wnt/PCP signaling. Manuscript is awaiting submission to *Cell Reports.*

3.1 Abstract

The extreme anterior domain (EAD) is a signaling center that facilitates migration of cranial neural crest (NC) towards the facial midline in *Xenopus*. We show here that cranial NC reciprocally signals to the EAD to mediate mouth formation (Figure 3.1). Initially, the EAD forms a wide and short epithelial mass that becomes narrower and longer after arrival of cranial NC. Cells and nuclei change shape, indicating convergent extension, and the narrowed region opens to form the mouth. Since EAD convergent extension does not occur in the absence of cranial NC, we hypothesized that this tissue sends a Wnt/PCP signal to mediate EAD morphogenesis. In support of this, the receptor Fzl7 is locally required in the EAD while Wnt11 ligand is required more globally. Heterologous cells expressing Wnt11 are sufficient to substitute for cranial NC in mediating EAD convergent extension. The study identifies a crucial mechanism during normal mouth development.

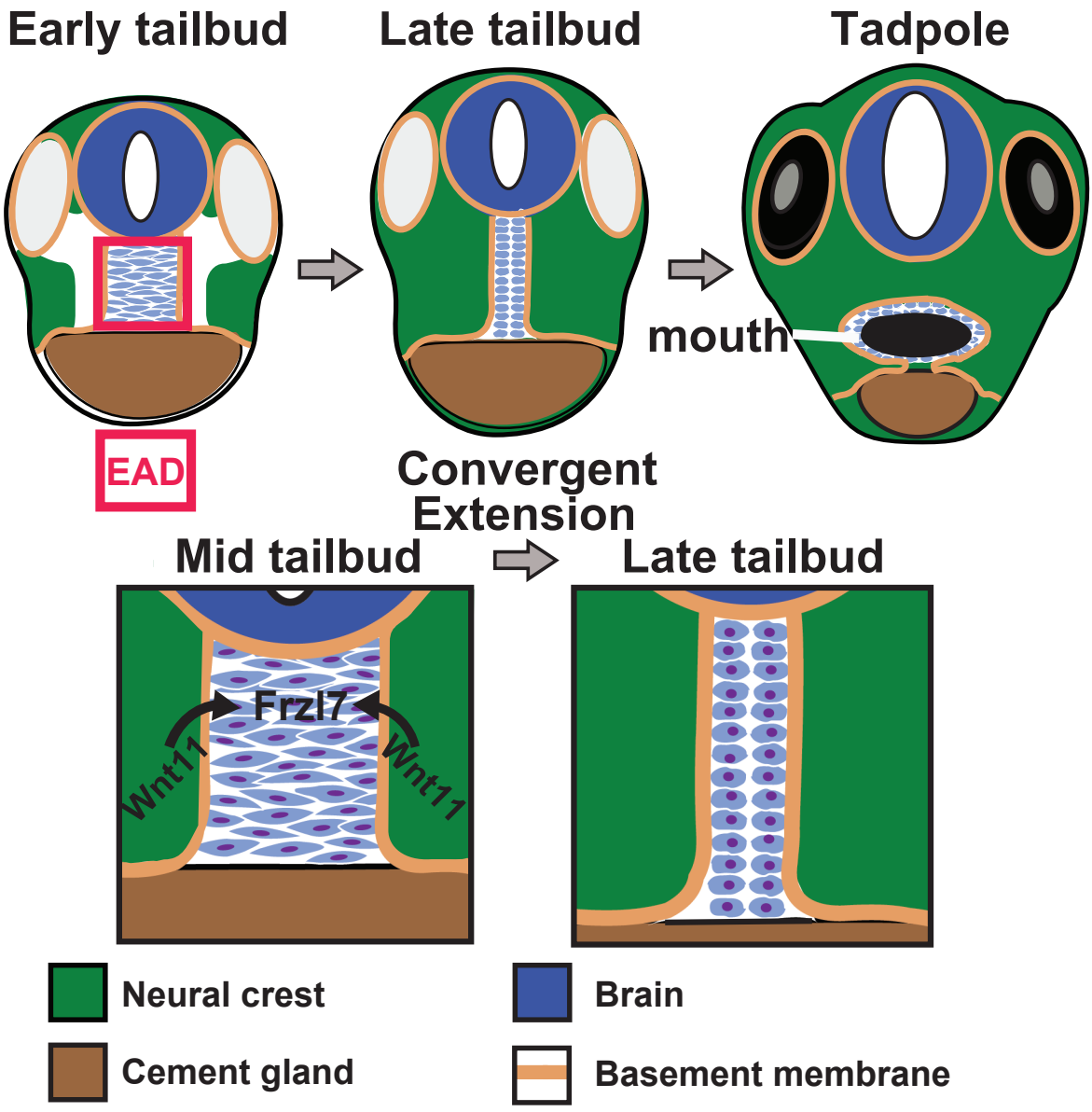

Figure 3.1: Graphical Abstract

3.2 Introduction

The extreme anterior domain (EAD) is a conserved region throughout deuterostomes, where anterior ectoderm and endoderm are directly juxtaposed, without intervening mesoderm (Dickinson and Sive, 2006). Our previous work in *Xenopus* showed that this region is a craniofacial organizer that is required for neural crest (NC) ingression towards the midline (Jacox and Sindelka et al., 2014).

The EAD also contributes to the initial mouth opening of the tadpole (Dickinson and Sive, 2006; Dickinson and Sive, 2009; Jacox and Sindelka et al. 2014). Mouth development from the EAD occurs through multiple sequential steps. These include setting aside the anterior region of the nascent face characterized by expression of *pitx* genes, at neurula. The basement membrane (BM) between EAD ectoderm and endoderm then dissolutes. Tissue morphogenesis forms the stomodeal invagination and the ectoderm undergoes a burst of apoptosis, thinning the tissue (Dickinson and Sive, 2006). Thinned ectoderm and endoderm layers intercalate to form the buccopharyngeal membrane, which perforates to open the mouth at swimming tadpole stage.

The EAD is the earliest facial element, and is present across the anterior midline before the NC migrates into the face (Dickinson and Sive, 2007; Spokony, 2002). The NC comes to lie on either side of the EAD prior to its differentiation to form the bulk of facial tissue. In a previous study (Jacox and Sindelka et al., 2014), we noticed that prior to NC ingression, the EAD ectoderm forms a wide, short mass. Subsequent to NC arrival, EAD tissue becomes longer and narrower, suggestive of convergent extension associated with or caused by the adjacent NC.

Convergent extension (CE) is a major morphogenetic process whereby a group of epithelial cells rearranges by intercalation to extend the length of the cell sheet. CE has been

studied extensively in *Xenopus* and zebrafish axial mesoderm during gastrulation, and is mediated by non-canonical Wnt or Planar Cell Polarity (PCP) signaling factors (Roszko et al., 2009). These factors are expressed on the migrating NC where they are required for proper NC migration, mediating contact inhibition of locomotion in *Xenopus* (Carmona-Fontaine et al., 2008).

Based on bulk EAD elongation, we hypothesized that the EAD undergoes CE under instruction of the incoming first arch cranial NC, and via Wnt/PCP signaling. We present data that supports this hypothesis and identifies an essential reciprocal interaction between the cranial NC and EAD required for normal craniofacial and mouth development.

3.3 Methods

3.3 a. Embryo Preparation

Xenopus laevis embryos were cultured using standard methods (Sive et al., 2000). *Xenopus* embryos were staged according to Nieuwkoop and Faber, 1994.

3.3 b. DiI Labeling and Transplants

All fate mapping and transplants were done in 0.5x Modified Barth's Solution (MBS). Fate mapping was performed by injecting 5-10nl drop of 1,1-dioctadecyl-3,3,3,3-tetramethylindocarbocyanin (DiI; 2mg/ml, Molecular Probes) or DiO (2mg/ml, Molecular Probes) into the EAD or ANR ectoderm at early or late neurula stages. Embryos were photographed and fixed at tail bud and tadpole stages for immunohistochemistry. EAD transplants were performed according to Jacox et al., 2014. NC transplants were performed according to Mancilla and Mayor, 1996. Animal cap transplants were performed on late neurula control or *sox9* morphants, injected with 5-7ng of morpholino. Tissue lateral to the EAD in morphants was extirpated using a 1mm diameter capillary tube pulled to a fine point. Animal caps were removed from embryos injected with 1000ng of either inactive MMP11 (control) or Wnt11 mRNA plus 1000ng of mApple mRNA. Animal cap tissue was transplanted into the face of extirpated morphants, and held in place with glass bridges for 1-2 hours. Transplants were cultured until late tail bud, photographed, fixed, and sectioned for immunohistochemistry.

3.3 c. In Situ Hybridization

cDNA sequences used to transcribe in situ hybridization probes including *cpn* (BC059995), *sox9* (AY035397), *frzl7* (De Calisto et al., 2005), *wnt11* (Tada and Smith, 2000), *pitx1* (Schweickert et al., 2001), *pitx2c* (Schweickert et al., 2001), *frzb1* (BC108885), and *XCG*

(Sive, 1989). In situ hybridization was performed as described by Sive et al., 2000, without proteinase K treatment. Double-staining protocol adapted from Wiellette and Sive, 2003.

3.3 d. Morpholinos and RNA Rescues

Xenopus antisense morpholino-modified oligonucleotides ("morpholinos; MOs") included start site MOs targeting *fzl7* (31ng injected, Winklbauer et al., 2001), *wnt11* (9ng injected, Pandur et al., 2002), and *sox9* (5ng injected, Spokony et al., 2002). Referenced studies demonstrated morpholino specificity via morpholino and RNA co-injection at the one cell stage; RNA prevented morphant phenotypes. *wnt11* mRNA (De Rienzo et al., 2011), truncated *Dep+ disheveled* mRNA (Sokol, 1996; Tada and Smith, 2000) and noncatalytic *mmp11* (gift of Malcolm Whitman) were generated from plasmids.

3.3 e. Immunohistochemistry

Immunohistochemistry was performed as described (Dickinson and Sive, 2006). Caspase-3 and PH3 labeling were performed according to Kennedy and Dickinson, 2012 and Dickinson and Sive, 2009. Primary antibodies included a rabbit, polyclonal anti-Laminin antibody (Sigma L-9393) diluted 1:150, a rabbit, polyclonal anti-β-catenin antibody (Invitrogen) diluted 1:100, a mouse, monoclonal anti-brdu antibody (Becton Dickinson 347580) diluted 1:750, and a mouse, monoclonal anti-Zo-1 antibody (Invitrogen) diluted 1:100.

The secondary antibodies included Alexa 488 and 647 goat anti-rabbit (Molecular Probes) and Alexa 488 goat anti-mouse (Molecular Probes) diluted 1:500 with 0.1% propidium iodide (Invitrogen) or Hoersch (Life Technologies) as a counterstain. Phalloidin (Life Technologies), an actin dye, was used in combination with DiI labeling. Sections were imaged

on a Zeiss LSM 710 Laser Scanning Confocal microscope. Images were analyzed using Imaris (Bitplane) and Photoshop (Adobe).

3.3 f. Wnt/PCP Inhibitor Assays

Rock inhibitor (Y-27632 Calbiochem, stock: 20mM in DMSO, working: 200μM in 2% DMSO, -80°C storage), Rac1 inhibitor (NSC23766 Santa Cruz, stock: 37mM in DMSO, working: 200μM in 2% DMSO, -20°C storage), Rho inhibitor (CCG-1423 Calbiochem, stock: 22mM in DMSO, working: 200μM in 2% DMSO, -20°C storage), and Jnk inhibitor (SP600125 Sigma, stock: 20mM in DMSO, working: 200μM in 2% DMSO, 4°C storage) were resuspended in DMSO, aliquoted, and stored at stock concentrations until incubation with beads. AG 1-X2 Resin beads (Bio Rad, 140-1231, 50-100 mesh) were washed in ethanol, dried, mixed with diluted, working concentration inhibitor solution, and incubated overnight at 4°C. Late neurula embryos had a small incision cut in their facial midline where the bead was inserted into the foregut behind the EAD. Embryos were grown to late tail bud for fixation and immunohistochemistry and to swimming tadpole for live imaging.

3.4 Results

3.4 a. Extreme Anterior Domain (EAD) Ectoderm Contributes to the Tadpole Face and Is Derived from the Anterior Neural Ridge

Prior work (Dickinson and Sive, 2006) showed that the EAD contributed to the initial mouth opening of the tadpole ('primary mouth'), however only limited lineage labeling analysis was performed. To determine the derivatives and source of the EAD ectoderm, a fate map for the EAD was assembled by labeling EAD ectoderm tissue with a lipophilic dye, DiI, and tracking development from late neurula (stage 20) to mouth opening at swimming tadpole stage (stage 40) (Fig. 3.2A). We initially hypothesized that EAD tissue apoptosed to produce the oral opening. Though a wave of apopotosis does occur (Dickinson and Sive, 2006), remaining EAD ectoderm contributed to the tadpole face as demonstrated by DiI labeling of the anterior pituitary (AP) and the lining of the nostrils and oral cavity (Fig. 3.2B-I, h-i). To assay cell mixing in the EAD, DiI and DiO were injected into top and bottom or lateral regions of EAD ectoderm (Fig. 3.2J-Y). Minimal cell mixing was observed both vertically and laterally in the EAD ectoderm.

Published chick, zebrafish, mammal and *Xenopus* studies suggest that anterior neural ridge (ANR) gives rise to presumptive oral ectoderm, however only limited analysis has been performed (Chapman et al., 2005; Couly and LeDouarin, 1985, 1987; Eagleson et al., 1995; Osumi-Yamashita et al.,1994; Schwind, 1928). ANR labeled with diI at early neurula localized to the EAD ectoderm and brain at late neurula and to the AP, lining of the nostrils, and oral cavity, at swimming tadpole stages, akin to EAD ectoderm fatemaps (Figures 3.2A, Z-g, j, Figure 3.2k: orange- future nostril lining; purple- future AP; blue- future oral cavity lining).

Figure 3.2: The Extreme Anterior Domain (EAD) gives rise to the anterior pituitary (AP), and the lining of the mouth and nostrils, and derives from the anterior neural ridge (ANR). (**A**) Schematic. (**B-E**) Representative embryo, labeled with DiI in the EAD ectoderm, photographed at four time points (n= 23 from 7 experiments, 78% with label in AP, 100% with label in oral lining, 44% with label in nostril lining). ap, anterior pituitary. cg, cement gland. mo, mouth. Scale bars: 200 μm. (**F-I**) Representative DiI labeled embryo sections at st. 24 (**F**), st. 35 (**G**), and st. 41 (**H, I**) with actin counterstain. Scale bar: 200μm. (**J-M**) Representative embryo, labeled with DiI in the superior half of the EAD ectoderm, photographed over time (n=12 from 3 experiments, 100% with label in AP, 100% with label in upper oral lining, 0% in lower oral lining, 100% with label in nostril lining). (**N-Q**) Representative embryo, labeled with DiI in the inferior half of the EAD ectoderm, photographed over time (n=11, 9% with label in AP, 45% with label in upper oral lining, 100% in lower oral lining, 18% with label in nostril lining). (**R-U**) Representative embryo sections at stage 41, either DiI-labeled in the top (**R, S**) or bottom (**T,U**) half of EAD, with actin counterstain. (**V-Y**) Representative embryo, labeled with DiI in the middle EAD ectoderm and DiO in the lateral EAD ectoderm, photographed over time (n=14 from 3 experiments). (**Z-c**) Representative embryo labeled with DiI in the anterior neural ridge, photographed at four time points. (n= 37 from 8 independent experiments, 73% with label in AP, 100% with label in mouth, 64% with label in nostrils). (**d-g, j**) Representative DiI labeled embryo sections at stage 20 (**d**), stage 26 (**e**), stage 35 (**f**), and stage 41 (**g,j**) with actin counterstain. (**h,i**) In situ hybridization for *pitx1* and *pitx2c.* ap, anterior pituitary. cg, cement gland. Scale bars (**A-Z, a-g**): 200μm. Scale bar (**h**): 1000μm. (**k**) Schematic of EAD development. Purple: Future anterior pituitary and lining of upper mouth. Orange: Future nostril

lining. Blue: future lining of lower mouth. ANR, anterior neural ridge. EAD, extreme anterior domain. ap, anterior pituitary. cg, cement gland. no, nose. nt, neural tube.

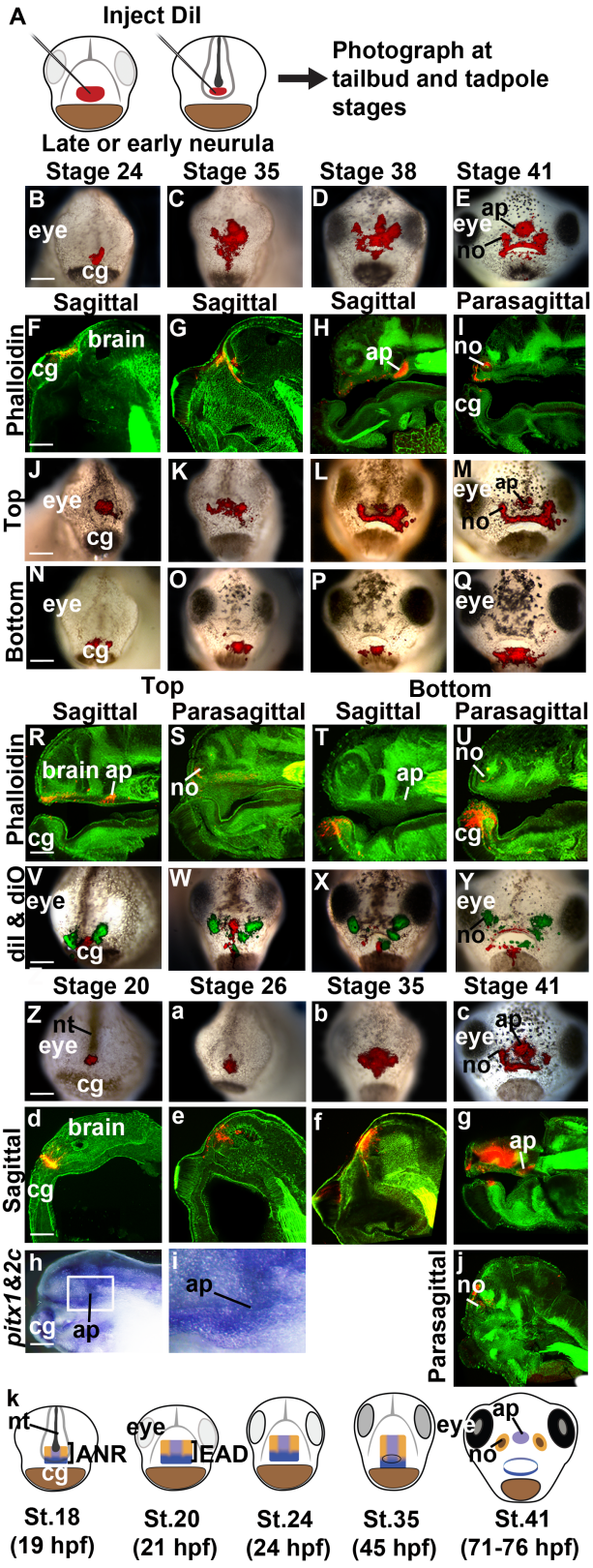
A
Inject DiI
Photograph at tailbud and tadpole stages
Late or early neurula
Stage 24
Stage 35
Stage 38
Stage 41
Sagittal
Parasagittal
Phalloidin
Top
Bottom
dil & diO
Stage 20
Stage 26
pitx1&2c
eye
cg
brain
ap
no
nt
ANR
EAD
St.18 (19 hpf)
St.20 (21 hpf)
St.24 (24 hpf)
St.35 (45 hpf)
St.41 (71-76 hpf)

Figure 3.2

3.4 b. EAD Ectoderm Undergoes Basement Membrane Remodeling, Convergent Extension and Subsequently Opens to Form the Mouth

To understand how the early EAD develops into its derivatives, we performed a coronal and sagittal time course study, analyzing adherens junction (β-catenin) and basement membrane (laminin) localization from late neurula (stage 22) to swimming tadpole (stage 40) (Figures 3.3, 3.4).

Sagittally, β-catenin positive ectoderm began as a triangular region, continuous with brain tissue at neurula (stage 20) (bracket, Figures 3.3B, B', J, J'), and enlarged to form a thin rectangle between the brain and cement gland by late neurula (stage 22) (bracket, Figures 3.3C, C'). At stage 21-22, basement membrane (BM) divided the brain and EAD into distinct regions (Figures 3.3K, K'), and two patchy BMs appeared, separating inner from outer ectoderm and ectoderm from endoderm. Parasagittaly, the β-catenin-enriched, outer ectoderm remained one to two cells thick but lengthened in height (Figures 3.3F-I, F'-I'). A patchy BM between brain and EAD is seen at stage 20 (Figures 3.3N, N'), and at stage 22, BM separates inner and outer ectoderm (Figure 3.3O, O').

At tail bud stages (stages 26, 28), sagittal EAD ectoderm lengthened and widened, forming a large rectangle stretching from brain to cement gland (bracket, Figures 3.3D-E, D'-E'). A thick sheet of laminin coated these midline cells at stage 26, concomitant with NC abutting the midline (Figures 3.3L, L', 3.5K-L). At stage 28, the laminin wall dissipated to form a patchy haze (Figures 3.3M, M'). Parasagittally, at stage 26, a thin perimeter of laminin wrapped around the EAD ectoderm, separating it from the brain superiorly, cement gland inferiorly, outer ectoderm anteriorly, and endoderm posteriorly (Figures 3.3P-P'). By stage 28, the parasagittal laminin BM separating the ectoderm from endoderm disappeared (Figures 3.3Q-

Q'). The roles of particular BMs and the rationale for their carefully timed deposition and breakdown are not known and are being investigated separately.

Figure 3.3: Sagittal anatomy of *Xenopus* face between late neurula and swimming tadpole**.** (**A**) Schematic of sagittal facial development from stages 22-28. (**B-I, B'-I'**) Sagittal and parasagittal sections assayed in 2 independent experiments (n=5-9) with β-catenin immunolabeling. Midline region with bright β-catenin labeling is EAD ectoderm. Bracket: region of 10x image (**B-E**) enlarged in 25x view (**B'-E'**). cg, cement gland. Scale bar (10x): 170μm. Scale bar (25x): 68μm. (**J-Q, J'-Q'**) Sagittal and parasagittal sections assayed in 2 independent experiments (n=5-9) with Laminin (green) immunolabeling with Propidium Iodide (PI) nuclear counterstain (red). Bracket: region of 10x image (**F-I**) enlarged in 25x view (**F'-I'**). cg, cement gland. Scale bar (10x): 170μm. Scale bar (25x): 68μm.

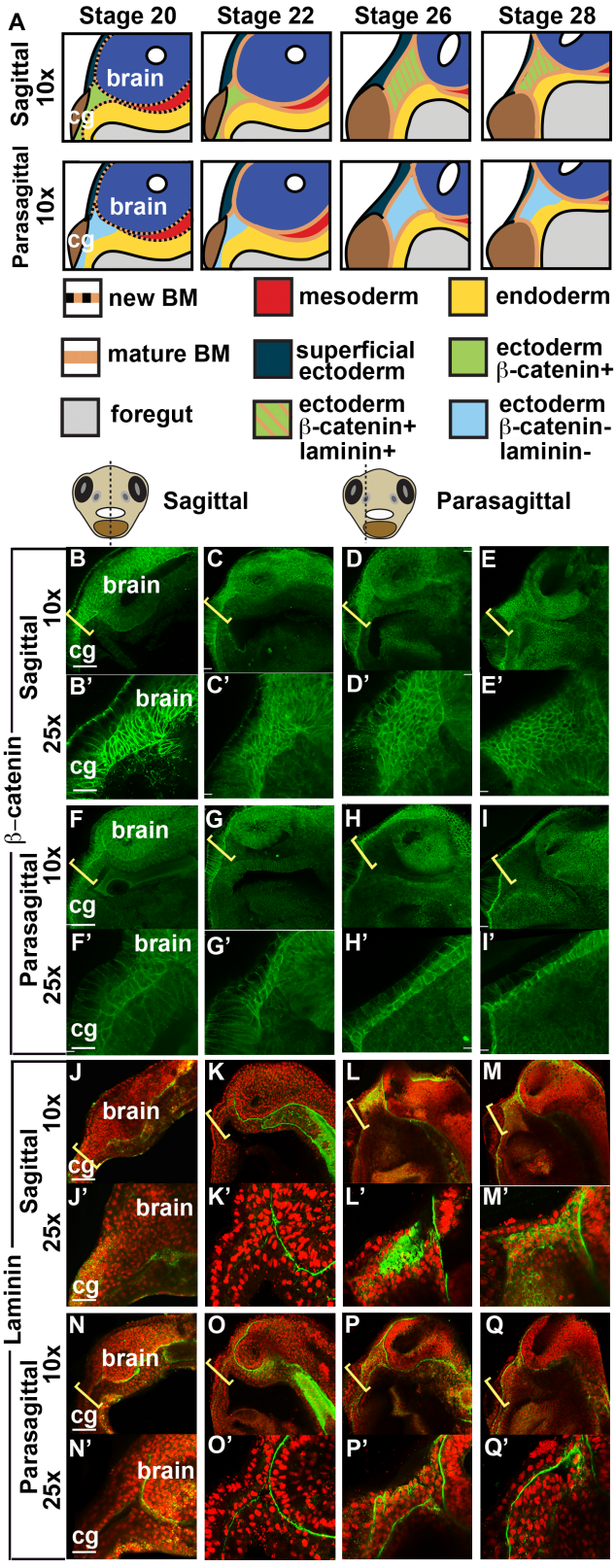
A
Stage 20
Stage 22
Stage 26
Stage 28
Sagittal 10x
Parasagittal 10x
brain
cg
new BM
mature BM
foregut
mesoderm
superficial ectoderm
ectoderm β-catenin+ laminin+
endoderm
ectoderm β-catenin+
ectoderm β-catenin- laminin-
Sagittal
Parasagittal
β-catenin
Laminin
B
B'
C
C'
D
D'
E
E'
F
F'
G
G'
H
H'
I
I'
J
J'
K
K'
L
L'
M
M'
N
N'
O
O'
P
P'
Q
Q'
10x
25x

Figure 3.3

Figure 3.4: Coronal anatomy of *Xenopus* face between late neurula and swimming tadpole, demonstrating convergent extension of midline ectoderm. (**A**) Schematic of facial development from st. 22-28. (**B-E, B'-E'**) Coronal sections assayed in 2 independent experiments (n=5-9) with β-catenin immunolabeling. Midline region with bright β-catenin labeling is EAD ectoderm. Bracket: region of 10x image (**B-E**) enlarged in 25x view (**B'-E'**). cg, cement gland. Scale bar (10x): 170μm. Scale bar (25x): 68μm. (**F-I, F'-I', F''-G''**) Coronal sections assayed in 2 independent experiments (n=5-9) with Laminin (green) immunolabeling with Propidium Iodide (PI) nuclear counterstain (red). Bracket: region of 10x image (**F-I**) enlarged in 25x view (**F'-I'**). White box: region of 25x image (**F'-G'**) enlarged in (**F''-G''**) view. cg, cement gland. Scale bar (10x): 170μm. Scale bar (25x): 68μm. (**J**) Quantification of height over width of EAD midline tissue. Height was counted as number of cells between the top of the cement gland and the bottom of the brain. Width was counted as the number of cells between the left and right borders of the bright, β-catenin positive midline or between the left and right midline Laminin basement membranes. Error bar: standard deviation. (**K-N, K'-N'**) Coronal sections with β-catenin (green) immunolabeling with PI nuclear counterstain (red) from stages 22-28. (**K'-N'**) Cell membranes traced in white, 6 representative cells per panel. (**K''-N''**) Cell outlines of traced cells in black. (**K'''-N'''**) Nuclei of traced cells. Dotted line: top of cement gland, cg. Scale bars (40x): 43μm. (**O**) Schematic of facial development from st. 35/36-40. (**P-S, P'-S'**) Coronal sections assayed in 2 independent experiments (n=5-9) with β-catenin immunolabeling. Bracket: region of 10x image (**P-S**) enlarged in 25x view (**P'-S'**). cg, cement gland. Scale bar (10x): 170μm. Scale bar (25x): 68μm. (**T-W, T'-W'**) Coronal sections assayed in 2 independent experiments with Laminin (green) immunolabeling with PI nuclear counterstain (red). Representative image shown (n=5-9). Bracket: region of 10x image (**T-W**) enlarged in 25x view (**T'-W'**). cg, cement

gland. Scale bar (10x): 170μm. Scale bar (25x): 68μm. (**X-a**) Still frames from claymation of mouth opening.

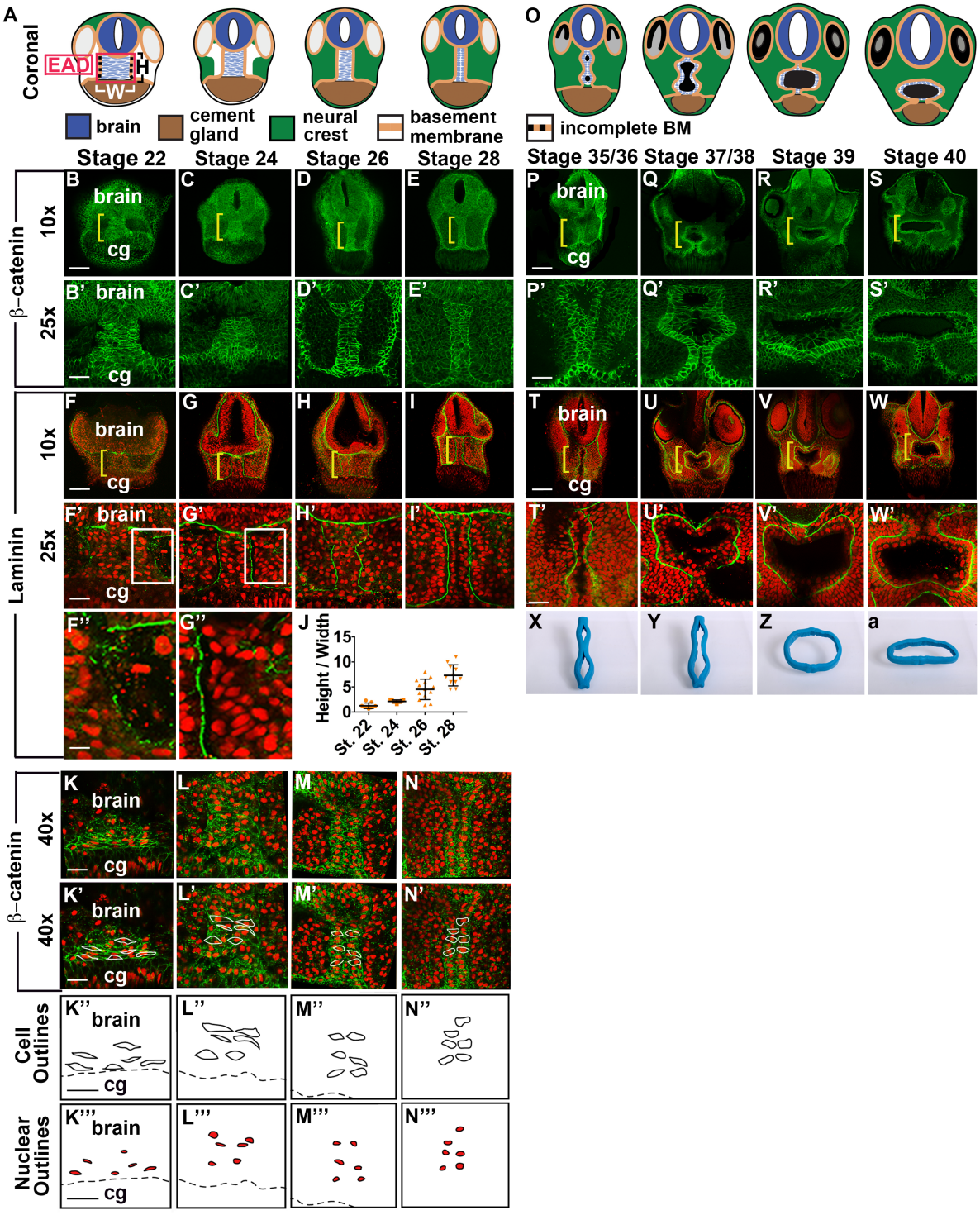
A
Coronal
EAD
H
W
brain
cement gland
neural crest
basement membrane
O
incomplete BM
Stage 22
Stage 24
Stage 26
Stage 28
Stage 35/36
Stage 37/38
Stage 39
Stage 40
β-catenin
10x
25x
Laminin
40x
Cell Outlines
Nuclear Outlines
brain
cg
Height / Width
St. 22
St. 24
St. 26
St. 28

Figure 3.4

Figure 3.5: Midline ectoderm undergoes convergent extension (CE) as the cranial neural crest (NC) approaches the midline and midline CE fails to occur in *sox9* morphants. (**A**) Experimental schematic. (**B-F, B'-F', B''-F''**) Representative embryo with mGFP labeled cranial NC and mCherry labeled EAD tissue from late neurula (stage 21) to swimming tadpole (stage 40) (n= 13, from 3 experiments). (**B-F**) bright field with cranial NC channel (green) and EAD channel (red) overlaid. (**B'-F'**) Green, cranial NC, mGFP channel. (**B''-F''**) Red mCherry, EAD channel. cg, cement gland. Scale bars: 200µm. (**G-L**) In situ hybridization for *cpn* (**G-I**) and *sox9* (**J-L**) at late neurula, early and late tail bud. RNA is purple. Cement gland marker (*xcg*) is red. Bracket: presumptive mouth. cg, cement gland. Scale bars: 200µm. (**M-N**) Frontal view of control and *sox9* morphants at swimming tadpole (stage 40) assayed in 2 experiments (*control* MO (**M**) n=24; *sox9* MO (**N**) n=30.) Bracket: unopened mouth. Dots surround open mouth. cg, cement gland. Scale bar: 200µm. (**O-P, O'-P'**) Coronal sections assayed in 4 independent experiments (n=23) with β-catenin immunolabeling. Midline region with bright β-catenin labeling is EAD ectoderm. Bracket: region of 10x image (**O-P**) enlarged in 25x view (**O'-P'**). cg, cement gland. Scale bar (10x): 170µm. Scale bar (25x): 68µm. (**Q**) Graph depicting percent of morphants, displaying mouth, face, nostrils and pigment formation phenotypes at st. 40 in control and *sox9* morphants. (**R**) Quantification of height over width of EAD midline tissue. Height was counted as number of cells between the top of the cement gland and the bottom of the brain. Width was counted as the number of cells between the left and right borders of the bright, β-catenin positive midline. Error bar: standard deviation.

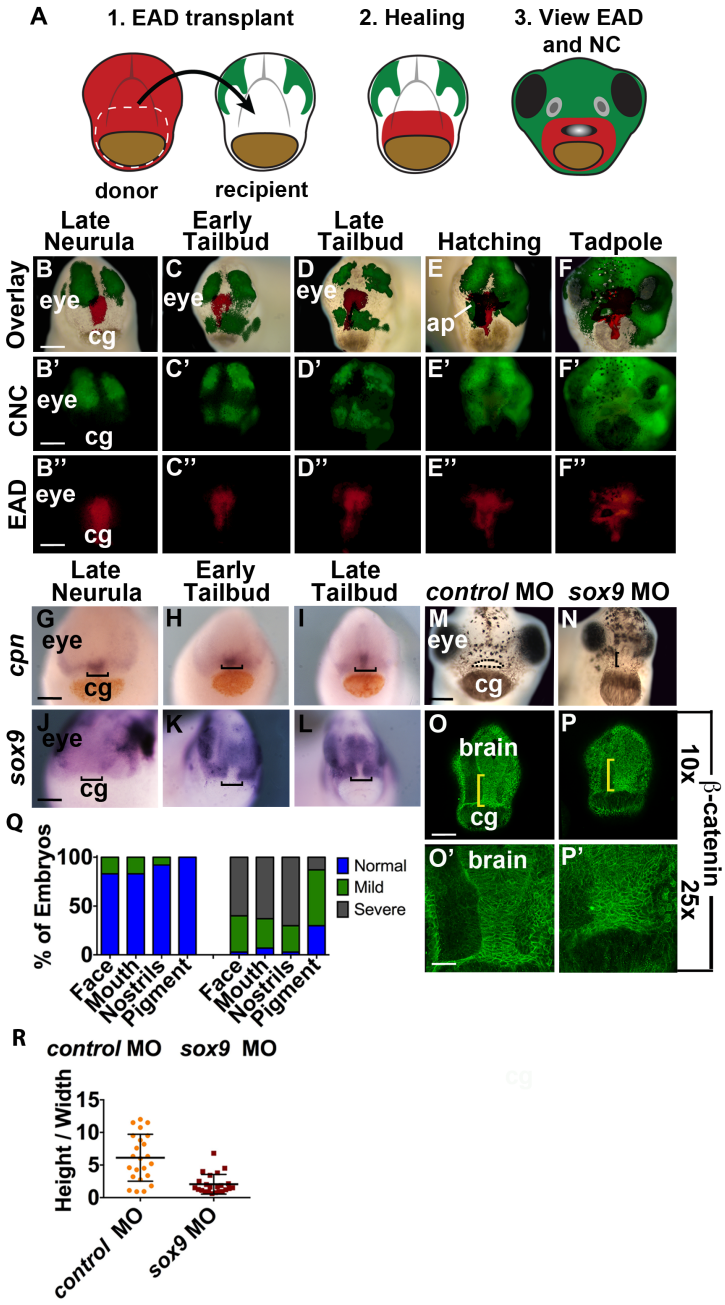
A
1. EAD transplant
2. Healing
3. View EAD and NC
donor
recipient
Late Neurula
Early Tailbud
Late Tailbud
Hatching
Tadpole
Overlay
CNC
EAD
eye
cg
ap
cpn
sox9
control MO
sox9 MO
brain
β-catenin
10x
25x
Q
% of Embryos
Normal
Mild
Severe
Face
Mouth
Nostrils
Pigment
R
Height / Width
control MO
sox9 MO

Figure 3.5

Coronally, we observed midline EAD ectoderm with high levels of membrane-bound β-catenin (Figures 3.4B-E, B'-E') bordered by basement membrane (BM) separating it from neural crest (NC) regions laterally, brain superiorly, and cement gland inferiorly (Figures 3.4F-I, F'-I'). Lateral BM was established before NC started migrating into the face at stage 24 (Figures 3.4A, F, F', 3.5K). The region adjacent to the midline ectoderm appears to form a 'pocket' and was devoid of nuclei at stage 22 (Figures 3.4F', F'', J), while at stage 24, this pocket was filled with nuclei, presumably those of NC cells that had migrated in to lie on either side of the midline (Figures 3.4A, G', G'', 3.5K). No NC cells cross the midline as defined by the EAD.

Between late neurula and swimming tadpole stages, this midline tissue underwent a marked lengthening in height and thinning in width, transitioning from flat, elongated cells (6-7 cells across and 7-9 cells wide), to a tall column of rectangular cells arranged in two parallel rows with basally localized nuclei (2-3 cells wide by 15-20 cells tall) (Figures 3.4A-N, B'-N', K''-N'', K'''-N'''). This morphogenetic process is consistent with convergent extension (CE), where cells rearrange to lengthen and narrow the EAD while undergoing stereotypical cell shape and nuclear polarity changes (Figures 3.4K-N, K'-N', K''-N'', K'''-N''') (Wallingford et al., 2002; Yin et al., 2009).

As *Xenopus* embryos enter hatching stages (stage 35-36), mouth lumen opening has begun as the two rows of β-catenin-positive cells separate down the middle and open into an oval shaped, oral orifice (stage 39-40), surrounded by a perimeter of BM (Figures 3.4O-W, P'-W'). We also used claymation to demonstrate the sequence of EAD ectoderm elongation and mouth opening (Fig. 3.4X-a).

The basal localization of midline nuclei and BM at tail bud stages (Fig. 3.4I, I') indicate polarity determination precedes midline unzipping, but many apical markers localize after the

oral opening has formed, including Zo-1 (Figure 3.6A-E, A'-E'), aPKC, and actin (data not shown). Apical polarity is likely established with an early marker upstream of aPKC, and may be involved in cellular detachment at the midline, as is being investigated independently.

These data newly revealed a morphogenetic process during mouth formation, consistent with CE. This appears to occur in the EAD concomitantly with arrival of NC on either side of the facial midline.

Figure 3.6: Apical polarity marker, Zo-1, is localized to apical membrane after oral opening. (**A-E, A'-E'**) Coronal sections assayed with immunolabeling from late neurula to late hatching. Midline opening with bright labeling at late hatching is part of the EAD ectoderm and the early oral orifice. Representative image shown (n=5-9). Bracket: region of 10x image (**A-E**) enlarged in 25x view (**A'-E'**). cg, cement gland. Scale bar: 170μm.

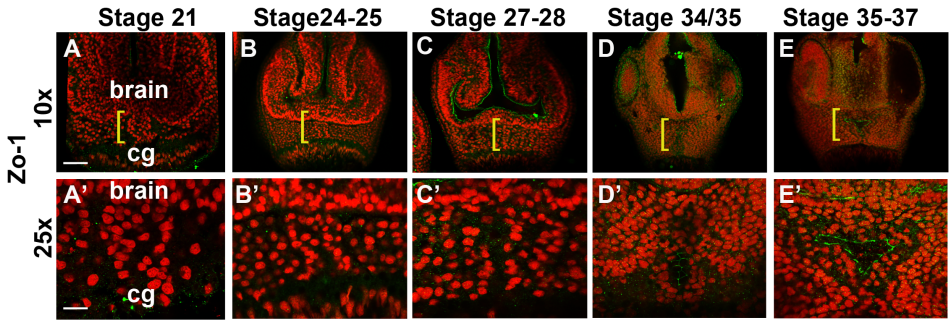
Stage 21
Stage24-25
Stage 27-28
Stage 34/35
Stage 35-37
Zo-1
10x
25x
A
B
C
D
E
brain
cg
A'
B'
C'
D'
E'
brain
cg

Figure 3.6

3.4 c. Midline Convergent Extension Is Neural Crest Dependent

Our data suggested that EAD CE was tightly associated with NC arrival in the region. In order to better characterize this relationship, lineage labeling was performed using a dual transplant approach. mApple-labeled EAD tissue was transplanted into a recipient with mGFP-labeled cranial NC (Figure 3.5A). At late neurula, the EAD transplant (red) was a rectangle at the facial midline, and the bilateral NC (green) was beginning to migrate into the face (Figures 3.5B, B', B''). By tail bud (stage 26), NC had migrated into lateral portions of the face to lie on either side of the lower half of the EAD transplant, which narrowed width-wise and lengthened in height as the NC encroached on the midline (Figures 3.5C-D, C'-D', C''-D''). The superior portion of the EAD broadened (Figures 3.5B-D, B''-D''), and formed distinct streams towards the future nostrils and a midline cell expansion for the developing anterior pituitary (AP) (Figures 3.5E, E', E''). The EAD inferior portion split into two fluorescent columns and separated down the midline, forming an open mouth, lined by red fluorescence, open red nostrils, and a red AP (Figures 3.5F, F', F''). Nearly the entire head was green, as facial cartilage, nerves, and connective tissue are predominantly NC-derived (Santagati and Rijli, 2003). This live imaging demonstrates that the lower portion of the transplant undergoes CE simultaneously with cranial NC approaching the midline.

To examine the relative location of EAD ectoderm and cranial NC, we performed double in situ hybridization with an EAD marker, *cpn,* and a cranial NC marker, *sox9*, in stage-matched embryos (Figures 3.5G-L). As in the live study, the EAD ectoderm, *cpn* domain (bracket) became narrower in width and lengthened in height as the cranial NC, *sox9* domain approached the midline bilaterally, leaving a narrow, NC-free zone.

The tight association of cranial NC arrival on either side of the EAD and EAD morphogenesis prompted us to test the hypothesis that cranial NC is required for EAD morphogenesis. Sox9 is essential for cranial NC formation (Spokony et al., 2002). Loss of function (LOF) in *sox9*, due to injection of morpholino-modified antisense oligonucleotides (MOs) yielded embryos which did not exhibit EAD CE, consistent with a requirement for cranial NC in this process. Later, morphant embryos failed to form mouths, nostrils, and had highly aberrant faces and pigmentation, compared with controls (Figures 3.5M-N, R; Figures 3.9S-T, S'-T').

3.4 d. EAD Convergent Extension Requires the NC and Wnt/PCP Signaling

How might the NC control EAD CE? Based on control of CE during gastrulation (Roszko et al., 2009), we hypothesized that a secreted, non-canonical Wnt was released by cranial NC and bound a receptor on the EAD to initiate CE (Figure 3.7A). To test this, we assayed EAD CE in embryos injected with Dep+ mRNA, a *disheveled* (*dvl*) truncated construct that lacks non-canonical capacity (Tada and Smith, 2000). Dep+ mRNA injected embryos failed to undergo midline CE and later formed abnormal, closed mouths and nostrils, and aberrant faces (Figures 3.7B-G). To identify which non-canonical Wnt ligand and receptor mediated CE, we assayed expression of *wnt11* and *frizzled7* (*fzl7*), which are expressed in NC (De Calisto et al., 2005). In situ hybridization of *fzl7* demonstrated expression throughout the head from stages 22-28 as CE takes place, while *wnt11* was expressed in cranial NC, but not in the midline (bracket) (Figures 3.8A-F, A'-F'), consistent with a mechanism by which the NC might regulate EAD CE.

Figure 3.7: Non-canonical Wnt factors are required for midline convergent extension, normal mouth formation, basement membrane deposition and EAD cell proliferation. (**A**) Schematic of hypotheses. Cranial NC releases Wnt11 which acts on Fzl7 receptors expressed on midline EAD cells. (**B-C**) Frontal view of control and Dep+ RNA injected embryos at swimming tadpole (st. 40) assayed in 3 experiments. ((**B**) control RNA n=56; (**C**) Dep+ RNA n=49.) Bracket: unopened mouth. Dots surround open mouths. cg, cement gland. Scale bar: 200µm. (**D-E, D'-E'**) Coronal sections assayed in 3 independent experiments ((**D, D'**) control RNA n= 16; (**E, E'**) Dep+ RNA n= 21) with β-catenin immunolabeling. Midline region with bright β-catenin labeling is EAD ectoderm. Bracket: region of 10x image (**D-E**) enlarged in 25x view (**D'-E'**). cg, cement gland. Scale bar (10x): 170µm. Scale bar (25x): 68µm. (**F**) Graph depicting percent of morphants, displaying mouth, face, nostrils and pigment formation phenotypes at stage 40 in control and *sox9* morphants. (**G**) Quantification of height over width of EAD midline tissue. Height was counted as number of cells between the top of the cement gland and the bottom of the brain. Width was counted as the number of cells between the left and right borders of the bright, β-catenin positive midline. Error bar: standard deviation. (**H-J**) Frontal view of control MO, *fzl7* MO, and *wnt11* MO injected embryos at swimming tadpole (stage 40) assayed in 3 experiments ((**H**) control MO n=40; (**I**) *fzl7* MO n=34; (**J**) *wnt11* MO n=30). Dots surround open mouths. cg, cement gland. Scale bar: 200µm. (**K-M, K'-M'**) Coronal sections assayed in 3 independent experiments ((**K, K'**) control MO n=13; (**L, L'**) *fzl7* MO n=20; (**M, M'**) *wnt11* MO n=22) with β-catenin immunolabeling. Midline region with bright β-catenin labeling is EAD ectoderm. Bracket: region of 10x image (**K-M**) enlarged in 25x view (**K'-M'**). cg, cement gland. Scale bar (10x): 170µm. Scale bar (25x): 68µm. (**N**) Graph depicting percent of morphants, displaying mouth, face, nostrils and pigment formation phenotypes at stage 40 in control and *sox9*

morphants. (**O**) Quantification of height over width of EAD midline tissue. (**P-S, P'-S'**) Coronal sections of control, *sox9*, *fzl7*, and *wnt11* morphants assayed with Laminin (green) immunolabeling with Propidium Iodide (PI) nuclear counterstain (red) ((**P, P'**) control MO n=5, 100% normal; (**Q, Q'**) *sox9* MO n=10, 0% normal; (**R, R'**) *fzl7* MO n=14, 14% normal; (**S, S'**) *wnt11* MO n=11, 9% normal). Bracket: region of 10x image (**P-S**) enlarged in 25x view (**P'-S'**). cg, cement gland. Scale bar (10x): 170μm. Scale bar (25x): 68μm. (**T-W, T'-W'**) Coronal sections of control, *sox9*, *fzl7*, and *wnt11* morphants assayed with Ph3 (green) immunolabeling with Hoechst nuclear counterstain (blue) ((**T, T'**) control MO n=21; (**U, U'**) *sox9* MO n=21; (**V, V'**) *fzl7* MO n=18; (**W, W'**) *wnt11* MO n=20). Yellow bracket: region of 10x image (**T-W**) enlarged in 25x view (**T'-W'**). cg, cement gland. White bracket: region of included Ph3 positive cells. Scale bar (10x): 170μm. Scale bar (25x): 68μm. (**X-Y**) Quantification of Ph3 and cleaved Caspase-3 positive cells in the EAD of morphants. Error bar: standard deviation.

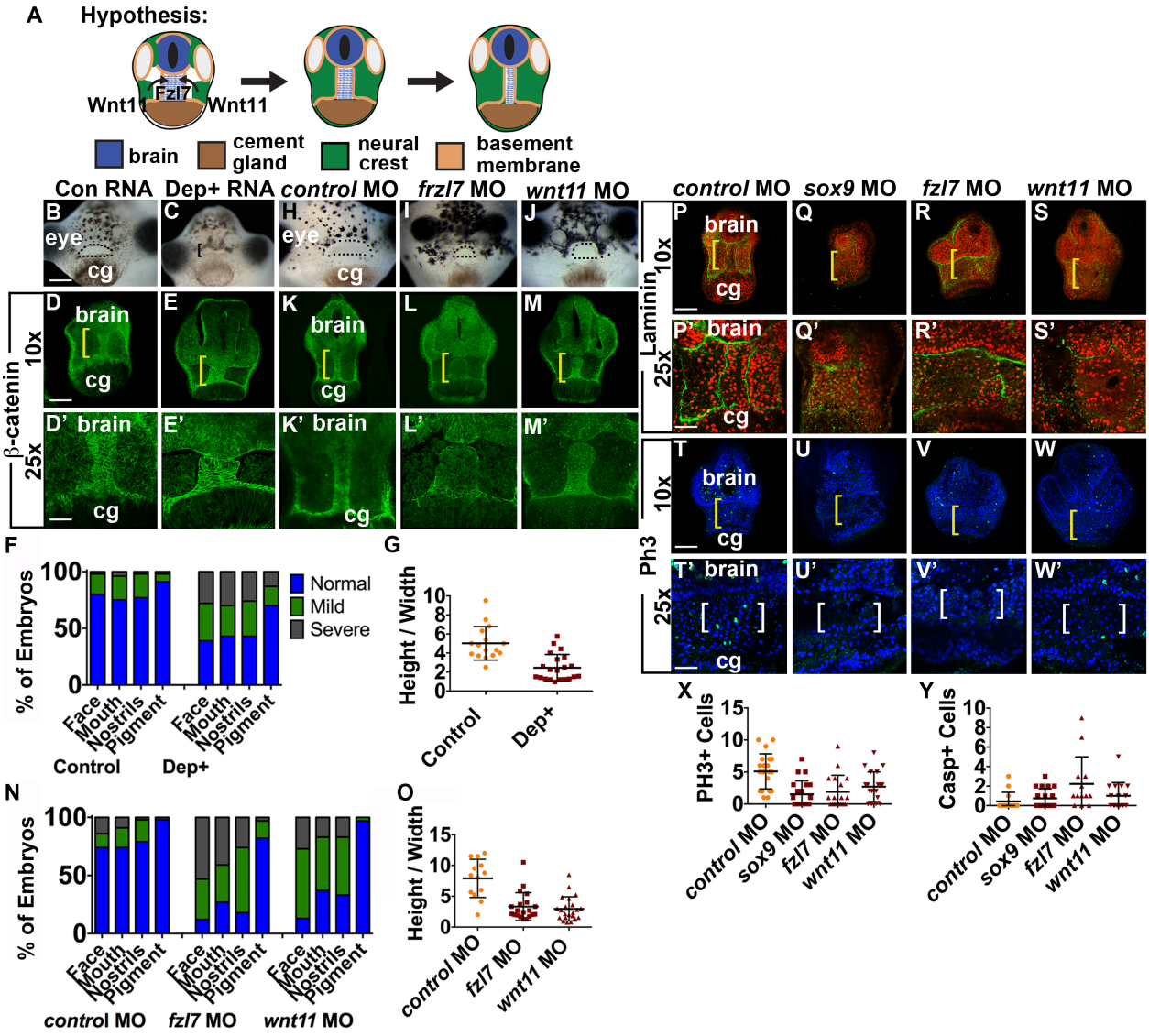
A Hypothesis:
Wnt11
Fzl7
Wnt11
brain
cement gland
neural crest
basement membrane
Con RNA
Dep+ RNA
control MO
frzl7 MO
wnt11 MO
β-catenin
10x
25x
eye
cg
brain
control MO
sox9 MO
fzl7 MO
wnt11 MO
Laminin
Ph3
F
% of Embryos
Normal
Mild
Severe
Face
Mouth
Nostrils
Pigment
Control
Dep+
G
Height / Width
Control
Dep+
N
control MO
fzl7 MO
wnt11 MO
O
X
PH3+ Cells
Y
Casp+ Cells
sox9 MO

Figure 3.7

Figure 3.8: *Frizzled7 (fzl7)* and *wnt11* are expressed throughout the head, except *wnt11* expression is low in the midline. The mouth is properly specified in *fzl7*, *wnt11*, and *sox9* morphants. (**A-F, A'-F', A''-C''**) In situ hybridization for *fzl7* (**A-C, A'-C', A''-C''**) and *wnt11* (**D-F, D'-F'**) at late neurula, middle, and late tail bud. RNA is purple. Cement gland marker (*xcg*) is red. Bracket: presumptive mouth. cg, cement gland. Scale bars: 200μm. (**G-N**) Control, sox9, fzl7, and *wnt11*morphants at stage 22 express presumptive mouth markers, *frzb1* and *xanf*1. Scale bar: 200μm.

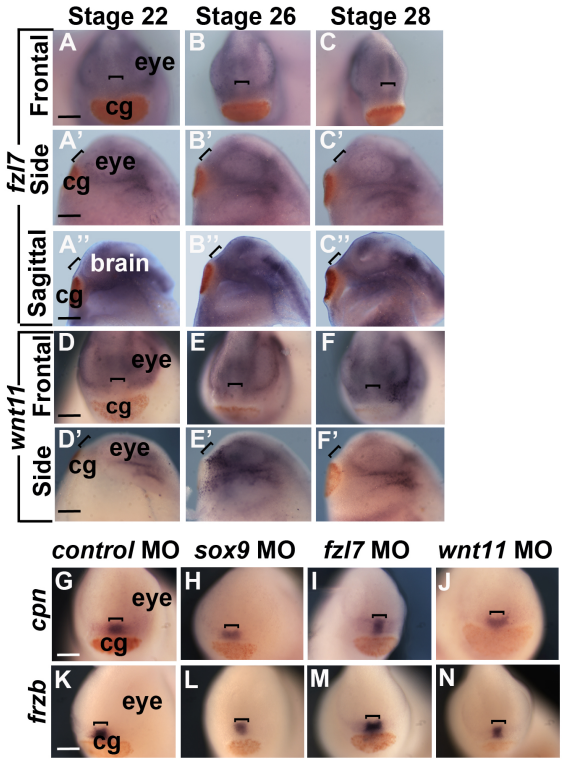
Stage 22
Stage 26
Stage 28
fzl7
Frontal
Side
Sagittal
wnt11
Frontal
Side
A
B
C
A'
B'
C'
A''
B''
C''
D
E
F
D'
E'
F'
eye
cg
brain
control MO
sox9 MO
fzl7 MO
wnt11 MO
cpn
frzb
G
H
I
J
K
L
M
N

Figure 3.8

Morpholino LOF in receptor and ligand resulted in markedly diminished CE and aberrant craniofacial development, with morphants exhibiting tiny, deformed mouths, lack of nostrils, and abnormally shaped faces, when compared with controls (Figures 3.7H-O, K'-M'). In situ hybridization of EAD markers, *cpn* and *frzb,* in control, *frzl7, wnt11,* and *sox9* morphants were normal indicating proper EAD specification (Figures 3.8G-N). To assess whether the CE-defective morphants (*frzl7, wnt11,* and *sox9*) eventually recover, midline ectoderm was viewed in siblings at late tail bud (stage 27-28) and early hatching (stage 32) stages, when the oral invagination first forms (Nieuwkoop and Faber, 1994). Midline CE did not occur in the older CE morphants demonstrating that diminished CE was not a function of developmental delay (Figures 3.9A-I, A'-H'). Sagittally, stage 28 morphants had a slightly reduced height/depth ratio, when compared with controls, consistent with the coronal views (Figures 3.9J-M, J'-M', R). Parasagittally, morphants matched controls (Figures 3.9N-Q, N'-Q').

To assay BM in CE morphants, laminin immunostaining was performed at tail bud (stage 27-28). Morphants lacked the contiguous, laminin staining seen adjacent to the midline ectoderm of control morphants (Figures 3.7P-S, P'-S'). Spots of disordered laminin appeared in the EAD region of all three CE morphants. Phospho-Histone-3 (PH3) immunolabeling during EAD CE (stage 24-25) highlighted a random scatter of dividing cells in control midline tissue (white brackets), which was markedly decreased in CE morphants (Figures 3.7T-X, T'-W'). However, minimal cell death was observed in the EAD midline ectoderm of all morphants and controls (Figures 3.7Y, 3.9W-Z, W'-Z'). These data demonstrate that non-canonical Wnt signaling is required for proper midline proliferation and BM deposition, but does not affect apoptosis.

Figure 3.9: *sox9*, *frizzled7 (fzl7),* and *wnt11* morphants fail to recover from convergent extension defects and sagittal views demonstrate a lower length to depth ratio. (**A-H, A'-H'**) Control, *sox9*, *fzl7,* and *wnt11* morphants at stages 28 and 32. (**A, A', E, E'**) Control morphants (stage 28 n=6; stage 32 n=15). (**B, B', F, F'**) *sox9* morphants (stage 28 n=8; stage 32 n=12). (**C, C', G, G'**) *fzl7* morphants (stage 28 n=11; stage 32 n=24). (**D, D', H, H'**) *wnt11* morphants (stage 28 n=14; stage 32 n=19). Height / width was calculated by counting the number of cells between the brain and cement gland (height) and between the right and left boundaries (width) of the midline ectoderm with high β-catenin labeling. Bracket: region of 10x image (**A-H**) enlarged in 25x view (**A'-H'**). cg, cement gland. Scale bar (10x): 170μm. Scale bar (25x): 68μm. (**I**) Graph depicting the ratios of height / width of EAD ectoderm in morphants. (**J-Q, J'-Q'**) Sagittal and parasagittal sections of stage 28 control, *sox9*, *fzl7,* and *wnt11* morphants with β-catenin immunolabeling. Midline region with bright β-catenin labeling is EAD ectoderm. Representative images shown (control morphants n=5, *sox9* morphants n=5, *fzl7* morphants n=7, and *wnt11* morphants n=4). Length / depth was calculated by counting the number of cells between the brain and cement gland (length) and between the top / left and bottom / right boundaries (depth) of the deep ectoderm with high β-catenin labeling. Bracket: region of 10x image (**J-Q**) enlarged in 25x view (**J'-Q'**). cg, cement gland. Scale bar (10x): 170μm. Scale bar (25x): 68μm. (**R**) Graph depicting the ratios of length / depth of EAD ectoderm in sagittal sections of morphants. (**S-T, S'-T'**) In situ hybridization of *sox9* in control and *sox9* morphants assayed in 2 experiments (n=14). (**S-T**) frontal. (**S'-T'**) side view. Bracket: midline ectoderm. Scale bar: 200μm. (**U-V, U'-V'**) In situ hybridization of *sox9* in control and *fzl7* morphant EAD transplants assayed in 2 experiments (n=16). (**U-V**) frontal. (**U'-V'**) side view. Bracket: midline ectoderm. Scale bar: 200μm. (**W-Z, W'-Z'**) Coronal sections of stage 24 control, *sox9*, *fzl7,* and *wnt11* morphants

with cleaved caspase-3 immunolabeling (control n=14; *fzl7* n= 13; *wnt11* n= 16; *sox9* n=19). Bracket: region of 10x image (**W-Z**) enlarged in 25x view (**W'-Z'**). cg, cement gland. Scale bar (10x): 170μm. Scale bar (25x): 68μm.

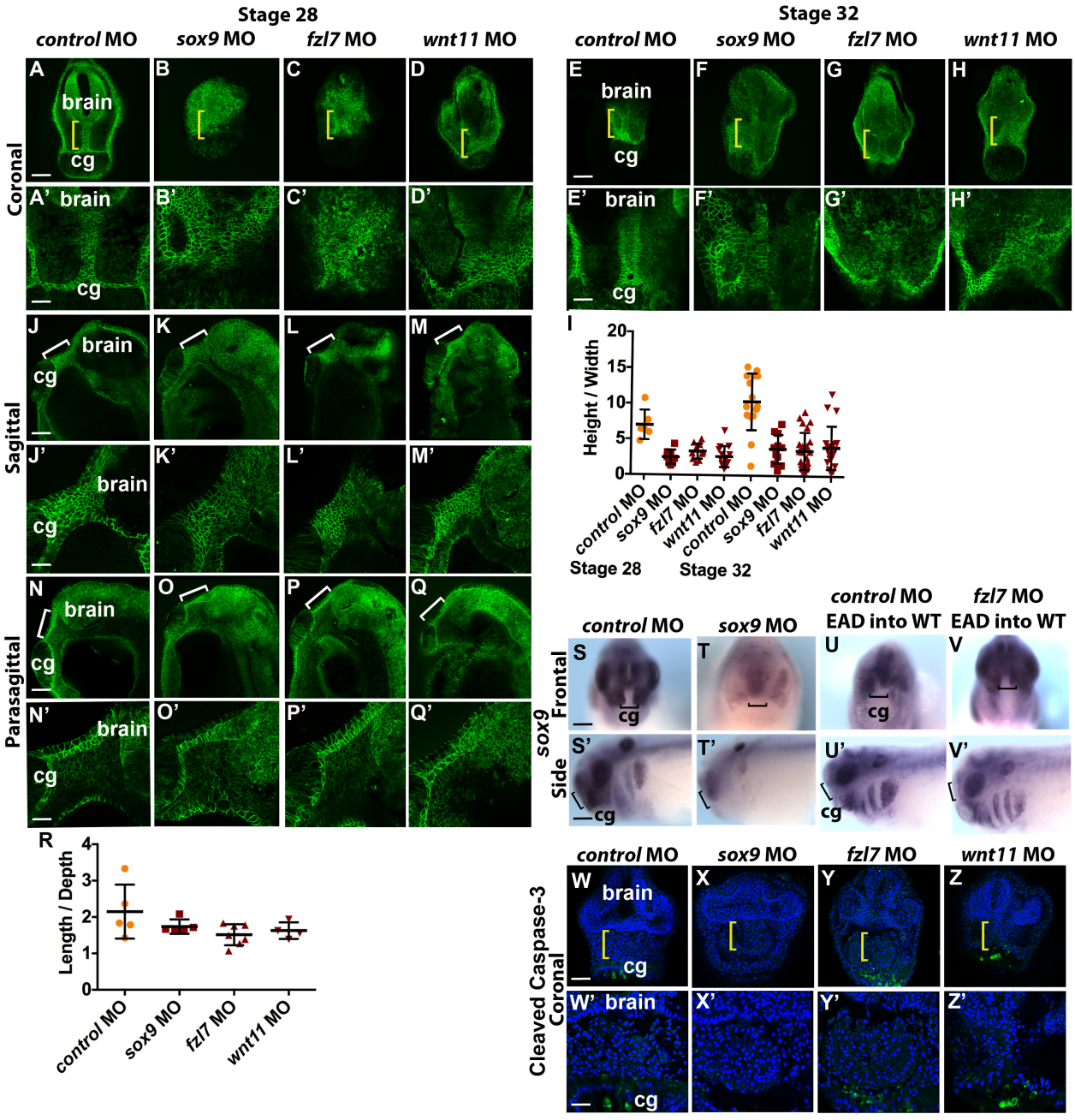
Stage 28
control MO
sox9 MO
fzl7 MO
wnt11 MO
Stage 32
control MO
sox9 MO
fzl7 MO
wnt11 MO
Coronal
Sagittal
Parasagittal
brain
cg
Height / Width
Stage 28
Stage 32
control MO
fzl7 MO
EAD into WT
EAD into WT
sox9
Frontal
Side
Length / Depth
Cleaved Caspase-3
Coronal

Figure 3.9

3.4 e. EAD Transplants Demonstrate a Localized Requirement for Non-Canonical Wnt Signaling in the EAD

Based on LOF phenotypes and RNA expression, we hypothesized that intracellular signaling mediator, *dvl,* and the receptor *frzl7* are locally required in the EAD for CE, while the ligand *wnt11* is not. This was tested using a facial transplant protocol (Jacox et al., 2014). EAD was removed from Dep+ embryos, *frzl7* and *wnt11* morphants at early tail bud (stage 22) and transplanted to sibling controls (Figure 3.10A) (Jacox et al., 2014). Control RNA or MO-to-control transplants underwent normal EAD CE, mouth opening, nostril formation and pigmentation (Figures 3.10B, B', D, D', H, H', K, K', and quantified in F, G, N, O). However, when *frzl7* LOF or Dep+ EAD was transplanted into control embryos, midline CE did not occur and small, deformed mouths and nostrils formed (Figures 3.10C, C', E-G, E', I, I', L, L', N, O). In contrast, transplant of *wnt11* LOF EAD produced normal midline CE and facial phenotypes, leading us to conclude neighboring tissue to the EAD can supply Wnt11 (Figures 3.10J, J', M-O, M').

The requirement for *frzl7* expression in the EAD during CE and mouth formation led us to test whether *fzl7* is also required for cranial NC development. No difference was noted in NC marker, *sox9*, expression in *fzl7* MO transplants compared with controls, suggesting that a reciprocal mechanism does not operate (Figures 3.9U-V, U'-V').

These results show that the NC likely supplies Wnt11 protein that activates Fzl7 receptors on EAD to elicit CE of the EAD through the Wnt/PCP pathway.

Figure 3.10: Fzl7 is locally required in the EAD for midline convergent extension and Wnt11 is sufficient for EAD convergent extension. Local requirement of Dsh, *fzl7*, and *wnt11* expression tested with an EAD transplant technique. (**A**) Experimental design: donor morphant tissue was transplanted to uninjected sibling recipients. (**B-C, B'-C'**) EAD transplant outcome from control or Dep+ RNA donor tissue assayed in 3 experiments. ((**B, B'**) control RNA n=23; (**C, C'**) Dep+ RNA n=22.) (**B'-C'**) Overlay of (**B-C**) with GFP fluorescence indicating location of donor transplant in recipient. Dots surround open mouths. Bracket: unopened mouth. Frontal view. cg, cement gland. Scale bar: 200μm. (**D-E, D'-E'**) Coronal sections of EAD transplants with control or Dep+ donor tissue assayed in 3 independent experiments ((**D, D'**) control RNA n=10; (**E, E'**) Dep+ RNA n=14) with β-catenin immunolabeling. Midline region with bright β-catenin labeling is EAD ectoderm. Bracket: region of 10x image (**D-E**) enlarged in 25x view (**D'-E'**). cg, cement gland. Scale bar (10x): 170μm. Scale bar (25x): 68μm. (**F**) Quantification of normal or abnormal structure development depending on background of facial tissue. (**G**) Quantification of height over width of EAD midline tissue. Height was counted as number of cells between the top of the cement gland and the bottom of the brain. Width was counted as the number of cells between the left and right borders of the bright, β-catenin positive midline. Error bar: standard deviation. (**H-J)** EAD transplant outcome from control, *fzl7*, or *wnt11* morphant donor tissue assayed in 4 independent experiments. ((**H, H'**) control MO n=27; (**I, I'**) *fzl7* MO n=30; (**J, J'**) *wnt11* MO n=30.) (**H'-J'**) Overlay of (**H-J**) with GFP fluorescence indicating location of donor transplant in recipient. Dots surround open mouths. Bracket: unopened mouth. Frontal view. cg, cement gland. Scale bar: 200μm. (**K-M, K'-M'**) Coronal sections of EAD transplants with control, *fzl7*, or *wnt11* donor tissue assayed in 4 independent experiments with β-catenin immunolabeling ((**K, K'**) control MO n=19; (**L, L'**) *fzl7* MO n=17; (**M, M'**) *wnt11* MO n=14). Midline region with

bright β-catenin labeling is EAD ectoderm. Bracket: region of 10x image (**K-M**) enlarged in 25x view (**K'-M'**). cg, cement gland. Scale bar (10x): 170μm. Scale bar (25x): 68μm. (**N**) Quantification of normal or abnormal structure development depending on morphant background of facial tissue. (**O**) Quantification of height over width of EAD midline tissue in transplants. (**P**) Sufficiency of Wnt11 for midline CE was tested with an animal cap transplant technique. Experimental schematic of bilateral transplants with mApple, animal cap overexpressing Wnt11 or a control, secreted protein (inactive MMP11). (**Q-T**) Overlay of brightfield images with mApple fluorescence indicating location of donor transplant in late tail bud recipients (stage 28). cg, cement gland. Scale bar: 200μm. (**U-X, U'-X'**) Coronal sections of animal cap transplants with *mmp11* or *wnt11* overexpressing donor tissue assayed in 3 experiments with β-catenin immunolabeling ((**U, U'**) control MO+*mmp11* n=15; (**V, V'**) control MO+*wnt11* n=14; (**W, W'**) *sox9* MO+*mmp11* n=18; (**X, X'**) *sox9* MO+*wnt11* n=22). Midline region with bright β-catenin labeling is EAD ectoderm. Bracket: region of 10x image (**U-X**) enlarged in 25x view (**U'-X'**). cg, cement gland. Scale bar (10x): 170μm. Scale bar (25x): 68μm. (**Y**) Quantification of height over width of EAD midline tissue. Error bar: standard deviation.

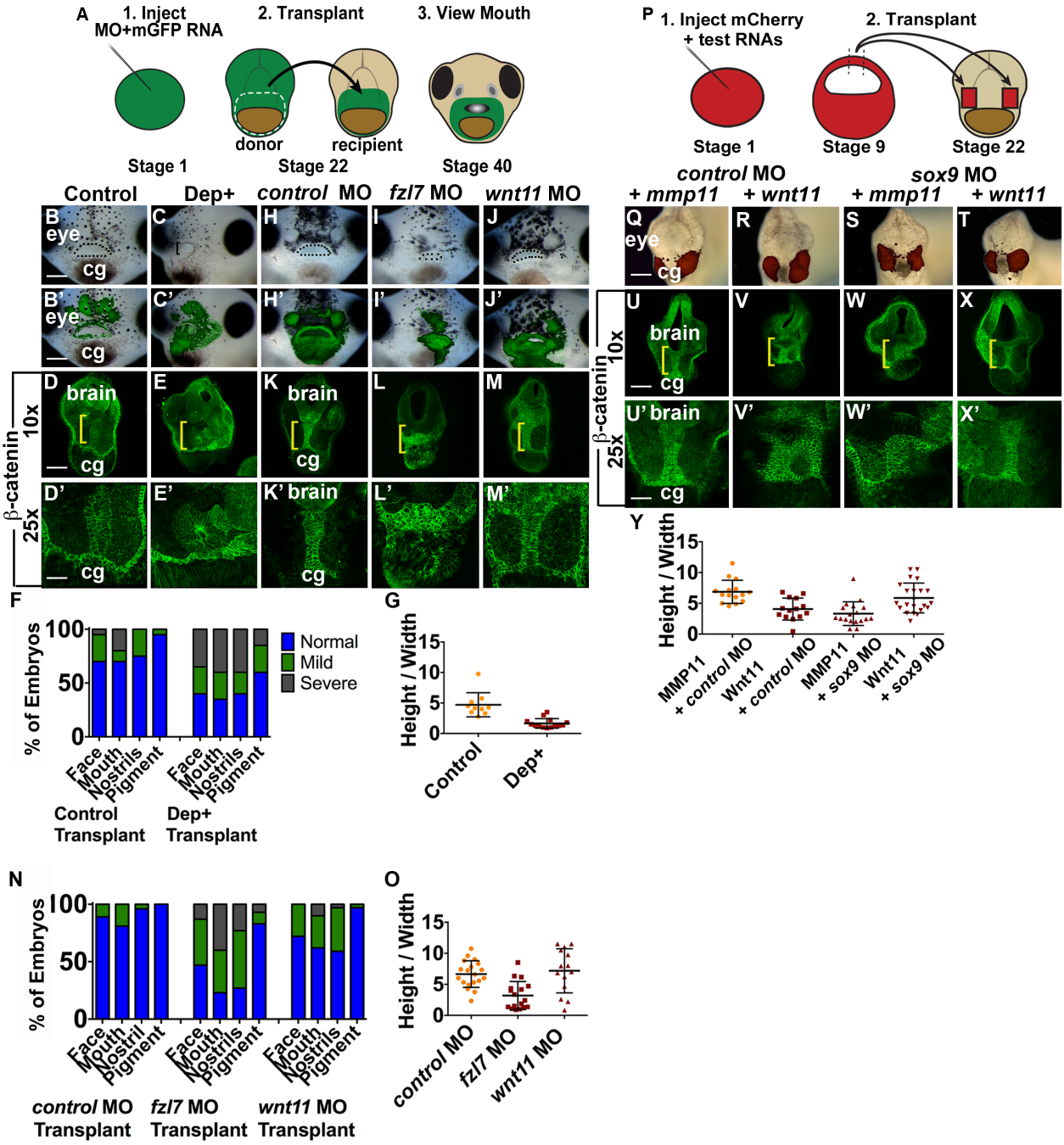
A
1. Inject MO+mGFP RNA
2. Transplant
3. View Mouth
donor
recipient
Stage 1
Stage 22
Stage 40
Control
Dep+
control MO
fzl7 MO
wnt11 MO
eye
cg
brain
β-catenin
10x
25x
F
% of Embryos
Normal
Mild
Severe
Face
Mouth
Nostrils
Pigment
Control Transplant
Dep+ Transplant
G
Height / Width
Control
Dep+
N
Nostril
control MO Transplant
fzl7 MO Transplant
wnt11 MO Transplant
O
control MO
fzl7 MO
wnt11 MO
P
1. Inject mCherry + test RNAs
2. Transplant
Stage 1
Stage 9
Stage 22
control MO
sox9 MO
+ mmp11
+ wnt11
Y
MMP11 + control MO
Wnt11 + control MO
MMP11 + sox9 MO
Wnt11 + sox9 MO

Figure 3.10

3.4 f. Wnt11 Is Sufficient for Midline Convergent Extension in the EAD

EAD transplants demonstrated that localized non-canonical signaling is necessary for midline CE. From this, we hypothesized that Wnt11 is sufficient for EAD CE. This was tested in a transplant assay where red animal cap tissue, overexpressing a control, secreted protein (inactive MMP11) or Wnt11, was surgically implanted on either side of the EAD in control and *sox9* morphants at stage 22 (Figure 3.10P). Embryos were grown until stage 28, when EAD CE has reached completion, and scored for CE. Control morphants implanted with control animal caps demonstrated normal CE (Figures 3.10Q, U, U'), while controls implanted with *wnt11* tissue had reduced CE, consistent with data demonstrating a reduction in gastrulation CE with *wnt11* overexpression (Figures 3.10R, V, V') (Yin et al., 2009). *sox9* morphants implanted with control animal caps had greatly diminished CE (Figures 3.10S, W, W'), while *sox9* siblings implanted with animal caps expressing *Wnt11* showed significant rescue of EAD CE.

These data support the hypothesis that NC supplies Wnt11 to modulate CE by showing that ectopic expression of Wnt11 is sufficient to stimulate midline CE (Figures 3.10T, X, X',Y). Non-canonical Wnt signaling is therefore both necessary and sufficient for EAD CE.

3.4 g. Downstream GTPase Effectors, Rock and Jnk, are Required for Midline Convergent Extension

Non-canonical Wnt signaling has a number of downstream branches made up of GTPase effectors. We determined which GTPases mediate midline CE, using non-canonical Wnt inhibitors. Beads were soaked overnight in inhibitors diluted in DMSO and then implanted in the foregut behind the EAD at stage 22 (Figure 3.11A). DMSO control, ROCK inhibitor, and Rho inhibitor beads produced normal faces and midline CE (Figures 3.11B, G, G', E-F, J-K, J'-K', L, M). Rac1 and Jnk inhibitors were associated with markedly reduced CE, failure of mouth and

nostril formation, and abnormally shaped faces (Figures 3.11C-D, H-I, H'-I', L, M). In other systems, Rac1 acts downstream of Dvl and phosphorylates JNK, targeting it to the nucleus to modulate signaling (Yin et al., 2009). Visualization of p-JNK demonstrated maximal nuclear localization in EAD cells during CE (stage 23, Figures 3.11O, O', T). Prior to CE, few nuclei exhibit p-JNK labeling (Figures 3.11N, N', T), and by tail bud, the number of p-JNK positive nuclei is reduced relative to stage 23, the peak of CE (Figures 3.11P, P', T). p-JNK positive nuclei appeared randomly distributed in the EAD of control morphants. *frzl7* morphants demonstrate low levels of p-JNK positive nuclei at all stages, concomitant with failed CE (Figures 3.11Q-T, Q'-S'). These data are consistent with the Rac1 and Jnk branch of Wnt/PCP signaling mediating midline CE.

The mechanism of CE in the *Xenopus* EAD remains an area of further inquiry. Live two-photon imaging of cellular movements has provided great insight into CE in other settings (Ulrich et al., 2003). Unfortunately, the high lipid content of *Xenopus* cells prevented us from obtaining similar insight due to high refractivity. Separation of the brain from the EAD appreciably reduced midline CE, suggesting that the structural brain-EAD connection is required for proper EAD CE (Figures 3.12A-D, A'-C').

Figure 3.11: Inhibition of GTPases Jnk and Rac1 is associated with a reduction in EAD convergent extension. (**A**) Experimental schematic of inhibitor loaded bead implantation in the presumptive mouth, EAD region. (**B-F**) Frontal view of swimming tadpole (stage 40) embryos with inhibitor loaded beads implanted in their presumptive mouths, assayed in 3 experiments. ((**B**) control DMSO n=97; (**C**) Rac1 n=40; (**D**) Jnk inhibitor n=44; (**E**) Rock inhibitor n=75;(**F**) Rho inhibitor n=39.) Bracket: unopened mouth. Dots surround open mouths. cg, cement gland. Scale bar: 200μm. (**G-K**, **G'-K'**) Coronal sections assayed in 3 independent experiments. ((**G, G'**) control DMSO n=31; (**H, H'**) Rac1 inhibitor n=27; (**I, I'**) Jnk inhibitor n=24; (**J, J'**) Rock inhibitor n=9; (**K, K'**) Rho inhibitor n=12.)) with β-catenin immunolabeling. Midline region with bright β-catenin labeling is EAD ectoderm. Bracket: region of 10x image (**G-K**) enlarged in 25x view (**G'-K'**). cg, cement gland. Scale bar (10x): 170μm. Scale bar (25x): 68μm. (**L**) Graph depicting percentage of embryos, displaying mouth, face, nostrils and pigment formation phenotypes at stage 40. (**M**) Quantification of height over width of EAD midline tissue. Height was counted as number of cells between the top of the cement gland and the bottom of the brain. Width was counted as the number of cells between the left and right borders of the bright, β-catenin positive midline. Error bar: standard deviation. (**N-P, N'-P'**) Control morphants at stage 20 (**N, N'**, n=19), stage 23 (**O, O'**, n= 23), and stage 26 (**P, P'**, n=21) with p-JNK immunolabeling (green), mApple cell membranes (red), and with Hoechst nuclear counterstain (blue in **N-P**) assayed in 2 experiments. (**Q-S, Q'-S'**) *fz17* morphants at stage 20 (**Q, Q'**, n=26), stage 23 (**R, R'**, n=23), and stage 26 (**S, S'**, n=16) with p-JNK immunolabeling (green), mApple cell membranes (red), and with Hoechst nuclear counterstain (blue in **Q-S**) assayed in 2 experiments. Bracket: EAD. cg, cement gland. Scale bars (40x): 43μm. (**T**) Quantification of

cells with p-JNK positive nuclei in the EAD ectoderm. Total number of EAD nuclei was equivalent between stage matched control and *frzl7* morphants.

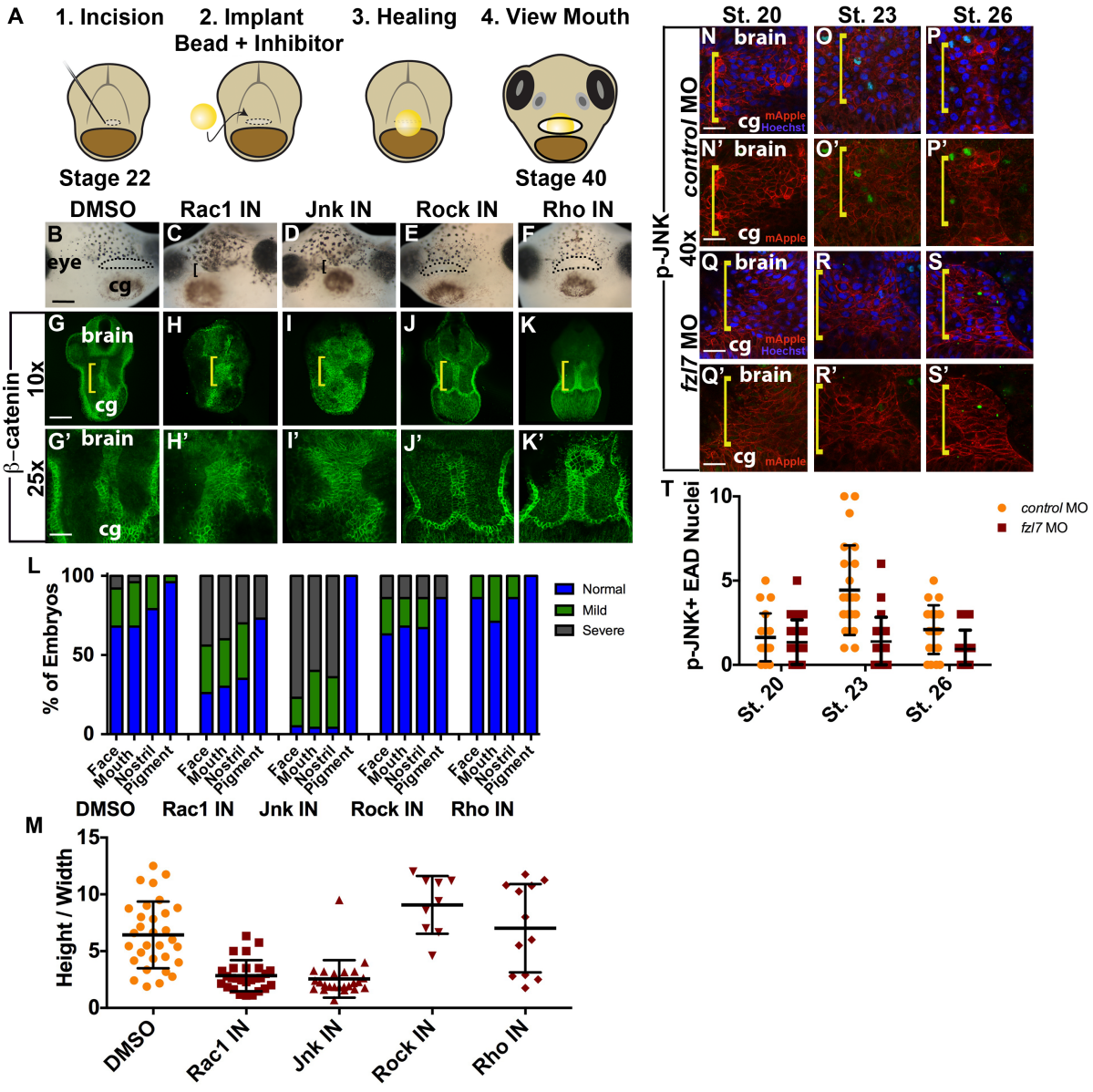
A
1. Incision
2. Implant Bead + Inhibitor
3. Healing
4. View Mouth
Stage 22
Stage 40
DMSO
Rac1 IN
Jnk IN
Rock IN
Rho IN
β-catenin
10x
25x
brain
eye
cg
p-JNK
40x
control MO
fzl7 MO
mApple
Hoechst
St. 20
St. 23
St. 26
T
p-JNK+ EAD Nuclei
control MO
fzl7 MO
L
% of Embryos
Normal
Mild
Severe
Face
Mouth
Nostril
Pigment
M
Height / Width

Figure 3.11

Figure 3.12: Brain-EAD separation is associated with reduced convergent extension. (**A-C, A'-C'**) (**A, A'**) Control, wild-type embryos with "foil" had a tiny triangle of aluminum foil inserted into the brain adjacent to EAD, but placed such that it did not disrupt the brain-EAD connection (n=29 from 3 independent experiments). (**B, B'**) Control, wild-type embryos without aluminum foil (n=21 from 3 independent experiments). (**C, C'**) Wild-type embryos with an aluminum foil triangle inserted such that it bisects the connection between the lower margin of the brain and upper margin of the EAD (n=23 from 3 independent experiments). Height / width was calculated by counting the number of cells between the brain and cement gland (height) and between the right and left boundaries (width) of the midline ectoderm with high β-catenin labeling. Bracket: region of 10x image (**A-C**) enlarged in 25x view (**A'-C'**). cg, cement gland. Scale bar (10x): 170μm. Scale bar (25x): 68μm. (**D**) Graph depicting the ratios of height / width of EAD ectoderm.

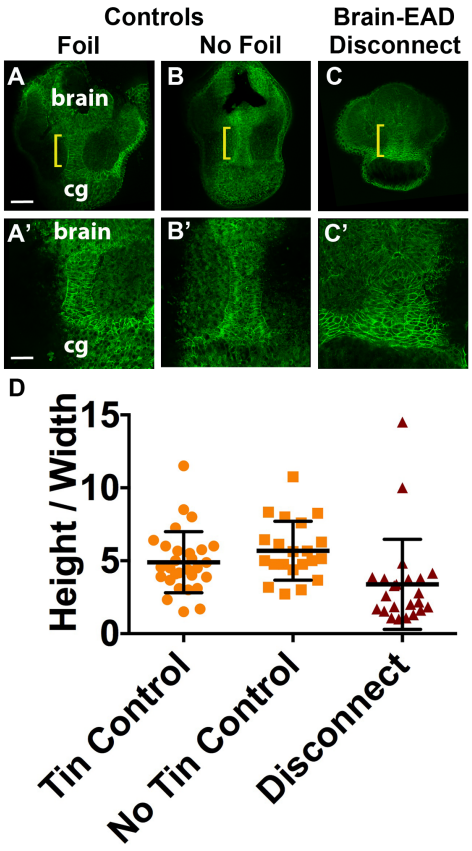
Controls
Foil
No Foil
Brain-EAD
Disconnect
A
brain
cg
B
C
A'
brain
cg
B'
C'
D
Height / Width
15
10
5
0
Tin Control
No Tin Control
Disconnect

Figure 3.12

3.5 Discussion

This study is the first to identify midline convergent extension (CE) as a morphogenetic phase of mouth formation, mediated by a non-canonical Wnt ligand secreted by cranial NC. Three major conclusions are reached. First, EAD ectoderm undergoes CE. Failure of CE is associated with abnormally small or absent mouth openings and other craniofacial abnormalities, suggesting it is a necessary phase of mouth and face development. Second, EAD CE is dependent on non-canonical Wnt signaling. Third, this signaling occurs from the cranial NC to the EAD, uncovering a new phase of the EAD-NC signaling conversation. These findings add new insight into mouth morphogenesis and the reciprocal signaling required for craniofacial development.

Key stages of mouth development appear widely conserved (Dickinson and Sive, 2006, 2007), including formation of a presumptive mouth tissue that invaginates, thins, and perforates, forming an open mouth. While an EAD is present in all vertebrates, the CE described here has not been described previously.

Our prior analyses demonstrated that the EAD is an organizer, required for ingression of first arch cranial NC into the nascent face through Kinin-Kallikrein signaling (Jacox and Sindelka et al., 2014). More limited analysis showed that *frzb1*, expressed exclusively from the EAD is necessary both locally and more globally (Dickinson and Sive, 2009). Our demonstration of a reciprocal signaling event between the newly arrived NC and EAD demonstrates a novel signaling conversation during craniofacial development. NC cells and sensory placodes also signal reciprocally. In chicken, NC cells release the ligand Slit1 which bind the placodal receptor, Robo2, promoting placodal condensation and maturation to form cranial ganglions (Shiau and Bronner-Fraser, 2009). In *Xenopus*, reciprocal signaling between NC and placodal

cells is necessary for migration of both cell types via the "chase and run" mechanism, which also utilizes Wnt/PCP components (Steventon et al., 2014; Theveneau et al., 2013).

In *Xenopus*, zebrafish, and amniote axial mesoderm, mediolateral intercalation is the predominant cell movement of CE (Keller et al., 2000; Tada and Heisenberg, 2012; Yin et al., 2009). The cell shape and rearrangements observed in the EAD during CE are consistent with mediolateral intercalation. It is likely that additional Wnt/PCP factors, such as Glypican4, Prickled, Vangl2, Sdc4, collude with Dvl and the effector GTPases to mediate the intracellular processes required for CE. Wnt5 and Ror2 may also participate in midline CE signaling. Investigating the roles of other Wnt/PCP factors is a point of future interest.

Wnt/PCP signaling is not only required for proper NC migration in *Xenopus*, via contact inhibition of locomotion (Carmona-Fontaine et al., 2008), but also for chondrocyte stacking and transition from proliferative to hypertrophic phases in zebrafish and mice, where LOF is associated with skull and craniofacial defects (Dale et al., 2009; Topczewski et al., 2011). Our study demonstrates that localized Wnt/PCP LOF is associated with craniofacial abnormalities in *Xenopus*, including deformed mouths, reduced nostrils, and abnormal facial shape, stemming from aborted midline CE. Craniofacial abnormalities related to Wnt/PCP LOF suggest common roles in tissue morphogenesis of the developing face.

Are there further NC/EAD interactions yet uncharacterized? We note with interest that the NC migrating into the face does not cross the EAD at the midline. This suggests perhaps, that the EAD acts as a physical barrier or chemical stop signal to the incoming NC, perhaps keeping NC identity distinct in the two halves of the face.

Our study newly defines midline CE as a novel phase of mouth formation and identifies a reciprocal signaling relationship between the migratory cranial NC and the EAD utilizing

Wnt/PCP factors. These findings suggest important future directions, including probing possible interactions between canonical and non-canonical Wnt factors expressed in and around the EAD and identification of other Wnt/PCP factors involved in midline CE.

3.6 Acknowledgements

We thank our colleagues for discussion, reagents, and critical input, especially Ryann Fame, Justin Chen, Jasmine McCammon, and Christian Cortez-Campos. We thank George Bell for help with bioinformatics, Tom diCesare for assistance with figures, and Wendy Salmon for imaging support. We also thank Sergei Sokol, Masazumi Tada, Malcolm Whitman, Axel Schweickert, Jean-Pierre Saint-Jeannet, Carl-Phillipe Heisenberg, Naoto Ueno, and Richard Harland for gifts of plasmids. We are grateful to the NIDCR for support (1R01 DE021109-01 to HLS and F30DE022989 to LJ) and to Harvard University for the Herschel Smith Graduate Fellowship (to LJ).

Chapter 4

Facial Transplants in *Xenopus laevis* Embryos

Author Contributions: L.J. conducted the transplants and prepared all materials featured in the figures and JOVE video. L.J. starred in the JOVE video and wrote and revised the manuscript. A.D. invented the face transplant technique and revised the manuscript. H.S. supervised the study and revised the manuscript.

Publication: Jacox, L.*, Dickinson, A.*, Sive, H. (2014). Facial Transplants in *Xenopus laevis* Embryos. *J. Vis. Exp.* (85), e50697, doi:10.3791/50697
(* equally-contributing first authors)

This chapter has been kept largely unchanged from its published form, with the exception of minor changes in figure and section order.

4.1 Abstract

Craniofacial birth defects occur in 1 out of every 700 live births, but etiology is rarely known due to limited understanding of craniofacial development. To identify where signaling pathways and tissues act during patterning of the developing face, a 'face transplant' technique has been developed in embryos of the frog *Xenopus laevis*. A region of presumptive facial tissue (the "Extreme Anterior Domain" (EAD)) is removed from a donor embryo at tailbud stage, and transplanted to a host embryo of the same stage, from which the equivalent region has been removed. This can be used to generate a chimeric face where the host or donor tissue has a loss or gain of function in a gene, and could include a lineage label. After healing, the outcome of development is monitored, and indicates roles of the signaling pathway within the donor or surrounding host tissues. *Xenopus* is a valuable model for face development, as the facial region is large and readily accessible for micromanipulation. Many embryos can be assayed, over a short time period since development occurs rapidly. Findings in the frog are relevant to human development, since craniofacial processes appear conserved between *Xenopus* and mammals.

4.2 Introduction

To understand mechanisms underlying craniofacial birth defects, important tissues and their signaling contributions during craniofacial development must be identified (Gorlin et al., 1990; Trainer, 2010). In the frog *Xenopus laevis,* part of the face, including the mouth and nostrils form from the Extreme Anterior Domain (EAD), where ectoderm and endoderm are directly juxtaposed (Dickinson and Sive, 2006; Dickinson and Sive, 2007). The EAD also acts as a signaling center to influence surrounding tissues, including the cranial neural crest, which forms the jaws and other facial regions (Dickinson and Sive, 2009). To identify genes that contribute to EAD function, a 'face transplant' technique was developed, where tissue is transplanted from a donor into a host embryo, after removing the corresponding host region. Following the transplant, resulting facial development is assessed. Thus, the effects of loss of function (LOF) or gain of function (GOF) for a specific gene in the EAD are analyzed locally, where the rest of the head and body is composed of wild type tissue. The reciprocal transplant can be performed, where wild type tissue is transplanted into embryos with global LOF or GOF in specific genes. Transplantation has been frequently used in *Xenopus* and chick studies (Gilbert, 2010). For example, *Xenopus* transplantation has addressed homogenetic neural induction, lens and neural competence, and neural crest migration (Borchers et al., 2000; Grunz, 1990; Servetnick and Grainger, 1991; Servetnick and Grainger, 1991). Quail-chick chimeric grafting has analyzed development of the anterior neural plate, anterior neural ridge, neural crest, and cranial bones (Couly et al., 1993; Couly and Le Douarin, 1985; Couly and Le Douarin, 1987; Lievre and Le Douarin, 1982). This is the first transplant technique for study of craniofacial development in *Xenopus.* This technique has demonstrated a novel role for the Wnt inhibitors *Frzb-1* and *Crescent* in regulating basement membrane formation in the presumptive mouth

(Dickinson and Sive, 2009). *Xenopus laevis* is an ideal model for study of craniofacial development as embryos are large, develop externally, and the face is readily visible, allowing micromanipulation and imaging of development. Mechanisms underlying facial development appear conserved, indicating that findings made in the frog provide insight into human development (Dickinson and Sive, 2007; Kennedy and Dickinson, 2012; Trainor and Tam, 1995).

4.3 Materials

Materials and reagents required for face transplants are included in Table 4.1.

Table 4.1: Detailed information about the materials and reagents required for face transplants.

Name of Reagent/Materials	Company	Catalog Number	Comments
Pasteur Pipette Size 5 ¾''	VWR	14672-400	Lime Glass Cotton Plugged Disposable
Graduated Transfer Pipette	VWR	16001-180	Disposable Polyethylene
#5/45 Forceps	Fine Science Tools by Dupont Medical	11251-35	Angled 45°
Standard Pattern Forceps	Fine Science Tools	11000-20	Straight Serrated Tip Stainless Steel 20cm long
Capillary Tubing (for needles)	FHC	30-30-1	Borosil 1.0mm OD x 0.5mm ID/Fiber 100mm each
Cover Slip Micro cover glass (for glass bridges) No. 1.5	VWR	48393 252 or 48393 230	24x60mm or 24x40mm
Ficoll 400	Sigma-Aldrich	F9378	
Needle Puller Model P-80	Sutter Instrument Co. Flaming/Brown Micropipette	Discontinued	The most similar, current available product is the P-97.
Stereomicroscope Zeiss Stemi 1000	Zeiss		
Stereomicroscope Lighting by Fostec	Fostec		Use a light box with 2 fiberoptic arms.
Nickel Plated Pin Holder	Fine Science Tools	26018-17	Jaw Opening Diameter: 0 to 1mm Length: 17cm
Moria Nickel Plated Pin Holder	Fine Science Tools	26016-12	Jaw Opening Diameter: 0 to 1 mm Length: 12cm
Tungsten Needles	Fine Science Tools	10130-05	0.125mm Rod diameter
Van Aken Plastalina Modeling Clay- white, red or yellow	Blick	#33268-2981	
mMessage mMachine Sp6 or T7 Kit	Ambion	AM1340	

4.4 Protocol

4.4 a. Preparing Reagents

1. 10x MBS: Prepare 1L of 10x Modified Barth's Saline (MBS) solution. Refer to Table 4.2: Reagents, ingredients, and instructions. Use distilled water for all solutions. Mix in a beaker, using a stir bar, until full dissolution. All solutions should be made at room temperature.

2. 1x MBS: Dilute 100ml of 10x MBS solution in 900ml of distilled water to make 1L of 1x MBS. Add 0.7ml of 1M $CaCl_2$ solution.

3. 0.1x MBS: Dilute 1x MBS to prepare 1L of 0.5x MBS solution and 2L of 0.1x MBS solution. To 1L of 0.1x MBS solution, add 1ml of 10mg/ml gentamycin solution. The 0.1x MBS solution with gentamycin will be used for long-term embryo culture.

4. Ficoll/MBS: Add 15grams of Ficoll 400 to 500ml of 0.5x MBS solution. Mix vigorously. Add a stir bar and mix until Ficoll is fully dissolved (several hours).

5. 70% ethanol: Dilute 100% ethanol to 70% ethanol using distilled water.

Table 4.2: Reagents, ingredients and instructions for making solutions.

Reagent	Ingredients	Instructions
1M $CaCl_2$ Solution	111g of $CaCl_2$ per liter	Autoclave and store in 1ml aliquotes at -20°C or 4°C.
10X Modified Barth's Saline (MBS) Solution	880 mM NaCl, 51.4g 10mM KCl, 745.5mg 10mM $MgSO_4$, 1.2g 50mM HEPES (pH 7.8), 11.9g 25mM $NaHCO_3$, 2.1g	Adjust volume up to 1L with distilled water. Adjust final pH to 7.8 with NaOH and then autoclave.
1X MBS Solution	Final Concentrations: 88mM NaCl 1mM KCl 0.7mM $CaCl_2$ 1mM $MgSO_4$ 5mM HEPES (pH7.8) 2.5mM $NaHCO_3$	Prepare 1XMBS solution by mixing 100ml of 10x MBS salts solution with 0.7ml of 1M $CaCl_2$ solution. Adjust volume up to 1L with distilled water. Dilute this solution to make 0.5XMBS and 0.1XMBS.

4.4 b. Preparing Glass Operating Tools

1. Needle preparation: Load capillary tubing into a needle puller.

a. Pull the needles according to the settings shown in Table 4.3: Needle puller settings. The settings are for a Sutter Instrument Co. Model P-80/PC micropipette puller and capillary tubings, as described in Table 4.1: Table of specific reagents and equipment. However, these settings are specific to the Sutter needle puller, and will need to be adjusted for other machines. Settings can be determined using a ramp test, as specified by the machine's manufacturer.

b. Pull 4-6 needles in preparation for the procedure. The needles should be broken such that the flexible, hair-like portion of the glass tip is fully removed, which is typically 2-3 mm long. The tip must be relatively rigid, but still narrow enough to be used as a cutting tool. See photo of an ideal needle in Figure 4.1A.

c. Store the needles in a Petri dish with a strip of clay down the center. Press the shaft of each needle into the clay, to hold it in place and to keep the fragile sharp tip away from the bottom and sides.

Table 4.3: Needle puller settings for a Sutter Instrument Co. Model P-80/PC Micropipette Puller. Needle Puller Settings vary from machine to machine so each lab will need to optimize their own needle puller settings.

Heat	**Pull**	**Velocity**	**Time**
800	70	40	50

Figure 4.1: Tools used for face transplants. (**A**) Shows an intact, unbroken needle and a broken needle after the flexible tip has been removed. (**B**) Depicts two pipette tools with their ends fully sealed and rounded. (**C**) Shows three sample glass bridges. Scale bars = 1mm.

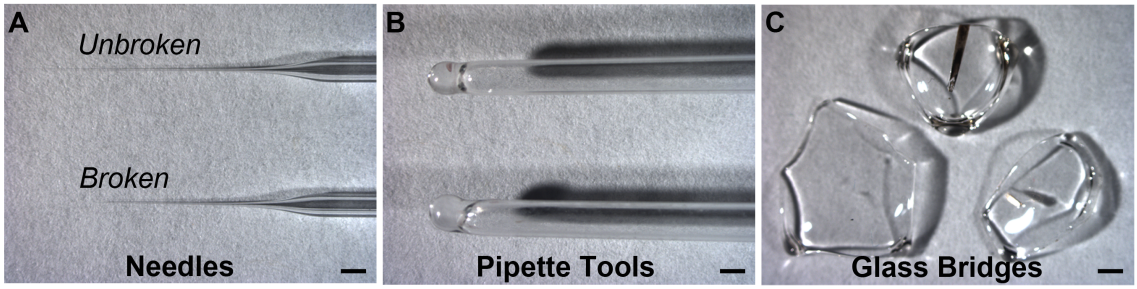

Figure 4.1

2. For additional tools, obtain glass cover slips, a pair of long standard pattern forceps, a Bunsen burner, and 3-4 glass Pasteur pipettes (Size 5 ¾ in).

3. Pipette tool: To make a pipette tool, light the Bunsen burner and place the tip of a glass Pasteur pipette into the blue part of the flame while rotating it, such that the tip melts and the hole completely seals, forming a closed, rounded end. The rounded, sealed tip is later used to make depressions in the clay dish that holds the embryos during the operation. See Figure 4.1B.

4. Glass bridges: To make glass bridges, use long standard pattern forceps to carefully break off 3 mm by 3 mm chunks of cover slip glass. While holding the piece of cover slip with tweezers, place the glass in the flame until all four edges soften and curve downward, forming a tiny glass dome. The edges should no longer be sharp. See Figure 4.1C.

5. Store the glass cover slip bridges by inserting them, edges down, into modeling clay, lining the bottom of a Petri dish. Insert the bridges such that the top of the bridge remains above the clay surface. Do not push too hard such that the bridge breaks, and do not fully embed the bridge into the clay because it can be difficult to remove. After sterilization with a flame or 70% ethanol, the bridges can be reused from experiment to experiment.

4.4 c. Preparing for the Embryo Operation

1. Line a small 60 mm plastic Petri dish with modeling clay. Between uses, the dish and clay surface is thoroughly washed with distilled water and then with 70% ethanol.

NOTE: Use red, white or yellow Van Aken Plastalina modeling clay, which can be bought at a local toy or art store. Black clay is not recommended because it releases residue.

2. Fill the dish with 3% Ficoll 0.5x MBS solution. The higher salt concentration prevents tissue dissociation, and the polysaccharide Ficoll helps to thicken the solution, which assists in holding

the face in position.

3. Use the flamed Pasteur pipette tool (see Figure 4.1) to make shallow, 2-3 mm depressions in the clay, about the depth of a stage 20 embryo body. Make 20-30 depressions, 1-2 mm apart, on each side of the dish, so there is a total of 40-60 depressions. Label one side LOF/GOF, and the other side wild type, by carving initials into the clay with forceps.

4.4 d. Preoperation Embryo Preparation

1. Obtain and culture *Xenopus laevis* embryos using standard methods (Sive et al., 2000). For a detailed description of frog husbandry, please see Sive et al. 2000.

a. Forty-eight hours prior to the experiment, obtain eggs from female frogs and perform in vitro fertilization.

b. Inject 0.5-1ng of capped membrane GFP mRNA, plus any desired mRNA or anti-sense morpholino-modified antisense oligonucleotides ("morpholinos") at the one cell stage or into 2 cells at the 2 cell stage. The one cell stage lasts approximately 70-90 minutes. Inject a total volume of 1-3nl. In place of RNA coding for a fluorescent protein (such as GFP or RFP RNA), one can inject FITC-labeled morpholino or fluorescently labeled dextran. The fluorescence is important for determining whether the transplanted tissue heals and remains in the head.

c. Capped mRNA can be prepared from a linearized plasmid using a mMessage mMachine SP6 or T7 kit. Morpholinos can be designed and ordered through Gene Tools LLC. The amount of morpholino required for a desired effect must be determined for each gene (Tandon et al., 2012).

d. Store the injected embryos at 15 °C for 48 hours, until they reach stage 19-20. (For all subsequent steps, stage embryos according to the Normal table of *Xenopus laevis* by Nieuwkoop and Faber, 1994.)

NOTE: On the day of the surgery, both recipient and donor embryos must be within one stage of each other for the transplants to work optimally. However, embryos injected with morpholinos ("morphants") sometimes develop more slowly than wild type or control morphant embryos, making it necessary to coordinate experiments so both morphant and wild type embryos are at the same stage. Morphants may need to be maintained at a higher temperature for 12-24 hours prior to the procedure. To increase the likelihood that embryos can be found at matching stages, embryos can be maintained at several temperatures. Twenty-four hours prior to the experiment, one should divide the embryos into a several dishes, and place morphants at 18-20°C and wild type embryos at 15-18°C.

2. On the day of the transplantation experiment, remove the embryos from the 15°C incubator and stage them according to Nieuwkoop and Faber, 1994. If they are younger than late neurula (stage 19), leave them at room temperature for 1-2 hours, until they reach stage 19.

3. Screen the injected embryos under a fluorescent microscope. Select embryos that show uniform, bright fluorescence for the experiment.

4. Remove clutter and possible contaminants near the operating area. Wipe down the operating surface, stereomicroscope, and all tools with 70% ethanol.

5. Once the embryos are at stage 19, remove the vitelline membrane using #5/45 Dumont forceps under a stereomicroscope.

a. Remove the vitelline membrane of 20-30 of each of donor and host embryos.

b. For the first several face transplant experiments, one should practice with a few

embryos for each condition. The method is challenging and requires careful practice before it can be used on a larger scale, quickly, and successfully. One can work up to completing 20 transplants per experiment.

6. Move host embryos into the operating dish using a plastic graduated transfer pipette with the tip cut off such that the opening is much wider than an embryo (at least a few millimeters). Be careful to avoid touching embryos to bubbles or the water surface, as embryos will explode in the surface tension.

7. Use #5/45 forceps to insert the embryos into the clay depressions, with the posterior of the embryo in the clay. Gently close the clay around the bases of the embryo using the forceps, leaving the top quarter of the embryo, the head, protruding from the depression.

8. Once all host embryos are secured in their depressions, move to the other side of the plate and begin to insert the donor embryos into their depressions. Repeat the process of securing the embryos in their wells.

4.4 e. Performing the Face Transplant Surgery

1. Cutting knife: As a cutting knife for removal of donor EAD tissue, use an appropriately broken glass capillary needle (see section 4.4 b. step 1 and Figure 4.1).

NOTE: One can directly hold the capillary between fingers (this works well for people with small hands) or one can mount the needle in an insect pin holder. Electrosharpened tungsten needles loaded into a pin holder may be used instead of a capillary tube needle (Sive et al., 2000). Please see suggested pin holders and tungsten needles in the Table 4.1.

2. Under a stereomicroscope, insert the needle into the head of the embryo to the left of the cement gland. The needle should be inserted deeply, so that it passes from outside the embryo,

through the head, and into the foregut. To transplant the entire EAD, cuts should extend from the outside of the embryo to the foregut. For ectoderm-only transplants, cuts should be shallow and extend only through the ectoderm.

3. Flick the needle from the left to the right side of the head, across the entire width of the cement gland. The flicking is important as the motion gives a clean cut. Refer to Figure 4.2A for a summary of the technique and Figure 4.2B for a demonstration of the cuts. The cement gland and eyes are important landmarks for the cuts. The order of the cuts does not affect the outcome and can vary based on user preference or handedness.

Figure 4.2: Summary of face transplant method. (**A**) General Transplant Scheme: Schematic of the face transplant method. **a.** Embryos are injected with a fluorescent agent and an antisense oligonucleotide morpholino at the 1 cell stage. The fluorescent agent can either be GFP mRNA, FITC-tagged morpholino, or fluorescent dextran. **b.** Presumptive mouth is removed at stage 22 from a host wild type embryo and a donor morphant embryo. The transplanted tissue can also be enlarged to include the presumptive nose, which lies directly above the mouth region. The donor morphant tissue is transplanted to the wild type host, and then is secured in place with a glass bridge. Grey arch: hatching gland. **c.** Facial development is scored at stages 40-41. (**B**) Experimental Considerations. **a.** Summary of incisions used to remove the face from a donor embryo. For surgical excision of the face, make incisions 1 through 4 in order. This is the preferred order of cuts, but the order of incisions can vary. **b.** The resulting donor is shown with the ectoderm and endoderm removed from the face, such that an opening exists from the outside of the embryo to the foregut. **c.** The diagram shows ideal placement of the glass bridge. The glass contacts both the transplant and host face, pressing the EAD tissue into the head to oppose extrusive forces from wound contraction during healing.

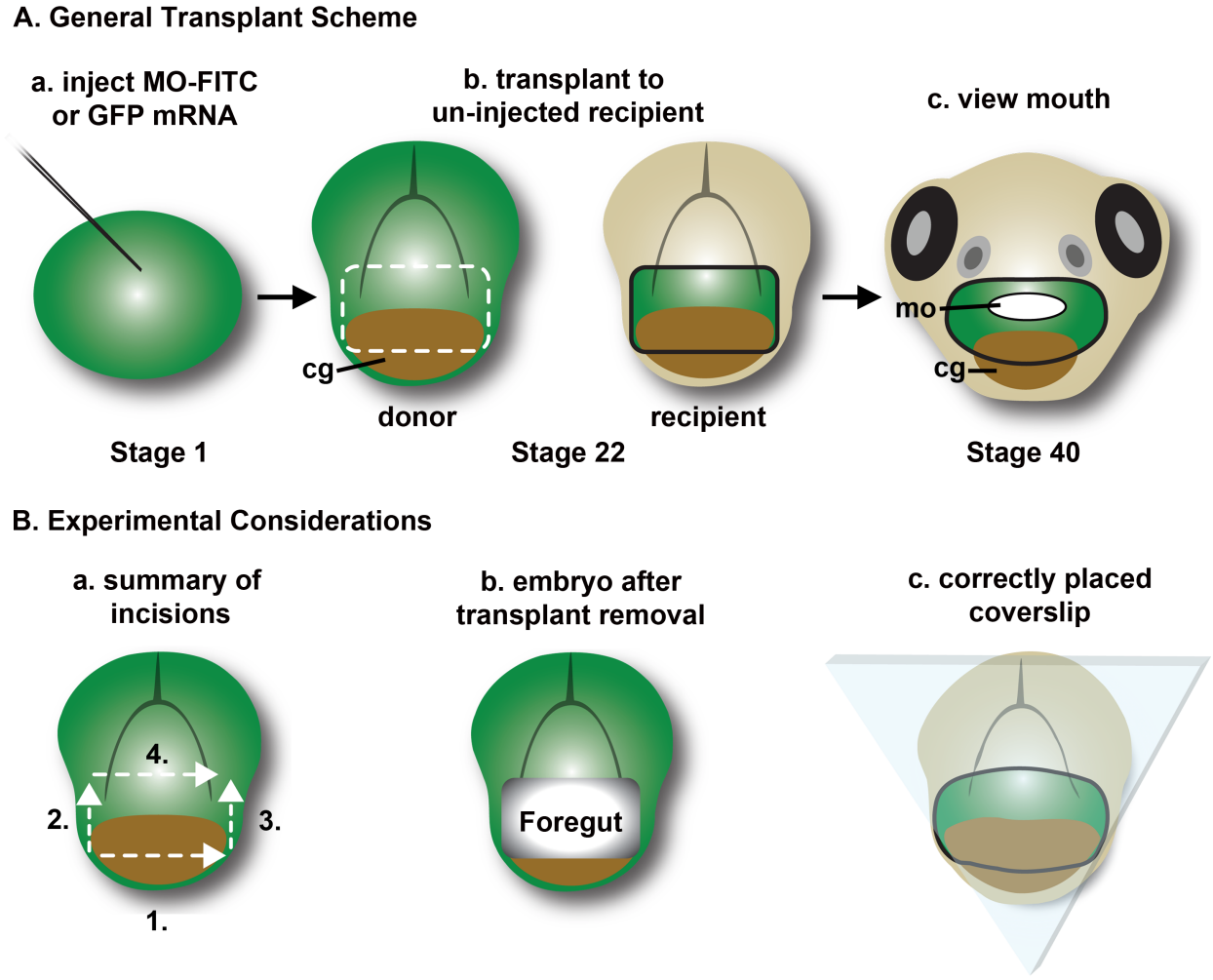
A. General Transplant Scheme
a. inject MO-FITC or GFP mRNA
b. transplant to un-injected recipient
c. view mouth
cg
mo
cg
donor
recipient
Stage 1
Stage 22
Stage 40
B. Experimental Considerations
a. summary of incisions
b. embryo after transplant removal
c. correctly placed coverslip
4.
2.
3.
1.
Foregut

Figure 4.2

4. Place the needle at the start of the previous cut, at the left border of the cement gland, and flick the needle upward until it reaches the bottom of the left eye. This will create a vertical cut from the left border of the cement gland to the bottom of the left eye.

5. Place the needle at the right border of the cement gland, and flick the needle upward until it reaches the bottom of the right eye. This will create a vertical cut from the right border of the cement gland to the bottom of the right eye.

6.To fully excise the tissue, flick the needle from the bottom of the left eye to the bottom of the right eye, creating a horizontal cut that will free the tissue. Cuts can extend from the outside of the embryo to the foregut, including both ectoderm and endoderm in the EAD explant. Alternately, shallow cuts can be used for ectoderm-only EAD transplants. Once the EAD tissue is removed, there should be a rectangular hole from the outside of the embryo into the foregut, stretching from the cement gland to just below the eyes (top to bottom). The hole should extend from the inside border of the left eye to the inside border of the right eye (side to side). See Figure 4.2Bb.

7. Gently push the excised tissue on the tip of the needle, and lift it through the buffer to the part of the dish containing host embryos. Do not expose the tissue to the surface air or it will become damaged.

8. Excise the same tissue from the host embryo, as for the donor. Discard the host EAD explant or save it to insert into the donor face, for reciprocal transplants.

9. Insert the donor explant into the resulting host hole using #5/45 forceps.

10. Once the donor tissue is correctly positioned and fully inserted, carefully place a glass bridge (see Figure 4.1 and Figure 4.2Bc) over the embryo's face to hold the transplant in place. The ends of the bridge should insert into the clay, holding it in place. The bridge should gently apply

pressure to the transplanted tissue, such that the transplant lies flush with the host head, without it sticking out of the head or lying deep within the head. The head can be slightly flattened by the cover slip, but be careful not to damage the embryo with too much pressure. Transplants should be performed within 5 minutes.

NOTE: An experienced investigator can perform around twenty transplants per experiment, over 2-3 hr. During this period the embryos will progress from stage 20-22. Completing the face transplants at stage 21 or 22 does not affect outcomes. Later transplants (at stages 22-26) can be done but are more difficult as the crest-free EAD midline region is narrowed as cranial neural crest moves into the face. Consistency across transplants is critical.

4.4 f. Face Transplant Post-operation Recovery

1. Healing typically takes 2-3 hr. Leave the embryos at room temperature undisturbed in their clay depressions with the glass bridges holding the donor tissue in place.

2. Once the transplants have healed, carefully remove the glass bridges, remove the clay from around the base of the embryos using forceps, and use a plastic graduated transfer pipette to gently vacuum the embryos out of their depressions.

3. Put the embryos into an appropriately labeled Petri dish, half filled with clean 0.1x MBS with gentamycin.

4. Grow the embryos at 15°C or 18°C for several days until they reach feeding tadpole stage at stage 40, when facial phenotypes can be scored.

a. The 0.1x MBS solution with gentamycin should be changed daily, and any dead embryos should be removed promptly to prevent contamination and death of other embryos.

b. The mouth opens at stage 40. At stage 40-41, one must check that the transplanted tissue remains healed in place by viewing its fluorescence. Transplants occasionally fall out, so one must ensure that all scored embryos have the donor tissue in place.

4.5 Representative Results

Transplanted tissue should be fully inserted into the host head after transplantation as shown in Figure 4.3A, and have a glass bridge appropriately placed on the embryo's face, as shown in Figure 4.2Bc. The transplanted donor tissue must be correctly sized for the host opening, for the transplant to be successful. The EAD tissue should not protrude from the head, in any way, as seen in Figures 4.3B and 4.3C. Additionally, the face transplant should not be rotated relative to its position in the donor body, as shown in Figure 4.3D. After several hours, the transplanted tissue and surrounding face should heal, and by the next day, the embryo should appear as the example shown in Figures 4.4A and 4.4A'. One can observe, under fluorescence, that the transplant remains in place in Figure 4.4B and 4.4B'. At stage 41, the transplanted control tissue will contribute to the mouth, and will remain florescent green, seen in Figure 4.4B'. Wild type EAD tissue transplanted into wild type hosts should give rise to normal faces, when compared with unperturbed wild type embryos. However, with LOF or GOF donor tissue, faces should heal and remain in the head, but these may or may not give rise to normal craniofacial structures, as shown in Figure 3 of Dickinson and Sive, 2009.

Figure 4.3: Schematic of embryos shortly after transplantation. Frontal views are shown. The transplanted tissue is outlined in red dots. (**A** and **A'**) depict an ideal outcome at stage 22. The tissue is fully inserted and correctly positioned in the head. (**B** and **B'**) show an incorrect transplant, with the tissue partially inserted into the head. (**C** and **C'**) show an incorrect transplant with most of the tissue inserted into the head, but the excess region is protruding from the healing site. This tissue will necrose, and inhibit healing of the surrounding, properly inserted regions. (**D** and **D'**) show an improper transplant, where the face has been rotated in the host, relative to its position in the donor. The tissue will heal into the head, but the face will not develop normally.

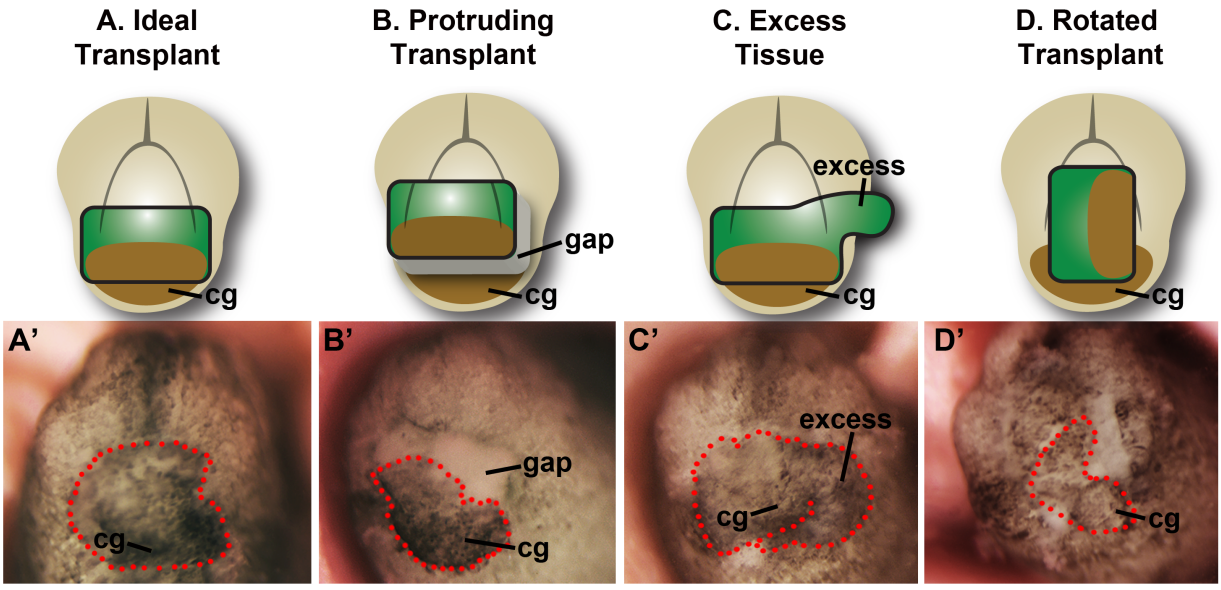
A. Ideal Transplant
B. Protruding Transplant
C. Excess Tissue
D. Rotated Transplant
cg
gap
excess
A'
B'
C'
D'

Figure 4.3

Figure 4.4: Older embryos with ideal outcomes. Frontal views are shown. cg, cement gland. mo, mouth. (**A**) Displays an embryo one day after transplantation, showing a properly healed transplant at stage 32. (**A'**) Shows this same embryo with a fluorescent overlay, confirming that the transplanted tissue remains in place. (**B**) Shows the same embryo at stage 42 which had a control morpholino, GFP+ transplant several days prior. The face has developed properly. (**B'**) Shows the same embryo with a fluorescent overlay, confirming that the transplanted tissue remains in the head and has contributed normally to facial structures.

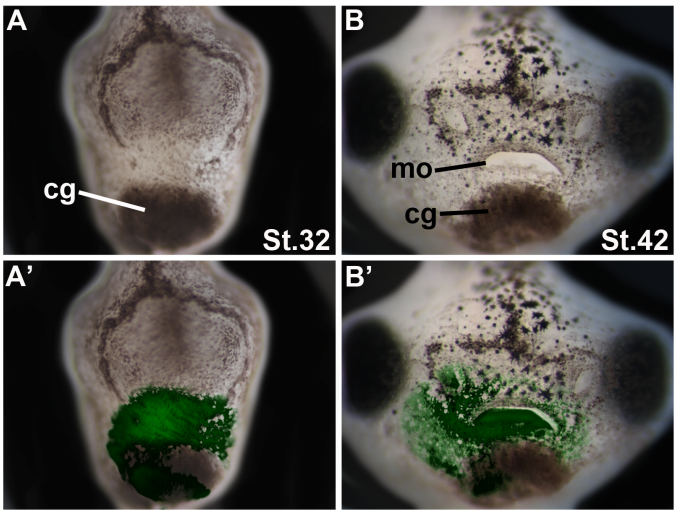

Figure 4.4

4.6 Discussion

4.6 a. Critical Steps and Limitations

The EAD face transplant procedure is time and work intensive. It requires practice, steady hands, and dexterity to perfect. The face transplant protocol relies on the researcher's ability to efficiently remove and transplant tissue. If one takes too long to insert the transplant into the host's face, the host face will begin to contract and heal. Forceps can be used to delicately expand the facial region. However, if significant wound contraction has occurred, the transplant will not heal as well and may need to be reduced in size to fit into the host's facial hole. The transplant's size and shape must roughly match the size and shape of the recipient's facial cavity, to allow successful insertion.

Face transplants are most successful when performed between stages 19-22, with embryos that are matched by stage. Older face transplants, between stages 22-26, are possible, but are more challenging and may disrupt neural crest migration into the sides of the face since the crest-free midline region becomes significantly narrower from stage 22-26.

Both the recipient and donor must be at similar stages for the transplant to work optimally. Ideally, they should be the same stage, and minimally have to be within a few hours of each other. Embryos injected with antisense-RNA morpholino oligonucleotides ("morphants") sometimes develop more slowly than wild type or control morphant embryos, requiring that morphants be grown at a higher temperature to match the wild type embryos' stages.

The donor face tissue should not be rotated in the host body relative to its original position in the donor embryo, otherwise the face will not develop normally. The cement gland does not need to be included in the face transplant for the procedure to work; the face develops normally without it. However, the cement gland is often included in the extirpated facial tissue

because it serves as a distinct marker to indicate and position the bottom of the transplant. This marker will help avoid accidently rotating the tissue during the transfer of the face tissue to the recipient. If the transplant has been inserted incorrectly in the host face, the donor tissue can be removed and discarded. One can attempt to insert a new transplant into the same host, if the opening has not begun to constrict. However, if the host opening has noticeably shrunk, then discard the host and begin anew.

It is crucial to place the glass bridge directly on the transplanted face, so that the transplant is held in the host's head during healing. If the transplant is not held in place, the transplant can be extruded from the host's face. Transplants that are not fully inserted into the face or that pop out during healing will undergo necrosis. Even in perfect transplants, small amounts of tissue death may occur around the edges of the transplant. Usually this does not cause adverse effects and a completely normal face can still be formed. In successful controls, we have not observed any malformation after four weeks of development suggesting that the cartilages formed normally and that rejection of the tissue is rare.

Finally, if a morpholino perturbs a protein required for normal wound healing, this technique may not work, as the transplanted LOF tissue may not be incorporated into the host head.

4.6 b. Possible Modifications and Trouble Shooting

Modifications can be made to the procedure. With practice, the researcher can learn to transplant smaller regions, for example, half of the EAD. Shallow incisions allow ectodermal transplants, leaving the deeper endoderm undisturbed. Other regions of embryonic tissue can be transplanted, using similar approaches.

If the transplanted tissue dies after insertion, there are a couple of possible causes. Transplanted tissue that is not completely inserted into the host or appropriately held in place with a glass bridge, will die and impede proper healing. Make sure to fully insert the transplanted tissue and secure it in place with a glass bridge. If the transplant is derived from a morpholino or RNA-injected donor, then the tissue may die due to toxicity from injected agents. Similarly, if the host embryos are morphants or RNA-injected and frequently die, then the amount of morpholino or RNA will need to be reduced. To resolve these issues, titrate the amount of injected RNA or morpholino and determine a safe amount for successful face transplants. Finally, increasing the salt concentration of the MBS solution above 0.1x can also assist healing.

4.6 c. Significance

The face transplant technique described allows analysis of the local requirements and activity of gene products during craniofacial development. This approach can clarify signaling between the developing non-crest, neural crest, and surrounding structures. It allows one to examine LOF or GOF (using any strategy) in all EAD-derived tissues, which is not possible with any single promoter driven construct. Though there is a long history of tissue transplantation in developmental biology, this is the first application of transplantation to the study of craniofacial development in frogs and is crucial for mechanistic studies. Thus the technique can help to unravel the complex mechanisms controlling patterning and formation of the vertebrate face and to clarify causes of craniofacial developmental defects.

4.7 Acknowledgements

We thank Radek Sindelka for his help, and Cas Bresilla for assisting with frog husbandry and embryo preparation. This work was funded by the NIH via the grant R01DE021109 to H.L.S. L.J. was funded by the Herschel Smith Graduate Fellowship at Harvard University and an F30 individual fellowship grant F30DE022989-01 through the NIDCR.

Chapter 5

Future Directions

Author Contributions: L.J. wrote and revised the chapter. H.S. directed and supervised the studies discussed and assisted in revising the chapter.

5.1 'An experiment is a question which science poses to Nature, and a measurement is the recording of Nature's answer.' – Max Planck

Craniofacial development is fertile with promising questions, yielding answers of astounding complexity and beauty. The face is the most complicated and critical region of living organisms, needed for communication, consumption and sensory input. Considering its varied roles and cell types, it is amazing that the face is simply derived from cranial neural crest (NC) and anterior embryonic tissues. However, the signaling conversations and morphogenetic processes needed for development are immensely nuanced. The extreme anterior domain (EAD) is a newly recognized organizer of craniofacial development, and is required for mouth formation and cranial NC migration and development in *Xenopus*. Chick and mouse also have a facial organizing domain, known as the frontonasal ectodermal zone (FEZ), which operates later in craniofacial development (Hu and Marcucio, 2009b). Research conducted in model organisms has provided great insight into face formation, and in the process, opened many new lines of inquiry. The topics discussed in these chapters lend themselves to future questions and hypotheses deserving investigation.

5.2 Classical Embryology Anew

Classical embryology has yielded some of the most striking results, such as body axis duplication resulting from blastopore lip grafting described by Spemann and Mangold (Spemann and Mangold, 1924). Our group's transplantation experiments demonstrate the organizing potential of the EAD (Jacox et al., 2014), and extirpation of superficial and deep EAD tissue results in marked craniofacial abnormalities (Dickinson and Sive, 2006). However, our early extirpation experiments were conducted prior to careful study of EAD tissue architecture and developmental timing. As a result, it would be useful to revisit these experiments to determine when the organizer operates and which portions of the EAD are necessary. *I hypothesize that the EAD ectoderm and endoderm are required for organizer signaling and that the organizer operates from early to mid tail bud stages (stages 22-24).* By stage 24, cranial NC has segregated into BA1 and migrated into the face, and *frzb-1* and *crescent* are down-regulated in the EAD (Dickinson and Sive, 2009). To test this hypothesis, one could selectively extirpate EAD ectoderm, endoderm or both, at intervals from late neurula (stage 20) through swimming tadpole (stage 30) and then score facial development at feeding tadpole stage (stage 40). One could observe when the organizer is required and which tissues are critical at various times.

Extirpation of EAD endoderm, endoderm zone 1 (EZ-1), is associated with failure of mouth and nostril formation in *Xenopus leavis* (Dickinson and Sive, 2006). EZ-1 directs overlying NC to form mesethmoid cartilage, the precursor to upper beak cartilage in chick and nasal septum and vomer bones in human (Benouaiche et al., 2008). Ablation of EZ-1 is associated with agenesis or reduction of the nasal capsule, nasal septum, and upper beak (Benouaiche et al., 2008; Couly et al., 2002). From chick and mammalian data, *I hypothesize that EZ-1 signals to an anterior NC domain to control nasal and maxillary development in Xenopus.*

It would be interesting to repeat Dickinson's EZ-1 extirpations followed by detailed bright field and confocal imaging to visualize NC, nostril, nasal septum and stomodeal development, using both morphology and tissue specific markers. In situ hybridization, fluorescent NC transplants, and alcian blue staining could be used to determine if NC arches and subsequent cartilages are altered. It would also be useful to see if early *shh* expression is limited to EZ-1, as in chicks, by in situ hybridization (Benouaiche et al., 2008). One could identify factors required for EZ-1 signaling, beginning with LOF and GOF studies in *shh*. Our prior studies have focused on EAD ectoderm, but an equally promising line of inquiry involves study of anterior endoderm.

Initial EAD grafting assays were quite crude and redesigning these experiments could yield greater insight (Dickinson and Sive, 2006). Transplantation of EAD tissue into flank did not induce a mouth, but transplantation of a large swath of facial tissue into the lateral head produced a second stomodeum (Dickinson and Sive, 2006). *I hypothesize that the EAD is capable of inducing a second mouth only when it is adjacent to NC and anterior brain tissue.* With use of fluorescent NC transplants, conducted at stage 18, one could selectively transplant EAD tissue alone, EAD plus fluorescent NC, and EAD with NC and brain tissue, into wild-type host faces and flanks at stages 20-22. Development could be imaged over time and scored at feeding tadpole stage (stage 40). Even if a mouth fails to form, embryos could be fixed and used for in situ hybridization of NC marker *sox9* to see if EAD signaling was exerting an effect on host NC.

Though late Hedgehog signaling regulates mouth size (Tabler et al., 2014), it is plausible that mouth and facial cartilage sizes correlate with EAD area. This is complicated by the contribution of the EAD to the mouth, though EAD tissue primarily gives rise to epithelial lining and not the bulk of facial cartilage and connective tissue (Chapter 3). FEZ grafting and

extirpation alter cartilage dimensions in chick, and *frzb-1* GOF in *Xenopus* is associated with an enlarged stomodeum, suggesting EAD-localized Wnt inhibitors influence mouth size (Dickinson and Sive, 2006; Hu et al., 2003). *Therefore, I hypothesize that mouth size is proportional to EAD area.* To test this theory, one could measure mouth and cartilage dimensions in wild-type embryos, embryos with grafted EAD tissue, and embryos with partial EAD extirpation. Alcian blue staining would facilitate visualization and measurement of cartilage segments. Data would indicate whether EAD size is a regulator of mouth and facial cartilage dimension.

5.3 Conservation of the FEZ Organizing Region

The EAD and FEZ are craniofacial organizing centers. However, they are distinct organizers active at different times in craniofacial development and studied in separate species. The EAD was identified in *Xenopus*, with early activity while cranial NC is migrating into the face (Jacox et al., 2014). The FEZ is a facial organizer studied in mice and chick, acting after cranial NC migration, during facial prominence development (Hu et al., 2003; Hu and Marcucio, 2009b; Hu et al., 2015).

All vertebrate faces have an EAD, with juxtaposed ectoderm and endoderm, but it is unclear whether the EAD serves organizer functions in species outside of *Xenopus* (Dickinson and Sive, 2006; Dickinson and Sive, 2007; Jacox et al., 2014). Similarly, all vertebrates have ectoderm overlying their cranial NC prominences, but it is unknown whether the tissue secretes SHH and FGF8 to pattern facial development in species beside mouse, chick and possibly zebrafish. *I hypothesize that vertebrates begin facial development with a conserved EAD organizer active during cranial NC migration, and later generate a FEZ organizer for prominence development and chondrogenesis.* To investigate presence of a FEZ organizer in *Xenopus,* one could use dual in situ hybridization to see *fgf8* and *shh* expression at several stages between late tail bud (stage 28) and feeding tadpole (stage 40). Juxtaposed *fgf8* and *shh* expression in *Xenopus* facial ectoderm would be consistent with my hypothesis. If a FEZ-like domain exists, extirpation, grafting, GOF and LOF studies, akin to the chick and mouse experiments described in Chapter 1, would clarify whether the region was functionally conserved in *Xenopus*.

Data are consistent with the zebrafish having a FEZ/EAD organizing domain in the stomodeal region, which promotes branchial arch 1 condensation and chondrogenesis (Jacox et

al., 2014). Zebrafish demonstrate *fgf8* expression in the lateral stomodeum and *shh* expression in the medial stomodeum, directly adjacent and without overlap (Eberhart et al., 2006). This region of oral ectoderm is required for formation of the anterior craniofacial skeleton, like the murine and avian FEZ (Eberhart et al., 2006). *I hypothesize that the zebrafish stomodeal region is a midline craniofacial organizer.* To further test this theory, one could extirpate the tissue, graft an ectopic stomodeal region into the zebrafish head, conduct GOF and LOF studies of *shh* and *fgf8* independently and concomitantly, and do in situ hybridizations of *Xenopus* EAD-specific genes including *frzb-1* and *cpn*. Confirming conservation of a craniofacial organizing domain in zebrafish would help cement the ubiquity of midline organizers in vertebrates and offer another model species for their study. Future inquiry into organizer conservation and development is necessary to address these hypotheses.

5.4 EAD Morphological Study

The morphological study of mouth formation described in Chapter 3 has spawned a number of questions. *First, what is the role of the extracellular laminin coating observed in the EAD ectoderm while NC approaches the midline bilaterally (stage 26) (Chapter 3, Figures 3.3L and L')?* This abundant laminin could be serving as a structural barrier for the migrating NC and may prevent NC from crossing the midline or fusing prematurely. NC cells are not observed crossing this midline region during tail bud (Chapter 3). This laminin layer becomes patchy by stage 28, once NC has arrived at the facial midline and the EAD has undergone convergent extension (CE), suggesting the layer serves a specific, time-sensitive role. Localized loss of laminin in the EAD combined with live imaging of NC cells could yield fascinating data and point to the function of the midline laminin enrichment.

When and how is apical-basal polarity determined in the midline EAD? Basal polarity is established early in EAD morphogenesis. EAD cells undergoing CE demonstrate basally localized nuclei and basement membrane (BM) at late tail bud, yet separation of EAD tissue to open into the mouth, indicating apical polarity, occurs significantly later during stomodeal invagination (stage 34/35). Many apical markers localize after the oral opening has formed, including Zo-1 (Figure 3.6A-E, A'-E'), aPKC, and actin (data not shown). Apical polarity is likely established with an early marker upstream of aPKC, and may be involved in cellular detachment at the midline. A more comprehensive immunohistochemistry study is needed to identify an upstream factor determining apical-basal polarity in the midline EAD ectoderm. Polarity determination in midline cells is an unexplored phase of mouth formation and investigation could enrich our understanding of lumen formation and identify additional pathways involved in EAD morphogenesis.

5.5 Organizing Effect of Wnt Inhibitors

The study of Wnt inhibitors by Dickinson and Sive exposed the ability of the EAD to signal to surrounding tissue, thereby influencing mouth formation (Dickinson and Sive, 2009). The failure of mouth formation in *frzb-1* and *crescent* morphants was attributed to aberrant BM turnover. However, the profound craniofacial phenotypes observed in wild-type host embryos with *frzb-1* and *crescent* morphant EAD transplants, cannot be fully explained by a BM abnormality (Dickinson and Sive, 2009). *I hypothesize that secretion of the Wnt inhibitors Frzb-1 and Crescent by the EAD are required for cranial NC development.* Consistent with this hypothesis, transplant embryos had abnormalities in both the morphant EAD and surrounding wild-type tissue; mouths and nostrils failed to form, the faces were abnormally narrow, and pigment cells were absent. The phenotype is consistent with *cpn* morphant EAD transplants, where cranial NC fails to migrate and develop normally. To test my hypothesis, one could conduct in situ hybridization assays of cranial NC markers, live cranial NC migration studies, and proliferation and apoptotic measurements of embryos with *frzb-1* and *crescent* morphant EAD transplants. The Wnt inhibitors are key organizing molecules released by the EAD, and investigating their role in face formation would be a valuable extension of prior work by Dickinson and Sive, 2009.

5.6 Extensions of the Kinin-Kallikrein Study

The Kinin-Kallikrein pathway is a well-studied signaling cascade in adult mammals, but its role in craniofacial development was recently discovered, as described in Chapter 2. In adult mammals, CPN acts on a number of substrates, including complement 3a (C3a), a peptide required for mutual cell attraction in migrating NC cells of *Xenopus* embryos (Carmona-Fontaine et al., 2011; Matthews et al., 2004). *I hypothesize that Cpn processes multiple small peptides in the EAD, thereby modulating several pathways active in and around the EAD.* Such multi-purpose peptidase activity could explain the more severe phenotype observed in *cpn* morphants, as compared to loss of function in other Kinin-Kallikrein members. To explore this hypothesis, the cloned *Xenopus cpn* gene could be Flag- or His-tagged, then overexpressed and isolated. In vitro activity of Cpn could be tested against a panel of *Xenopus* small peptides. Tagged *cpn* mRNA could be injected into embryos followed by co-immunoprecipitate (Co-IP) of tagged Cpn and ligand. Co-IP product could be submitted to mass spectroscopy analysis to identify ligand molecules. Knowing which ligands are processed by Cpn will identify other pathways involved in mouth formation and will extend our knowledge of Cpn function in craniofacial development.

Bradykinin and desArg-Bradykinin bead assays in live embryos suggest Kinin peptides exercise pro-migratory effects on cranial NC (Jacox et al., 2014). However, the migratory effects of Kinins have not been fully characterized. *I hypothesize that Kinin peptides serve as chemoattractants for migratory cranial NC cells.* To test this theory, one could do an in vitro assay with migratory NC placed in a Kinin peptide gradient, to see how NC cells respond. It would also be interesting to see the interaction of migratory NC with explanted EAD and prechordal plate.

Though the identified Kinin-Kallikrein components are pivotal for facial morphogenesis, the pathway is incomplete without a receptor to bind the extracellular Bradykinin (BK) peptides and activate intracellular NOS. In adult mammalian tissues, BK and desArg-BK activate B2 and B1 G protein-coupled receptors (GPCR), to stimulate NOS. A BKB receptor had not been identified in the *Xenopus* genomes. However, a search of the recently sequenced *Xenopus tropicalis* and *laevis* genomes identified one candidate receptor in *X. tropicalis* and two, nearly identical receptors in *X. laevis*, 66% similar to the human BKB2 receptor and 51% similar to the human BKB1 receptor. The putative BKB receptor in *X. laevis* was isolated, cloned, and sequenced in full. Expression analyses reveal activity in the EAD and NC regions of the developing face. Loss of function in the putative BK receptor is associated with a reduction in NO production, failure of mouth and nostril formation, and grossly abnormal facial development, consistent with loss of function in other Kinin-Kallikrein members. Data suggest that the putative BK receptor is a member of the Kinin-Kallikrein pathway in *Xenopus* and is required for craniofacial development. Further inquiry is needed to clarify the BK receptor's binding characteristics, to delineate its role in EAD and neural crest development, and to identify the signaling cascade downstream of receptor activation.

5.7 Closing Thoughts

Craniofacial development is an intricate process, involving cranial neural crest (NC) and anterior facial tissue. Anterior facial tissue and NC give rise to the beautiful, diverse, and specialized structures of the face. This delicate complexity is likely why head and neck anomalies account for one third of all birth defects (Gorlin, 1990), though the molecular pathologies underlying the deformities are rarely known. Much work needs to be done to understand the stages and regulators of early craniofacial development.

NC migration into the early face is regulated by multiple mechanisms and activity of one or more organizer regions. In *Xenopus*, the extreme anterior domain (EAD) is a craniofacial organizer required for mouth formation (Jacox et al., 2014). Work presented in this dissertation explores the organizing role of the EAD in craniofacial development and its reciprocal signaling with cranial NC. Prior data suggests that the EAD possesses organizer traits and demonstrates enrichment of Kinin-Kallikrein gene expression. My thesis project began by exploring the activity and necessity of the putative EAD organizer and the Kinin-Kallikrein pathway in mouth formation of *Xenopus* and zebrafish. The mouth fails to form and NC development and migration are abnormal after loss of function in Kinin-Kallikrein genes. Facial transplants demonstrate that EAD-localized Kinin-Kallikrein function is required for migration of first arch cranial NC into the face and for mouth opening. Our data reveal that the EAD is a novel and essential craniofacial organizer acting through Kinin-Kallikrein signaling.

During a histological study of EAD development, we noted a novel phase of EAD morphogenesis. Initially, the EAD forms a wide and short epithelial mass that narrows and lengthens after arrival of cranial NC. Cells and nuclei undergo stereotypical changes indicative of convergent extension, and the narrowed region opens to form the mouth. The concomitant

timing of convergent extension and NC migration into the face prompted investigation into whether cranial NC reciprocally signals to the EAD to mediate mouth formation. Data indicate that cranial NC sends a crucial Wnt/PCP signal to mediate EAD morphogenesis during normal mouth development.

The EAD is a pivotal organizer of craniofacial development that reciprocally signals with cranial NC to mediate migration, morphogenesis, and mouth formation. These early phases of craniofacial development are widely conserved, so findings in *Xenopus* are likely relevant to vertebrates (Dickinson and Sive, 2007; Young et al., 2014). Future investigation into organizers of craniofacial development will greatly enrich our knowledge of face formation and provide insight into causes and potential treatments of craniofacial anomalies.

References

Abu-Issa, R., Smyth, G., and Smoak, I., Yamamura, K.I., and Meyers, E. N. (2002). Fgf8 is required for pharyngeal arch and cardiovascular development in the mouse. Development. *129(19)*, 4613-4625.

Abzhanov, A., Cordero, D., Sen, J., Tabin, C., and Helms, J. (2007). Cross-regulatory interactions between *Fgf8* and *Shh* in the avian frontonasal prominence. Congenit Anom (Kyoto) *47*, 136-148.

Abzhanov, A., Protas, M., Grant, R., Grant, P., and Tabin, C. (2004). Bmp4 and morphological variation of beaks in Darwin's finches. Science. *305*, 1462-1645.

Abzhanov, A., and Tabin, C. (2004). Shh and Fgf8 act synergistically to drive cartilage outgrowth during cranial development. Dev. Biol. *273*, 134-148.

Adams, E. (1931). Some effects of the removal of endoderm from the mouth region of the early Amblystoma punctatum embryos. J. Exp. Biol. *58*, 147-163.

Aoki, Y., Saint-Germain, N., Gyda, M., Magner-Fink, E., Lee, Y.H., Credidio, C., and Saint-Jeannet, J.P. (2003). Sox10 regulates the development of neural crest-derived melanocytes in *Xenopus*. Dev. Biol. *259*, 19–33.

Barr, M., Jr., and Cohen, M.M., Jr. (1991). ACE inhibitor fetopathy and hypocalvaria: the kidney-skull connection. Teratology. *44*, 485-495.

Belloni, E., Muenke, M., Roessler, E, Traverso, G., Siegel-Bartelt, J., Frumkin, A., Mitchell, H., Donis-Keller, H., Helms, C., Hing, A., Heng, H., Koop, B., Martindale, D, Rommens, J., Tsui, L., and Scherer, S. (1996). Identification of Sonic hedgehog as a candidate gene in holoprosencephay. Nature Genetics. *14*, 353-356.

Benouaiche, L., Gitton, Y., Vincent, C., Couly, G., and Levi, G. (2008). Sonic hedgehog signaling from foregut endoderm patterns the avian nasal capsule. Development. *135*, 2221-2225.

Borchers, A., Epperlein, H. H., and Wedlich, D. (2000). An assay system to study migratory behavior of cranial neural crest cells in *Xenopus*. Dev. Genes Evol. *210*, 217-222.

Borgono, C.A., Michael, I.P., and Diamandis, E.P. (2004). Human tissue kallikreins: physiologic roles and applications in cancer. Mol. Cancer Res. *2*, 257-280.

Bradley, S., Tossell, K., Lockley, R., and McDearmid, J.R. (2010). Nitric oxide synthase regulates morphogenesis of zebrafish spinal cord motoneurons. J. Neurosci. *30*, 16818-16831.

Brugmann, S., and Moody, S. (2005). Induction and specification of the vertebrate ectodermal placodes: precursors of the cranial sensory organs. Biol. Cell. *97*, 303-319.

Bryant, J.W., and Shariat-Madar, Z. (2009). Human plasma kallikrein-kinin system: physiological and biochemical parameters. Cardiovasc. Hematol. Agents Med. Chem. *7*, 234-250.

Carmona-Fontaine, C. (2011). PhD Thesis. University College of London. Epub. http://carloscarmonafontaine.wikispaces.com/Thesis

Carmona-Fontaine, C., Matthews, H., Kuriyama, S., Moreno, M., Dunn, G., Parsons, M., Stren, C., and Mayor, R. (2008). Contact inhibition of locomotion in vivo controls neural crest directional migration. Nature. *456 (7224)*, 957-961.

Carmona-Fontaine, C., Theveneau, E., Tzekou, A., Tada, M., Woods, M., Page, K.M., Parsons, M., Lambris, J.D., and Mayor, R. (2011). Complement fragment C3a controls mutual cell attraction during collective cell migration. Dev. Cell. *21*, 1026–1037.

Chang, A.C., Fu, Y., Garside, V.C., Niessen, K., Chang, L., Fuller, M., Setiadi, A., Smrz, J., Kyle, A., Minchinton, A., Marra, M., Hoodless, P.A., and Karsan, A. (2011). Notch initiates the endothelial-to-mesenchymal transition in the atrioventricular canal through autocrine activation of soluble guanylyl cyclase. Dev. Cell. *21*, 288–300.

Chapman, S., Sawitzke, A., Campbell, D., and Schoenwolf, G. (2005). A three-dimensional atlas of pituitary gland development in the Zebrafish. J. Comp. Neurol. *487*, 428–40.

Chen, W., Burgess, S., and Hopkins, N. (2001). Analysis of the zebrafish *smoothened* mutant reveals conserved and divergent functions of hedgehog activity. Development. *128*, 2385-2396.

Chen, A., Kumar, S.M., Sahley, C.L., and Muller, K.J. (2000). Nitric oxide influences injury-induced microglial migration and accumulation in the leech CNS. J. Neurosci. *20*, 1036-1043.

Cheung, P.P., Kunapuli, S.P., Scott, C.F., Wachtfogel, Y.T., and Colman, R.W. (1993). Genetic basis of total kininogen deficiency in Williams' trait. J. Biol. Chem. *268*, 23361-23365.

Chiang, C., Litingtung, Y., Lee, E., Yorng, K, Corden, J., Westphal, H., and Beachy, P. (1996). Cyclopia and defective axial patterning in mice lacking Sonic hedgehog gene function. Nature. *383*, 407-413.

Cloutheir, D.E., Garcia, E., and Schilling, T.F. (2010). Regulation of facial morphogenesis by endothelin signaling: Insights from mice and fish. Am. J. Med. Genet. Par. A. *152A*, 2962-2973.

Contestabile, A., and Ciani, E. (2004). Role of nitric oxide in the regulation of neuronal proliferation, survival and differentiation. Neurochem. Int. *45*, 903–914.

Cooke, J.P. (2003). NO and angiogenesis. Atheroscler. Suppl. *4*, 53–60.

Couly, G., Coltey, P., and Le Douarin, N. (1993). The triple origin of skull in higher vertebrates: a study in quail-chick chimeras. Development. *117*, 409-429.

Couly, G., Creuzet, S., Bennaceur, S., Vincent, C., and Le Douarin, N. (2002). Interactions between Hox-negative cephalic neural crest cells and the foregut endoderm in patterning the facial skeleton in the vertebrate head. Development. *129*, 1061-1073.

Couly, G. F., and Le Douarin, N. M. (1985). Mapping of the early neural primordium in quail-chick chimeras. I. Developmental relationships between placodes, facial ectoderm, prosencephalon. Dev. Biol. *110*, 422–439.

Couly, G. F. and Le Douarin, N. M. (1987). Mapping of the early neural primordium in quail-chick chimeras. II. The prosencephalic neural plate and neural folds, implications for the genesis of cephalic human congenital abnormalities. Dev. Biol. *120*, 198 -214.

Creuzet, S., Schuler, B., Couly, G., and Le Douarin, N.M. (2004). Reciprocal relationships between Fgf8 and neural crest cells in facial and forebrain development. Proc. Natl. Acad. Sci. USA. *101*, 4843-4847.

Crump J., Maves, L., Lawson, N., Weinstein, B., and Kimmel, C. (2004). An essential role for FGFs in endodermal pouch formation influences later craniofacial skeletal patterning. Development. *131*, 5703-5716.

Cuddapah, V.A., Turner, K.L., Seifert, S., and Sontheimer, H. (2013). Bradykinin-induced chemotaxis of human gliomas requires the activation of KCa3.1 and ClC-3. J. Neurosci. *33*, 1427-1440.

Curtin, E., Hickey, G., Kamel, G., Davidson, A.J., and Liao, E.C. (2011). Zebrafish *wnt9a* is expressed in pharyngeal ectoderm and is required for palate and lower jaw development. Mech. Dev. *128*, 104-115.

Dale, R.M., Sisson, B.E., and Topczewski, J. (2009). The emerging role of Wnt/PCP signaling in organ formation. Zebrafish. *6(1),* 9-14.

David, N., Saint-Etienne, L., Tsang, M., Schilling, T., and Roas, F. (2002). Requirement for endoderm and FGF3 in ventral head skeleton formation. Development. *129*, 4457-4468.

De Calisto, J., Araya, C., Marchant, L., Riaz, C.F., and Mayor, R. (2005). Essential role of non-canonical Wnt signaling in neural crest migration. Development. *132,* 2587-2597.

De Rienzo, G., Bishop, J.A., Mao, Y., Pan, L., Ma, T.P., Moens, C.B., Tsai, L.H., and Sive, H. (2011). Disc1 regulates both β-catenin-mediated and noncanonical Wnt signaling during vertebrate embryogenesis. FASB. *25(12),* 4184-97.

Dickinson, A.J., and Sive, H.L. (2006). Development of the primary mouth in *Xenopus laevis*. Dev. Biol. *295*, 700-713.

Dickinson, A., and Sive, H.L. (2007). Positioning the extreme anterior in *Xenopus*: cement gland, primary mouth and anterior pituitary. Semin. Cell Dev. Biol. *18*, 525-533.

Dickinson, A.J., and Sive, H.L. (2009). The Wnt antagonists Frzb-1 and Crescent locally regulate basement membrane dissolution in the developing primary mouth. Development. *136(7)*, 1071-1081.

Duband J. L. (2010). Diversity in the molecular and cellular strategies of epithelium-to-mesenchyme transitions: Insights from the neural crest. Cell Adh. Migr. *4*, 458-482.

Dupin E., Creuzet S., and Le Douarin N. M. (2006). The contribution of the neural crest to the vertebrate body. Adv. Exp. Med. Biol. *589*, 96-119.

Eagleson, G., Ferreiro, B., and Harris, W. A. (1995). Fate of the anterior neural ridge and the morphogenesis of the Xenopus forebrain. J. Neurobiol. *28(2)*, 146-158.

Eagleson, G., Jenks, B., and Van Overbeeke, A. P. (1986). The pituitary adrenocorticotropes originate from neural ridge tissue in *Xenopus* laevis. J. Embryol. Exp. Morphol. *95*,1-14.

Eberhart, J., Swartz, M., Crump, J., and Kimmel, C. (2006). Early Hedgehog signaling from neural to oral epithelium organizes anterior craniofacial development. Development. *133*, 1069-1077.

Erices, R., Corthorn, J., Lisboa, F., and Valdes, G. (2011). Bradykinin promotes migration and invasion of human immortalized trophoblasts. Reprod. Biol. Endocrinol. *9*, 97.

Ermakova, G.V., Solovieva, E.A., Martynova, N.Y., and Zaraisky, A.G. (2007). The homeodomain factor Xanf represses expression of genes in the presumptive rostral forebrain that specify more caudal brain regions. Dev. Biol. *307*, 483–497.

Filippin, L.I., Cuevas, M.J., Lima, E., Marroni, N.P., Gonzalez-Gallego, J., and Xavier, R.M. (2011). Nitric oxide regulates the repair of injured skeletal muscle. Nitric Oxide. *24*, 43-49.

Foppiano, S., Hu, D. and Marcucio, R. S. (2007). Signaling by bone morphogenetic proteins directs formation of an ectodermal signaling center that regulates craniofacial development. Dev. Biol. *312*, 103-114.

Fowles, L.F., Bennetts, J.S., Berkman, J.L., Williams, E., Koopman, P., Teasdale, R.D., and Wicking, C. (2003). Genomic screen for genes involved in mammalian craniofacial development. Genesis. *35*, 73-87.

Gorlin, R.J., Cohen, M., Levin, L. (1990). Syndromes of the head and neck. Oxford, UK: Oxford University Press.

Gilbert, S. (2010). Developmental biology. 9th Ed. (Sinauer Associates: Sunderland, MA).

Grunz, H. (1990). Homoiogenetic neural inducing activity of the presumptive neural plate of *Xenopus laevis*. Dev. Growth Differ. *32*, 583-589.

Hamburger, V., and Hamilton, H. (1951). A series of normal stages in the development of the chick embryos. J. Morphol. *88*, 49-67.

Hardin, J., and Armstrong, N. (1997). Short-range cell-cell signals control ectodermal patterning in the oral region of the sea urchin embryo. Dev. Biol. *182*, 134-149.

Haworth, K., Healy, C., Morgan, P., and Sharpe, P. (2004). Regionalisation of early head ectoderm is regulated by endoderm and prepatterns the orofacial epithelium. Development. *131*, 4797-4806.

Haworth, K., Wilson, J., Grevellec, A., Cobourne, M., Healy, C., Helms, J., Sharpe, P., and Tucker, A. (2007). Sonic hedgehog in the pharyngeal endoderm controls arch pattern via regulation of Fgf8 in head ectoderm. Dev. Biol. *303*, 244-258.

Helms, J., Kim, C., Hu, D., Minkoff, R., Thaller, C., Eichele, G. (1997). Sonic hedgehog participates in craniofacial morphogenesis and is down-regulated by teratogenic doses of retinoic acid. Dev. Bio. *187(1)*, 25-35.

Hu, D., and Helms, J. (1999). The role of Sonic hedgehog in normal and abnormal craniofacial morphogenesis. Development. *126*, 4873-4884.

Hu, D. and Marcucio, R. S. (2009a). A SHH-responsive signaling center in the forebrain regulates craniofacial morphogenesis via the facial ectoderm. Development. *136*, 107-116.

Hu, D. and Marcucio, R. S. (2009b). Unique organization of the frontonasal ectodermal zone in birds and mammals. Dev. Biol. *325*, 200-210.

Hu, D. and Marcucio, R. S. (2015). A dynamic *Shh* expression pattern, regulated by SHH and BMP signaling, coordinates fusion of primordial in the amniote face. Development. *142*, 567-574.

Hu, D., Marcucio, R., and Helms, J. (2003). A zone of frontonasal ectoderm regulates patterning and growth in the face. Development. *130*, 1749-1758.

Jacox, L.A., Dickinson, A.J., and Sive, H. (2014). Facial transplants in *Xenopus laevis* embryos. J. Vis. Exp. (85).

Jacox, L.*, Sindelka, R.*, Chen, J., Rothman, A., Dickinson, A., and Sive, H. (2014). The extreme anterior domain is an essential craniofacial organizer acting through Kinin Kallikrein signaling. Cell Rep. *8(2)*, 596-609. *Equal contribution.

Jeong, J., Mao, J., Tenzen, T., Kottmann, A., and McMahon, A. (2004). Hedgehog signaling in the neural crest cells regulates the patterning and growth of facial primordia. Genes Dev.*18*, 937-951.

Jeseta, M., Marin, M., Tichovska, H., Melicharova, P., Cailliau-Maggio, K., Martoriati, A., Lescuyer-Rousseau, A., Beaujois, R., Petr, J., Sedmikova, M., and Bodart, J.F. (2012). Nitric oxide-donor SNAP induces *Xenopus* eggs activation. PLoS ONE. *7*, e41509.

Kakoki, M., and Smithies, O. (2009). The kallikrein-kinin system in health and in diseases of the kidney. Kidney Int. *75*, 1019-1030.

Kamel, G., Hoyos, T., Rochard, L., Dougherty, M., Kong, Y., Tse, W., Shubinets, V., Grimaldi, M., Liao, E. (2013). Requirement for frzb and fzd7a in cranial neural crest convergence and extension mechanisms during zebrafish palate and jaw morphogenesis. Dev. Biol. *381*, 423-433.

Kawamura, K., Kouki, T., Kawahara, G., and Kikuyama, S. (2002). Hypophyseal development in vertebrates from amphibians to mammals. Gen. Comp. Endocrinol. *126*, 130-135.

Keller, R., Davidson, L., Edlund, A., Elul, T., Ezin, M., Shook, D., and Skoglund, P. (2000). Mechanisms of convergence and extension by cell intercalation. Philos. Trans. R. Soc. Lond. B Biol. Sci. *355*, 897-922.

Kennedy, A.E., and Dickinson, A.J. (2012). Median facial clefts in *Xenopus laevis*: Roles of retinoic acid signaling and homeobox genes. Dev. Biol. *365(1)*, 229–240.

Kimmel, C.B., Ballard, W.W., Kimmel, S.R., Ullmann, B., and Schilling, T.F. (1995). Stages of embryonic development of the zebrafish. Dev. Dyn. *203*, 253–310.

Knight, R.D., and Schilling, T.F. (2006). Cranial neural crest and development of the head skeleton. Adv. Exp. Med. Biol. *589*, 120–133.

Kong, Y., Grimaldi, M., Curtin, E., Dougherty, M., Kaufman, C., White, R.M., Zon, L.I., and Liao, E.C. (2014). Neural crest development and craniofacial morphogenesis is coordinated by nitric oxide and histone acetylation. Chem. Biol. *21*, 488–501.

Kozlowski, D. J., Murakami, T., Ho, R.K., and Weinberg, E.S. (1997). Regional cell movement and tissue patterning in the zebrafish embryo revealed by fate mapping with caged fluorescein. Biochem. Cell. Biol. *75*, 551-562.

Kurihara, Y., Kurihara, H., Suzuki, H., Kodama, T., Maemura, K., Nagai, R., Oda, H., Kuwaki, T., Cao, W.H., Kamada, N., et al. (1994). Elevated blood pressure and craniofacial abnormalities in mice deficient in endothelin-1. Nature. *368*, 703–710.

Kurosaka, H., Lulianella, A., Williams, T. and Trainor, P.A. (2014). Disrupting hedgehog and WNT signaling interactions promotes cleft lip pathogenesis. J. Clin. Invest. *124*, 1660-1671.

Kuzin, B., Roberts, I., Peunova, N., and Enikolopov, G. (1996). Nitric oxide regulates cell proliferation during Drosophila development. Cell. *87*, 639–649.

LaBonne, C., and Bronner-Fraser, M. (1998). Neural crest induction in *Xenopus*: evidence for a two-signal model. Development. *125*, 2403–2414.

Le Douarin N.M., Couly G., and Creuzet S.E. (2012). The neural crest is a powerful regulator of pre-otic brain development. Dev. Biol. *366*, 74-82.

Le Douarin, N.M., Creuzet, S., Couly, G., and Dupin, E. (2004). Neural crest cell plasticity and its limits. Development. *131*, 4637-4650.

Le Douarin, N., and Kalcheim, C. (1999). *The Neural Crest*. Cambridge/New York: Cambridge University Press.

Lepiller, S., Laurens, V., Bouchot, A., Herbomel, P., Solary, E., and Chluba, J. (2007). Imaging of nitric oxide in a living vertebrate using a diamino-fluorescein probe. Free Radic. Biol. Med. *43*, 619–627.

Lievre, A.L., and Le Douarin, N. (1982). The early development of cranial sensory ganglia and the potentialities of their component cells studied in quail-chick chimeras. Dev. Bio. *94*, 291-310.

Mancilla, A., and Mayor, R. (1996). Neural crest formation in *Xenopus laevis*: mechanisms of Xslug induction. Dev. Biol. *177*, 580–589.

Manni, L., Agnoletto, A., Zaniolo, G., and Burighel, P. (2005). Stomodeal and neurohypophysial placodes in *Ciona intestinalis*: insights into the origin of the pituitary gland. J. Exp. Zool. B. Mol. Dev. Evol. *304*, 324-339.

Marcucio, R., Cordero, D., Hu, D., and Helms, J. (2005). Molecular interactions coordinating the development of the forebrain and face. Dev. Biol. *284*, 48-61.

Marcucio, R.S., Tong, M., and Helms, J. (2001). Establishment of distinct signaling centers in the avian frontonasal process. Dev. Biol. *235*, A432.

Mashimo, H., and Goyal, R.K. (1999). Lessons from genetically engineered animal models. IV. Nitric oxide synthase gene knockout mice. Am. J. Physiol. *277*, G745–G750.

Matthews, K.W., Mueller-Ortiz, S.L., and Wetsel, R.A. (2004). Carboxypeptidase N: a pleiotropic regulator of inflammation. Mol. Immunol. *40*, 785–793.

Mayor, R., and Theveneau, E. (2013). The neural crest. Development. *140(11)*, 2247-2251.

McLean, D.L., and Sillar, K.T. (2000). The distribution of NADPH-diaphorase-labeled interneurons and the role of nitric oxide in the swimming system of *Xenopus laevis* larvae. J. Exp. Biol. *203*, 705-713.

Merkulov, S., Zhang, W.M., Komar, A.A., Schmaier, A.H., Barnes, E., Zhou, Y., Lu, X., Iwaki, T., Castellino, F.J., Luo, G., and McCrae, K.R. (2008). Deletion of murine kininogen gene 1 (mKng1) causes loss of plasma kininogen and delays thrombosis. Blood. *111*, 1274-1281.

Minoux, M., Rijli. F. (2010). Molecular mechanisms of cranial neural crest cell migration and patterning in craniofacial development. Development. *137*, 2605-2621.

Moncada, S., and Higgs, E.A. (1995). Molecular mechanisms and therapeutic strategies related to nitric oxide. FASEB J. *9*, 1319–1330.

Mori-Akiyama, Y., Akiyama, H., Rowitch, D.H., and de Crombrugghe, B. (2003). Sox9 is required for determination of the chondrogenic cell lineage in the cranial neural crest. Proc. Natl.

Acad. Sci. USA *100*, 9360–9365.

Mueller-Ortiz, S.L., Wang, D., Morales, J.E., Li, L., Chang, J.Y., and Wetsel, R.A. (2009). Targeted disruption of the gene encoding the murine small subunit of carboxypeptidase N (CPN1) causes susceptibility to C5a anaphylatoxin-mediated shock. J. Immunol. *182*, 6533–6539.

Nieuwkoop, P.D., and Faber, J. (1994). Normal table of *Xenopus laevis* (Daudin): A Systematical & Chronological Survey of the Development from the Fertilized Egg till the end of Metamorphosis (New York: Garland Publishing).

Noden, D. (1983). The role of the neural crest in patterning of avian cranial skeletal, connective, and muscle tissues. Dev. Biol. *96(1)*, 144-165.

Odent, S., Atti-Bitach, T., Blayau, M., Mathieu, M., Aug, J., Delezo, A. Gall, J., Le Marec, B., Munnich, A., David, V., and Vekemans, M. (1999). Expression of the Sonic hedgehog (SHH) gene during early human development and phenotypic expression of new mutations causing holoprosencephaly. Hum. Mol. Genet. *8(9)*,1683-1689.

Olson, S.Y., and Garban, H.J. (2008). Regulation of apoptosis-related genes by nitric oxide in cancer. Nitric Oxide. *19*, 170-176.

Ossipova, O., Dhawan, S., Sokol, S., and Green, J.B. (2005). Distinct PAR-1 proteins function in different branches of Wnt signaling during vertebrate development. Dev. Cell *8*, 829–841.

Osumi-Yamashita, N., Ninomiya, Y., Doi, H., and Eto, K. (1994). The contribution of both forebrain and midbrain crest cells to the mesenchyme in the frontonasal mass of mouse embryos. Dev. Biol. *164*, 409-419.

Pandur, P., Läsche, M., Eisenberg, L.M., and Kühl, M. (2002). Wnt-11 activation of a non-canonical Wnt signaling pathway is required for cardiogenesis. Nature. *418,* 636-41.

Papalopulu, N. (1995). Regionalization of the forebrain from neural plate to neural tube. Perspect. Dev. Neurobiol. *3*, 39-52.

Park, B. and Saint-Jeannet, J. (2010). Induction and segregation of the vertebrate cranial placodes. San Rafael (CA): Morgan & Claypool Life Sciences.

Peunova, N., Scheinker, V., Ravi, K., and Enikolopov, G. (2007). Nitric oxide coordinates cell proliferation and cell movements during early development of *Xenopus*. Cell Cycle. *6*, 3132-3144.

Piotrowski, T., and Nusslein-Volhard, C. (2000). The endoderm plays and important role in patterning the segmented pharyngeal region in Zebrafish (*Danio rerio)*. Dev. Biol. *225*, 339-356.

Poon, K.L., Richardson, M., and Korzh, V. (2008). Expression of zebrafish *nos2b* surrounds oral cavity. Dev. Dyn. *237*, 1662-1667.

Poon, K.L., Richardson, M., Lam, C.S., Khoo, H.E., and Korzh, V. (2003). Expression pattern of neuronal nitric oxide synthase in embryonic zebrafish. Gene Expr. Patterns. *3*, 463-466.

Ramachandran, S., Mamatha, G., Rajeshwari, G., Annigeri, S. and Shettar, S. (2010). Persistent buccopharyngeal membrane in an adult: An incidental finding. Int. J. of Dent. Clinics. *2(10)*, 74-76.

Roessler, E., Belloni, E., Gaudenz, K., Jay, P., Berta, P., Scherer, S., Tsui, L. and Muenke, M. (1996). Mutations in the human Sonic Hedgehog gene cause holoprosencephaly. Nat Genet. *14(3)*, 357-360.

Roszko, I., Sawada, A., and Solnica-Krezel, L. (2009). Regulation of convergence and extension movements during vertebrate gastrulation by the Wnt/PCP pathway. Sem. Cell Dev. Biol. *20,* 986-997.

Ruhin, B., Creuzet, S., Vincent, C., Benouaiche, L., Le Douarin, N. and Couly, G. (2003). Patterning of the hyoid cartilage depends on upon signals arising from the ventral foregut endoderm. Dev. Dyn. *228*, 239-246.

Santagati, F., and Rijli, F.M. (2003). Cranial neural crest and the building of the vertebrate head. Nat. Rev. Neurosci. *4(10)*, 806-818.

Sato, A., Scholl, A., Kuhn, E., Stadt, H., Decker, J., Pegram, K., Hutson, M., and Kirby, M. (2011). Fgf8 signaling is chemotactic for cardiac neural crest cells. Dev. Biol. *354(11)*, 18-30.

Schlosser, G. (2006). Induction and specification of cranial placodes. Dev. Biol. *294*, 303-351.

Schweickert, A., Steinbeisser, H., and Blum, M. (2001). Differential gene expression of *Xenopus* Pitx1, Pitx2b and Pitx2c during cement gland, stomodeum and pituitary development. Mech. of Dev. *107(1-2)*, 191-194.

Schwind, L. (1928). The development of the hypophysis cerebri of the albino rat. Am. J. Anut. *41*, 295-319.

Servetnick, M., and Grainger, R. M. (1991). Changes in neural and lens competence in *Xenopus* ectoderm: Evidence for an autonomous developmental timer. Dev. Bio. *112*, 177-188.

Servetnick, M., and Grainger, R. M. (1991). Homeogenetic neural induction in *Xenopus*. Dev. Bio. *147*, 73-82.

Sharma, J.N. (2009). Hypertension and the bradykinin system. Curr. Hypertens. Rep. *11*, 178-181.

Shiau, C.E., and Bronner-Fraser., M. (2009). N-cadherin acts in concert with Slit1-Robo2 signaling in regulation aggregation of placode-derived cranial sensory neurons. Development. *136(24),* 4155-4164.

Shigetani, Y., Nobusada, Y., and Kuratani, S. (2000). Ectodermally derived FGF8 defines the maxillomandibular region in the early chick embryo: Epithelial-mesenchymal interactions in the specification of the craniofacial ectomesenchyme. Dev. Biol. *228*, 73-85.

Sive, H.L., Grainger, R.M., and Harland, R.M. (2000). Early Development of *Xenopus laevis*: A laboratory manual (Cold Spring Harbor: Cold Spring Harbor Press).

Sive, H.L., Hattori, K., and Weintraub, H. (1989). Progressive determination during formation of the anteroposterior axis in *Xenopus laevis*. Cell. *58(1)*, 171–180.

Sokol, S.Y. (1996). Analysis of Dishevelled signaling pathways during *Xenopus* development. Current Biology. *6(11),* 1456-1467.

Spemann, H., and Mangold, H. (1924). Induction of Embryonic Primordia by Implantation of Organizers from a Different Species. Hafner, New York.

Spokony, R.F., Aoki, Y., Saint-Germain, N., Magner-Fink, E., and Saint-Jeannet, J.P. (2002). The transcription factor Sox9 is required for cranial neural crest development in *Xenopus*. Development. *129*, 421–432.

Steventon, B., Mayor, R., and Streit, A. (2014). Neural crest and placode interaction during the development of the cranial sensory system. Dev. Biol. *389*, 28-38.

Tabler, T., Bolger, T., Wallingford, J., and Liu, K. (2014). Hedgehog activity controls opening of the primary mouth. Dev. Biol. *396*, 1-7.

Tada, M., and Heisenberg, C.P. (2012). Convergent extension: using collective cell migration and cell intercalation to shape embryos. Development. *139,* 3897-3904.

Tada, M., and Smith, J.C. (2000). Xwnt11 is target of Xenopus Brachyury: regulation of gastrulation movements via Dishevelled, but not through the canonical Wnt pathway. Development. *127,* 2227-2238.

Tandon, P., Showell, C., Christine, K., and Conlon, F. (2012). Morpholino injection in *Xenopus*. Methods Mol. Biol. *843*, 29-46.

Theveneau E., and Mayor R. (2011). Collective cell migration of the cephalic neural crest: the art of integrating information. Genesis. *49*, 164-176.

Theveneau E., and Mayor R. (2012). Neural crest delamination and migration: from epithelium-to-mesenchyme transition to collective cell migration. Dev. Biol. *366*, 34-54.

Theveneau, E., Steventon, B., Scarpa, E., Garcia, S., Trepat, X., Streit, A., and Mayor, R. (2013). Chase-and-run between adjacent cell populations promotes directional collective migration. Nat. Cell Biol. *15*, 763-772.

Thomason, H., and Dixon, M. (2009). Craniofacial Defects and Cleft Lip and Palate. eLS, DOI: 10.1002/9780470015902.a0020915.

Topczewski, J., Dale, R.M., and Sisson, B.E. (2011). Planar cell polarity signaling in craniofacial development. Organogenesis. *7(4),* 255-59.

Trainor, P. (2010). Craniofacial birth defects: The role of neural crest cells in the etiology and pathogenesis of Treacher Collins syndrome and the potential for prevention. Am. J. Med. Gen. A. *152*, 2984-2994.

Trainor, P., Ariza-McNaughton, L., and Krumlauf, R. (2002). Role of the isthmus and FGFs in resolving the paradox of neural crest plasticity and prepatterning. Science. *295(5558)*, 1288-1291.

Trainor, P., and Tam, P. (1995). Cranial paraxial mesoderm and neural crest of the mouse embryo- codistribution in the craniofacial mesenchyme but distinct segregation in the branchial arches. Development. *121*, 2569-2582.

Trarbach, E.B., Abreu, A.P., Silveira, L., Garmes, H., Baptista, M., Teles, M, Costa, E., Mohammadi, M., Pitteloud, N., Mandonca, B., and Latronico, A. (2010). Nonsense mutations in FGF8 gene causing different degrees of human gonadotropin-releasing deficiency. J. Clin. Endocrinol. Metabl. *95(7)*, 3491-3496.

Trumpp, A., Depew, J., Rubenstein, J., Bishop, F., and Martin, G. (1999). Cre-mediated gene inactivation demonstrates that FGF8 is required for cell survival and patterning of the first branchial arch. Genes Dev.*13*, 3136-3148.

Tucker, A., Al Khamis, A., Ferguson, C., Bach, E., Rosenfeld, M. and Sharp, P. (1999). Conserved regulation of mesenchymal gene expression by FGF-8 in face and limb development. Development. *126*, 221-228.

Ulrich, F., Concha, M., Heid, P., Voss, E., Witzel, S., Roehl, H., Tada, M., Wilson, S., Adams, R., Soll, D., and Heisenberg, C. (2003). Slb/Wnt11 controls hypoblast cell migration and morphogenesis at the onset of zebrafish gastrulation. Development. *130*, 5375-5384.

Verma, S., and Geller, K. (2009). Persistent buccopharyngeal membrane: Report of a case and review of the literature. Int. J of Ped. Otorhinolaryng. *73(6)*, 877-880.

Wada, N., Javidan, Y., Nelson, S., Carney, T., Kelsh, R., and Schilling, T. (2005). Hedgehog signaling is required for cranial neural crest morphogenesis and chondrogenesis at the midline of the zebrafish skull. Development. *132(17)*, 3977-3988.

Wallingford, J.B., Fraser, S.E., and Harland, R.M. (2002). Convergent extension: The molecular control of polarized cell movement during embryonic development. Dev. Cell. *2(6),* 695-706.

Watanabe, K., Sasaki, F., and Takahama, H. (1984). The ultrastructure of oral (buccopharyngeal) membrane formation and rupture in the anuran embryo. Anat. Rec. *210*, 513-524.

Waterman, R. (1977). Ultrastructure of oral (buccopharyngeal) membrane formation and rupture in the hamster embryo. Dev. Biol. *58*, 219-229.

Waterman, R., and Balian, G. (1980). Indirect immunofluorescent staining of fibronectin associated with the floor of the foregut during formation and rupture of the oral membrane in the chick embryo. Anat. Rec. *198*, 619-635.

Waterman, R., and Schoenwolf, G. (1980). The ultrastructure of oral (buccopharyngeal) membrane formation and rupture in the chick embryo. Anat. Rec. *197*, 441-470.

Westerfield, M., Sprague, J., Doerry, E., and Douglas, S. (2001). The Zebrafish Information Network (ZFIN): a resource for genetic, genomic and developmental research. Nucleic Acids Res. *29*, 87-90.

Westermann, D., Schultheiss, H.P., and Tschope, C. (2008). New perspective on the tissue kallikrein-kinin system in myocardial infarction: role of angiogenesis and cardiac regeneration. Int. Immunopharmacol. *8*, 148–154.

Wiellette, E.L., and Sive, H. (2003). Vhnf1 and Fgf signals synergize to specify rhombomere identity in the zebrafish hindbrain. Development. *130(16)*, 3821–3829.

Winklbauer, R., Medina, A., Swain, R.K., and Steinbeisser, H. (2001). Frizzled-7 signaling controls tissue separation during *Xenopus* gastrulation. Nature. *413,* 856-60.

Wu, P., Jiang, T., Shen, J., Widelitz, R., and Chuong, C.M. (2006). Morphoregulation of avian beaks: comparative mapping of growth zone activities and morphological evolution. Dev. Dyn. *235*, 1400-1412.

Yan, Q., Feng, Q., and Beier, F. (2010). Endothelial nitric oxide synthase deficiency in mice results in reduced chondrocyte proliferation and endochondral bone growth. Arthritis Rheum. *62*, 2013-2022.

Yin, C., Ciruna, B., and Solnica-Krezel, L. (2009). Convergence and extension movements during vertebrate gastrulation. Cur. Topics Dev. Biol. *89,* 163-92.

Young, N. M., Hu, D., Lainoff, A. J., Smith, F. J., Diaz, R., Tucker, A. S., Trainor, P. A., Schneider, R. A., Hallgrimsson, B. and Marcucio, R. S. (2014). Embryonic bauplans and the developmental origins of facial diversity and constraint. Development. *141*, 1059-1063.

Yu, H.S., Lin, T.H., and Tang, C.H. (2013). Bradykinin enhances cell migration in human prostate cancer cells through B2 receptor/PKCd/c-Src dependent signaling pathway. Prostate. *73*, 89-100.